INTERFACIAL TENSIONS FOR CARBON DIOXIDE OR LIGHT HYDROCARBONS IN HYDROCARBON SOLVENTS: EXPERIMENTAL DATA AND CORRELATIONS

BY

PETER BRIAN DULCAMARA, JR.

Bachelor of Science in Chemistry
Cameron University
Lawton, Oklahoma
1983

Bachelor of Science in Chemical Engineering
Oklahoma State University
Stillwater, Oklahoma
1986

Submitted to the Faculty of the
Graduate College of the
Oklahoma State University
in partial fulfillment of
the requirements for
the Degree of
MASTER OF SCIENCE
December, 1987

INTERFACIAL TENSION FOR CARBON DIOXIDE OR LIGHT HYDROCARBONS IN HYDROCARBON SOLVENTS: EXPERIMENTAL DATA AND CORRELATIONS

Thesis approved:

Robert L. Robinson, Jr.
Thesis Adviser

Kenneth E. Starling

Mayis Seapan

Norman N. Durham
Dean of the Graduate College

ACKNOWLEDMENTS

There comes a time in life to decide what one has discovered about a minute part of nature, and to form the thoughts derived from that experience into words. It is the hope of this author that this humble work be of some enlightment to those that may come to read its contents.

During the course of any endeavor, more than one person's effort will eventually bring about the desired end of that work. I would like to offer my sincere appreciation to my adivsor and teacher, Professor Robert L. Robinson, Jr., for his guidance, expertise, and advice. I would also like to thank the members of my Advisory Committee, Dr. Ruth C. Erbar and Dr. Mayis Seapan.

There are not words which I may write on this page which could justly thank my friend, Dr. Khaled Gasem; without his insight, wisdom, and advice this work could not have been completed.

Many thanks must be extended to Anthony G. Lee, Steven C. Nichols, Jeff A. Graham, and Ronald D. Shaver for their dedication during the data acquisition of this work.

Most of all I wish to thank my family and friends for their love, patience, and understanding during the course of my studies, especially my mother and father, Carol and Peter B. Dulcamara.

TABLE OF CONTENTS

LIST OF TABLES

LIST OF FIGURES

Figure Page

NOMENCLATURE

a	- Surface area of interface
A	- Helmholtz free energy
a, b, n	- Scaling-law parameters (critical indices)
A, B, C, D	- Parameters in Equations 3-1
A_c	- Corresponding states parameter
A_i, B_i, G_i	- Parameters in Equations 4-1 through 4-5
AR	- Chromatograph dectector area ratio (solute-to-solvent)
b	- Radius of curvature at the vertex of a pendant drop
B	- Parameter for density coexistence
C	- Temperature independent constant
C_{ij}	- Hugill-Van Welsenes binary interaction parameter
g	- Acceleration due to gravity
k	- Scaling exponent Universal exponent used in Equation 2-17
K_1, K_2, n	- Universal constants used in Equations 2-18, 2-19 and 2-20
MW_1,MW_2	- Solute and solvent molecular weights
M	- Molecular weight
n	- moles
n_1,n_2	- Number of solute and solvent injections in a given calibration run
N_1,N_2	- Moles of solute and solvent in chromatograph calibration mixture

P	-	Pressure
P^*	-	Scaled pressure, (Pc-P)/Pc
P_c	-	Critical pressure
[P]	-	The parachor
Q	-	Heat transferred across interface
R	-	Radius of curvature of pendant drop
RF	-	Chromatograph response factor
S	-	Entropy of interface
	-	Shape factor
T	-	Temperature
T_{br}	-	Reduced normal boiling-point temperature
U	-	Internal energy
V	-	Total volume of equilibrium cell
V_c	-	Critical Volume
V^s	-	Interfacial volume
V_1, V_2	-	Volume of injected solute and solvent for a chromatograph calibration mixture
W	-	Total work done on interface
y	-	Vapor phase mole fraction
Y	-	General experimental variable
x	-	Liquid phase mole fraction
z_c	-	Critical composition (mole fraction)
1/H	-	Inverse shape parameter

GREEK

α	-	Riedel's Parameter
β	-	Density coexistence curve parameter
γ	-	Interfacial tension

γ_o	- van der Waals constant = $K_1 T_c V_c^{(-2/3)} = K_2 T_c^{(1/3)} P_c^{(2/3)}$
δ	- Ramsey and Shields temperature correction, usually taken as six degrees
Δ	- Wegner gap exponent
ε_Y	- Uncertainty in measured variable Y
θ	- Guggenheim scaling exponent = 11/9
μ	- Chemical potential
$\Delta\rho$	- Liquid phase density minus vapor phase density
ρ_a, ρ_w	- Air and water densities
ρ_c	- Critical density
ρ^L	- Liquid phase density
ρ^V	- Vapor phase density
ρ_1, ρ_2, ρ_M	- Solute, solvent, and mixture densities in chromatograph calibration mixture
σ	- Weighting factor in regressions
τ	- Density meter count (period of oscilation) for sample fluid
	- Thickness of interface, used in Equation 2-1
τ_a, τ_w	- Density meter counts for air and water
ϕ	- General "order parameter"
	- Angle made by the tangent at a point defined by R with the horizontal

CHAPTER I

INTRODUCTION

Various enhanced oil recovery processes are being evaluated as a means of recovering billions of barrels of crude oil that are unrecoverable through primary production mechanisms (1). In certain processes, the efficacy of the flooding medium is increased by the lowering the interfacial tension (IFT) between the injected fluid and the reservoir oil (2). Studies have shown that residual oil saturations and relative permeabilities can be strongly affected by the interfacial tension, especially when the IFT is lower than 0.01 mN/m (3). Without an adequate knowledge of the effects temperature and pressure have on the interfacial tension of the reservoir fluid, these sophisticated oil recovery processes can not be properly evaluated. Hence, the importance of acquiring accurate experimental data on interfacial tensions for hydrocarbon mixtures is warranted. However, due to the lack of experimental interfacial tension data in the literature, a renewed interest has been created for the development of correlations to predict interfacial tensions (4).

The primary objectives of this study were to measure and correlate the interfacial tension (IFT) of saturated liquid mixtures of ethane and heavier hydrocarbons in equilibrium with the corresponding vapor phases. In this work, several interfacial tension correlations were evaluated including: a) the Weinaug-Katz correlation (5), b) the Hugill-

Van Welsenes correlation (6) and c) the Lee-Chien correlation (7). These correlations were tested against both experimental data available in the literature and with data collected during this work. Evaluations of the ability of these models to predict surface tensions has been previously studied by Dickson (8) for carbon dioxide + hydrocarbon systems. The present study expands the work of Dickson to ethane and methane binary systems.

The interfacial tension measurements of primary interest to users of the models investigated in this work are those measurements on hydrocarbons prevalent in petroleum fluids. In order to complement the data currently available in the literature for ethane systems (primarily from investigations at the Oklahoma State University), the ethane + trans-decahydronaphthalene (trans-Decalin) system was investigated. The addition of the ethane + trans-Decalin data to the data base currently available is a logical extension to those data, since the data already accumulated include a paraffin (n-decane) and an aromatic (benzene). The addition of a naphthenic compound completes the study of solvents from the three major structural groups found in petroleum fluids.

CHAPTER II

LITERATURE REVIEW

Review of Surface Thermodynamics

The study of surface thermodynamics is important because surface forces play a vital role in the behavior of liquids in engineering operations which involve foaming, wetting, emulsifying, or droplet formation. Interfacial tensions are required for calculations related to the design of fractionators and absorbers, for two-phase flow calculations and in production of fluids from petroleum reservoirs. A brief review of surface thermodynamics is presented here.

The surface or interfacial tension of a two-phase fluid is a direct result of the molecules in the bulk liquid phase being subject to a balanced intermolecular attractive force exerted by the adjoining molecules, while molecules at the surface of the liquid are subject to unbalanced forces because there is a higher concentration of molecules in the bulk liquid than in the vapor phase above the interface. Thus, molecules in the surface layer are pulled inward and the liquid tends to assume a shape which has the smallest possible surface area for a given volume of liquid (i.e. a sphere) (9). Due to the influence of surface tension, a liquid behaves as if it were surrounded by an elastic skin with a tendency to contract. Drops of liquid, uninfluenced by external forces such as gravity, assume a truly spherical shape (10).

The definitions for boundary tensions found in the literature may

result in some confusion. In the most general sense, boundary tension has been defined by Andreas and co-workers (11) as a measure of the free energy of a fluid interface. The confusion often results over the distinction between the most common forms of boundary tension, surface tension and interfacial tension. Andreas and workers define surface tension as the boundary tension between a liquid and a gas, and interfacial tension as the boundary tension between two incompletely miscible liquids. Hough and workers (12) chose to define the surface tension as the boundary tension between two phases having the same composition. That is, the boundary tension between liquid and vapor phases of a pure component. Hough, et al. define interfacial tension as the boundary tension between two phases having different compositions for a mixture of two or more components. According to the definitions given by Hough, interfacial tension may be used to describe not only a liquid-liquid interface but also a gas-liquid interface. The definitions adopted during this work are those of Hough.

The total work done at the surface caused by the interactions of molecules within the surface is the sum of the force-displacement product parallel and perpendicular to the surface (13). The relationship between the thickness of the interface, τ, and the interfacial volume, V^S, and the surface area, a, may be stated as:

$$V^S = \tau a \qquad (2\text{-}1)$$

The work done on the interface by the forces perpendicular to the plane constituting the surface is $Pa\, d\tau$, where P is a pressure equal at all points on the surface. The work done by forces parallel to the plane

constituting the surface is independent of the shape perimeter, which for simplicity may be assumed to be a rectangle (13). Consequently the work done on the surface of the interface by the parallel surface forces may be stated as $(P_\tau - \gamma)\, da$, where γ is the interfacial tension. The total work done on the surface of the interface is the sum of the work done by the forces parallel and perpendicular to the surface interface (13) and may be stated as:

$$dW = Pa\, d\tau + (P_\tau - \gamma)\, da \tag{2-2}$$

$$= P(a d\tau + \tau\, da) - \gamma da \tag{2-3}$$

Since $$dV^S = a d\tau + \tau da \tag{2-4}$$

$$dW = P dV^S - \gamma da \tag{2-5}$$

From a classical approach of surfaces first treated by Gibbs (14), the interface may be considered a closed system of fixed composition, with γ, the tangential stress, as an intensive variable; that is to say, one in which the value for the system as a whole is not the sum of the values for that property at various points within the system, or simply put, the variable does not depend on the total mass within the system.

The first law of thermodynamics for a closed system which does not undergo a change in external potential or kinetic energy, but only changes in internal energy may be stated as (15):

$$dU = dQ - dW \tag{2-6}$$

Making the assumption that the heat transferred is a reversible process:

$$dQ_{rev} = TdS \tag{2-7}$$

The work on the surface may be defined as:

$$dW_{rev} = PdV^S - \gamma da \tag{2-8}$$

The expressions for reversible heat transition and work may be substituted into equation (2-6):

$$dU = TdS - PdV^S + \gamma da \tag{2-9}$$

The available free energy or Helmholtz free energy may be defined as (13):

$$A = U - TS \tag{2-10}$$

Upon differentiation of the Helmholtz free energy yields:

$$dA = dU - TdS - SdT \tag{2-11}$$

which on substitution of dU with equation (2-9) yields:

$$dA = -SdT - PdV^S + \gamma da \tag{2-12}$$

At constant temperature and volume this reduces to:

$$\gamma = \left(\frac{\partial A}{\partial a}\right)_{T,V^S,n} \tag{2-13}$$

Under these conditions a spontaneous contraction of the surface area (-da) will decrease A, provided γ is positive. Since the surface of a stable liquid phase does in fact tend to decrease in area, γ is always positive (16).

For an open system with varing composition, where μ_i and n_i are the chemical potential and number of moles of type i, then:

$$dU = TdS - PdV^S + \gamma da + \sum_i \mu_i \, dn_i \tag{2-14}$$

and consequently the following deduction (17) may be made:

$$dA = -SdT - PdV^S + \gamma da + \sum_i \mu_i \, dn_i \tag{2-15}$$

where upon the imposition of the previous assumptions for a closed system of constant temperature and volume reduces to equation (2-13).

Interfacial tension may be expressed as a free energy per unit area of surface, but because of the experimental methods employed in this work, the concept of a "tension", or more specifically of a force per unit length, was used to express the values of interfacial tension. This is analogous to expressing pressure in units of length (for instance, a "head" of liquid), where pressure is a measure of force per unit area. Customary units, then, may be dynes/cm instead of ergs/cm^2,

which are identical dimensionally.

At least twenty different methods of determining boundary tension are cited in the literature (18). Of these, only a few have found any widespread success. Some of the more adaptable methods for measuring interfacial tension include the capillary rise, drop weight, bubble pressure, and pendant drop methods. Adamson (18) presents a comprehensive analyses of the various methods used for measuring interfacial tension.

The measuring technique used in this investigation was the pendant drop method.

IFT Correlations

Many of the early attempts to predict interfacial tension are reviewed by Gambill (19, 20). In 1886, Eotvos (21) correlated interfacial tensions with temperature. Integration of his expression yields:

$$\gamma = k\ (T_c - T)(\rho^L/M)^{2/3} \qquad (2\text{-}16)$$

where γ = surface energy (interfacial tension)

ρ^L = liquid phase density

M = molecular weight

T_c = critical temperature

T = temperature of interest

k = universal constant

The Eotvos equation was modified seven years later by Ramsey and

Shields (22). They proposed that $(T_c - T)$ be replaced by $(T_c - T - \delta)$, where δ is usually taken as six degrees. In 1916, Katayama (23) modified these earlier equations in order to account for the vapor and liquid densities as well as temperature:

$$\gamma = k\ (T_c - T)\ (\frac{\Delta\rho}{M})^{2/3} \qquad (2\text{-}17)$$

where $\Delta\rho = \rho^L - \rho^V$

Later work by Walden (1912) and Jaeger (1917) cast serious doubt on the validity of the "universal constant" proposed by Eotvos. These equations were found to be applicable only for a narrowly defined group of liquids.

In 1894, J. D. van der Waals (24) proposed a relation for interfacial tension with reduced temperature as:

$$\gamma = K_1\ T_c\ V_c^{-2/3}\ (1 - T_r)^n \qquad (2\text{-}18)$$

$$= K_2\ T_c^{1/3}\ P_c^{2/3}\ (1 - T_r)^n \qquad (2\text{-}19)$$

$$= \gamma_o\ (1 - T_r)^n \qquad (2\text{-}20)$$

The constants K_1, K_2, and n were proposed to be universal constants for all liquids by van der Waals. The value of n was given as 1.5. In 1923, the equations proposed by van der Waals were confirmed by Ferguson (25) and Sugden (26), but both Ferguson and Sugden arrived at a value for the exponent of 1.2. Ferguson combined the Katayama and van der

Waals equations to arrive at the equation:

$$\gamma^{1/4} = C\ \Delta\rho \qquad (2\text{-}21)$$

where C is a temperature-independent constant for a given substance. Considering its simplicity, this equation is remarkably accurate up to about 30°C below the critical temperature. The Ferguson equation was reported on empirical grounds by Macleod (27) from the Ramsey-Shields data. Sugden, on the other hand, rewrote the van der Waals equation as:

$$\gamma = \gamma_o\ (1 - T_r)^{1.2} \qquad (2\text{-}22)$$

where: $\gamma_o = K_1\ T_c\ V_c^{-2/3} = K_2\ T_c^{1/3}\ P_c^{2/3}$

Sugden proposed that if Equation (2-21) is multiplied through by the molecular weight, an expression for the parachor is obtained:

$$[P] = MC^{1/4} = \frac{M(\gamma)^{1/4}}{\Delta\rho} \qquad (2\text{-}23)$$

The parachor is an additive and constitutive secondary physical property of organic and inorganic liquids. Through statistical mechanical considerations of a liquid in contact with its own vapor, Fowler (28) deduced independently the relationship of the parachor.

Reilly and Rae (29) argued that physical foundations of the parachor were rather weak. The following relation for the parachor was derived from a molecular similarity concept in order to provide a sounder basis for the existence of a parachor:

$$[P] = 0.41\ T_c^{1/4}\ V_c^{5/8} \tag{2-24}$$

In 1943, Weinaug and Katz (5) extended the parachor relationship to mixtures through the empirical relation:

$$\gamma^{1/4} = \frac{\rho^L}{M_L} \sum_i [P]_i\ x_i - \frac{\rho^V}{M_V} \sum_i [P]_i\ y_i \tag{2-25}$$

They found that the equation gave good agreement with their own experimental values for the methane-propane system.

The original Weinaug-Katz correlation was developed with an exponent of 1/4, but many other exponents have been suggested. Hough and Warren (30) found that an exponent with a value of 3/11 gave better results.

In 1984, a multicomponent interfacial tension correlation based on scaling theory was presented by Lee and Chien (7). In addition to the particular exponents usually employed, their correlation contains two new features: 1) a method to predict pure component parachors through estimation of the pseudocritical properties and 2) an approach to calculate the parachors of mixtures. The equation may be stated as:

$$\gamma^{\beta/\theta} = \frac{\rho^L}{M_L} [P]_L - \frac{\rho^V}{M_V} [P]_V \tag{2-26}$$

Scaling theory states that $\theta/\beta = 3.911...$ The above equation then may be written as:

$$\gamma^{1/k} = \frac{\rho^L}{M_L} [P]_L - \frac{\rho^V}{M_V} [P]_V \tag{2-27}$$

where $k = 3.911$

The parachor may then be evaluated from the following equation:

$$[P]_i = \frac{A_{ci}^{\beta/\theta} V_{ci}}{B_i} \tag{2-28}$$

where $A_{ci} = P_{ci}^{2/3} T_{ci}^{1/3} (0.133 \alpha_{ci} - 0.201)$

α_{ci} = Riedel Parameter = $0.9076(1 + (T_{br_i} \ln(P_{ci}))/(1-T_{br_i}))$

T_{br_i} = reduced boiling-point temperature for component i

β = density coexistence-curve exponent = 5/16

θ = scaling exponent = 11/9

V_{c_i} = critical volume

B_i = parameter for density coexistence curve

From the principle of corresponding states the evaluation of the parachor may be extended to either a liquid or vapor value for the parachor if the appropriate value for the mole fraction is used. Lee and Chien extended the evaluation of the parachor to obtain the following relation:

$$[P] = \frac{A_C^{\beta/\theta} V_C}{B} \tag{2-29}$$

where $A_C = P_C^{2/3} T_C^{1/3} (0.133 \alpha_C - 0.201)$

$$P_C = \sum_i z_i P_{ci}$$

$$T_C = \sum_i z_i \, T_{ci}$$

$$\alpha_C = \sum_i z_i \, \alpha_{ci}$$

$$V_C = \sum_i z_i \, V_{ci}$$

$$B = \sum_i z_i \, B_i$$

z = mole fraction in liquid ($z=x$) or vapor ($z=y$)

In 1986, Hugill and Van Welsenes (6) proposed that adjustable binary interaction parameters be incorporated in the parachor "mixing rules" in evaluating the Weinaug-Katz correlation. The Weinaug-Katz correlation may be rewritten as:

$$\gamma^{1/4} = \frac{\rho_L}{M_L} [P]_L - \frac{\rho_V}{M_V} [P]_V \qquad (2\text{-}30)$$

where $[P]_L = \sum_i [P]_i \, x_i$

$$[P]_V = \sum_i [P]_i \, y_i$$

Hugill and Van Welsenes (HVW) proposed that the parachors ($[P]_L$ and $[P]_V$) be determined by the following quadratic "mixing rules":

$$[P]_L = \sum_i \sum_j x_i \, x_j \, [P]_{ij}$$

$$[P]_V = \sum_i \sum_j y_i\, y_j\, [P]_{ij}$$

where $$[P]_{ij} = 1/2\ ([P]_{ii} + [P]_{jj})C_{ij}$$

C_{ij} = HVW binary interation parameter

If C_{ij} is equal to one, their proposed equation reduces to the original Weinaug-Katz correlation.

The correlations investigated during the course of this work are the Weinaug-Katz (WK), Hugill-Van Welsenes(HVW), and Lee-Chien (LC) correlations. The input variables required for these correlations were supplied by data sources available in the literature and data obtained in this work.

Previous Experimental Data

A literature survey for experimental interfacial tension, phase composition, and phase density data was conducted for hydrocarbon/hydrocarbon and carbon dioxide/hydrocarbon systems. The data available in the literature for measurements of interest (γ, x, y, ρ^L, ρ^V), for any one particular system, are very limited. Table I lists the data available, along with their references. The experimental data presented for the methane + n-heptane system by Warren (41) were "smoothed" in the present work so that the volumetric data presented by Sage, et al. (42) would be at identical pressures. The smoothing technique used is similar to the technique used during the smoothing of experimental data acquired during this investigation and is discussed in Chapter IV. The smoothing procedure was implemented so that the

TABLE I

AVAILABLE SOURCES FOR IFT, PHASE COMPOSITIONS, AND PHASE DENSITIES FOR CARBON DIOXIDE/HYDROCARBON AND HYDROCARBON/HYDROCARBON SYSTEMS

SYSTEM	REFERENCE NUMBER	
	IFT	PHASE COMPOSITION AND DENSITY
CO_2 + n-Butane	31	31
CO_2 + n-Decane	32	32
CO_2 + n-Tetradecane	33	33
CO_2 + n-Cyclohexane	34	34
CO_2 + n-Benzene	35	35
CO_2 + trans-Decalin	36	36
CH_4 + n-Propane	5	5
CH_4 + n-Butane	37	38
CH_4 + n-Pentane	39	40
CH_4 + n-Heptane	41 (smoothed)	42
CH_4 + n-Decane	41	43
C_2H_6 + n-Decane	44	44
C_2H_6 +Benzene	45	45

interfacial tension data along with the corresponding phase data could be used in the correlations investigated in this work.

CHAPTER III

EXPERIMENTAL APPARATUS AND PROCEDURE

The experimental apparatus used to obtain the data presented in this work was originally constructed by Dr. J. C. Hsu under the direction of Professor R. L. Robinson Jr. (31). The apparatus has undergone several modifications during the investigation of hydrocarbon systems. These modifications were performed by Drs. N. Nagarajan and K. A. M. Gasem, (32, 33, 34, 35, 36, 44, 45, 46, and 47). The apparatus was originally designed to measure interfacial tensions and volumetric and phase behavior data for multicomponent systems consisting of light solute gases and hydrocarbon solvents at reservoir conditions (to 300°F and 3000 psia). The system investigated during the present work was the ethane + trans-decahydronaphthalene (trans-Decalin) system. No major modifications to the apparatus were preformed, although the sampling valve for the gas chromatograph (GC) was repositioned in order to improve the reproduciblity in the vapor phase compositions.

General Description of the Apparatus

A schematic diagram of the apparatus appears in Figure 1. The experimental facility and procedures have been described in detail by Robinson, et al. (32, 33, 34, 35, 36, 44, 45, 46, and 47). A general description of the apparatus, with the minor changes made on the apparatus, will be discussed here. The three main sections of the

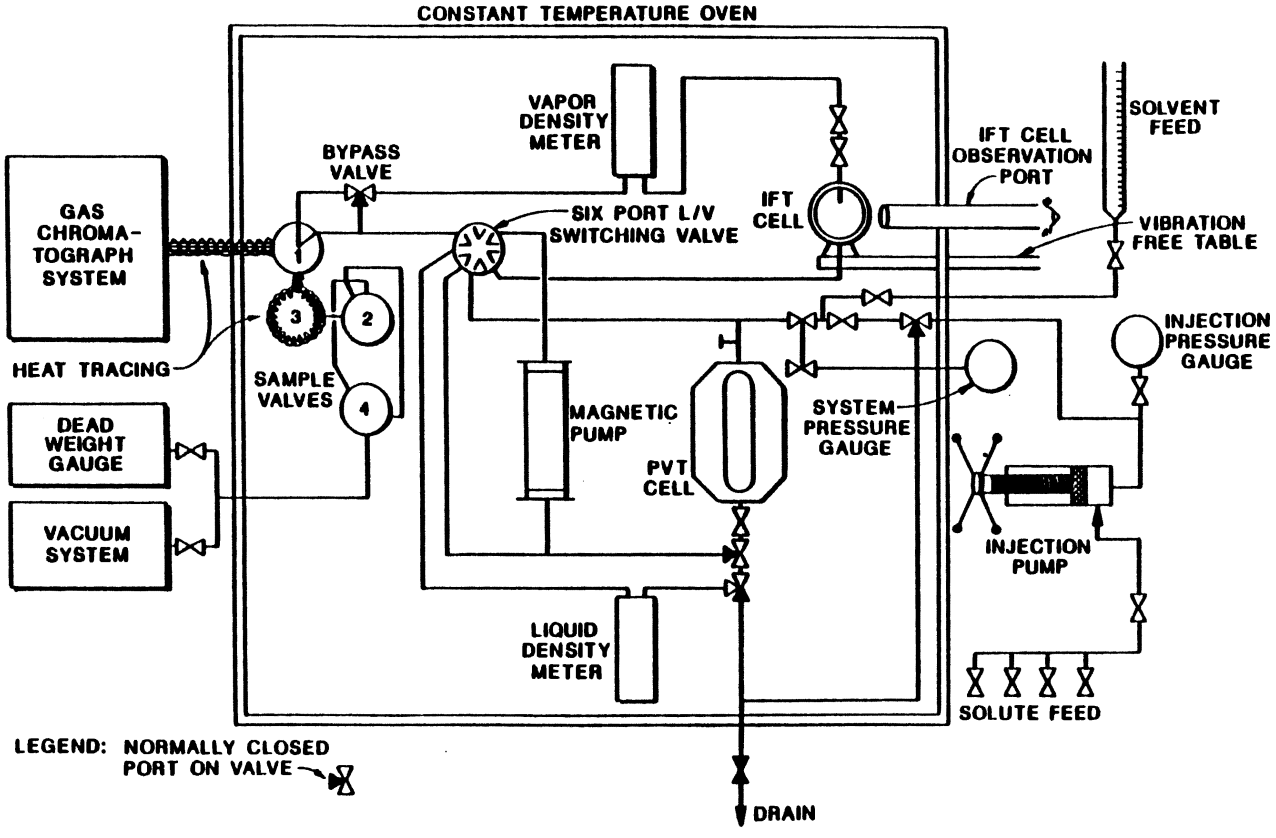

Figure 1. Schematic Diagram of the Experimental Apparatus

apparatus are the IFT cell, the gas chromatograph and the densitometers, all enclosed in a commercial oven.

IFT Cell

The pendant drop IFT cell was based on the original design presented by Schoettle (1) and was fabricated by Temco, Inc. of Tulsa, Oklahoma. The cell consists of a pressure vessel with observation ports on both ends. Within the core of the cell is a turret which may be rotated by the operator during data acquisition. The turret contains five needles, two of which contain wires which project beyond the needle tip. The needles project in a pentagonal manner, in a common plane, toward the center of the cell. The sizes of the needles are 0.018", 0.0103", and 0.0083", and the wires are 0.005" and 0.0035". The turret may be rotated to a selected needle (or wire) during usual operating conditions. The turret is turned in such a manner to align the needle with the inlet flow port to the cell (this is in the vertical position).

The verticality of the selected needle is critical during the photographing of the drop since the interfacial tension forces of interest are those which are parallel to the forces caused by the acceleration due to gravity. The needle (or wire) sizes were chosen to allow for the largest range of interfacial tension determinations. At low pressures, far removed from the critical, the larger needles are used, and as the critical region is approached, the selected of tip size become ever smaller until the progression is carried from the larger needles to the smallest wire. The interfacial tension of a substance tends toward zero as the critical is approached. The interfacial tensions for the ethane + trans-Decalin system were measured by the

pendant drop method. This technique is described in detail by Adams (48) and Jennings (49). The pendant drop method may be used to obtain interfacial tensions from approximately 20 to 0.005 mN/m (8). A list of advantages of this technique has been cited in the literature (50). The major advantages of the pendant drop method were summarized by Deam (51). They include: 1) it is an absolute method; that is, it has been subjected to a complete mathematical analysis and is free of any empirical correlations, 2) a calibration of the IFT cell using compounds of known interfacial tension is not required, 3) the measurements taken are directly convertable by analytical means to values of interfacial tension, 4) the method is easily adapted to a wide assortment of pressures and temperatures, 5) a photograph of a pendant drop serves as a permanent record for future reference, and 6) the drop is not disturbed by the measuring device. In addition, the results do not depend on the value of the contact angle, which is difficult to obtain experimentally.

Gas Chromatograph

The gas chromatograph used during this investigation and all proceeding data acquisitions was a Varian, model 3700, with the following support components: CDS-111 integrator, 9176 chart recorder, and an external events module, all manufactured by Varian. A thermal conductivity detector was used in all measurements. The following conditions were used to obtain the phase composition data for the ethane + trans-decalin system:

Column: 12' OV-101 Temperatures: Column - 200°C

Injector - 270°C

Detector - 270°C

Filament - 300°C

Carrier Gas: Helium

Pressure - 22 psig

Rate - 30 cc/min

The sampling system for the GC is a pneumatically sequenced set of valves controlled by a Valco Digital Valve Sequence Programmer.

During the early part of this work, vapor composition analyses were less reproducible than in previous studies using the same experimental apparatus. Several modifications of the sampling system were investigated. Finally, the chromatograph sampling valve used for gas sampling was repositioned so that both the inlet and outlet lines approach the valve vertically from below. This adjustment, designed to reduce the possibility of condensed liquid accumulating in the valve, resolved the observed difficulties. Thereafter, reproducibility of the vapor sample analyses was better than that obtained in previous studies using the above mentioned apparatus.

Constant Temperature Oven

The major apparatus which reside in the oven are the U-tube densitometers, IFT cell, the magnetic positive displacement pump, PVT cell, pneumatically actuated GC sampling valves, platinum resistance thermometer probe, and the various piping and valves which make up the closed loop circulatory system. The oven is used to maintain precise

temperature control for the required constant temperature equilibrium condition.

The oven is a commercial unit manufactured by Hotpack of Philadelphia, Pennsylvania. The temperature of the oven was brought to within five degrees of the desired temperature by the power unit supplied with the oven. The incremental heat load is then supplied by a Hallikainen Thermotrol connected in series to an ordinary 100 watt incandescent light bulb and a 6' long, 0.5" wide, 470 watt Samox heating tape. In order to maintain a uniform temperature profile within the oven, additional heaters are placed next to both U-tube densitometers, and the IFT cell. These heaters were controlled by variable autotransformers.

Densitometers

The vibrating U-tube densitometers are Mettler/Paar type 512 remote measuring cells. The densitometers are housed within the oven. The liquid densitometer is on the floor of the oven with the inlet and outlet ports pointing upward. The vapor densitometer is positioned at a higher elevation than any other apparatus and is inverted. The positioning of the densitometers was intentional and was done to help eliminate the possibilities of bubbles from being trapped in the liquid cell or liquid from accumulating in the bottom of the vapor cell. The configuration worked quite well.

System Flow Patterns

The flow patterns for the apparatus are shown in Figure 1. The appropriate flow path, liquid or vapor, may be chosen by manually

actuating the six port liquid/vapor (L/V) circulation valve shown in the figure. The liquid and vapor circulation patterns are shown schematically in Figures 2 and 3, respectively. In either case the fluid is pumped up through the magnetic positive displacement pump to the LV valve, where the flow is directed to the appropriate path. In liquid circulation (Figure 2), the liquid passes through the GC sampling valve. The GC sampling valve may be by-passed by opening the sampling by-pass valve and is by-passed during the circulation interval used to obtain equilibrium of the phases. The by-pass valve is then closed while samples of each phase are obtained. When the valve is in the closed position all flow is directed through the GC sampling valve. The liquid then passes through the vapor densitometer and on to the IFT cell, where pendant drop photographs may be taken. The liquid then passes through the L/V valve where it is directed to the top of the windowed PVT cell. Here the liquid falls through the vapor phase completing the closed circulation path. Vapor circulation is essentially the reverse of the liquid pattern with the vapor bubbling upward through liquid in both the IFT and PVT cell (Figure 3).

Calibrations and Integrity Check

To the extent possible, various consistency tests are routinely performed on both the experimental techniques and on the experimental data acquired. These tests constitute an integral part of the overall experimental effort. While rather elaborate techniques are required to assess the absolute thermodynamic consistency of phase equilibrium data, certain instrumental tests on the internal and external consistency of the experimental measurements are easily conducted. The following is a

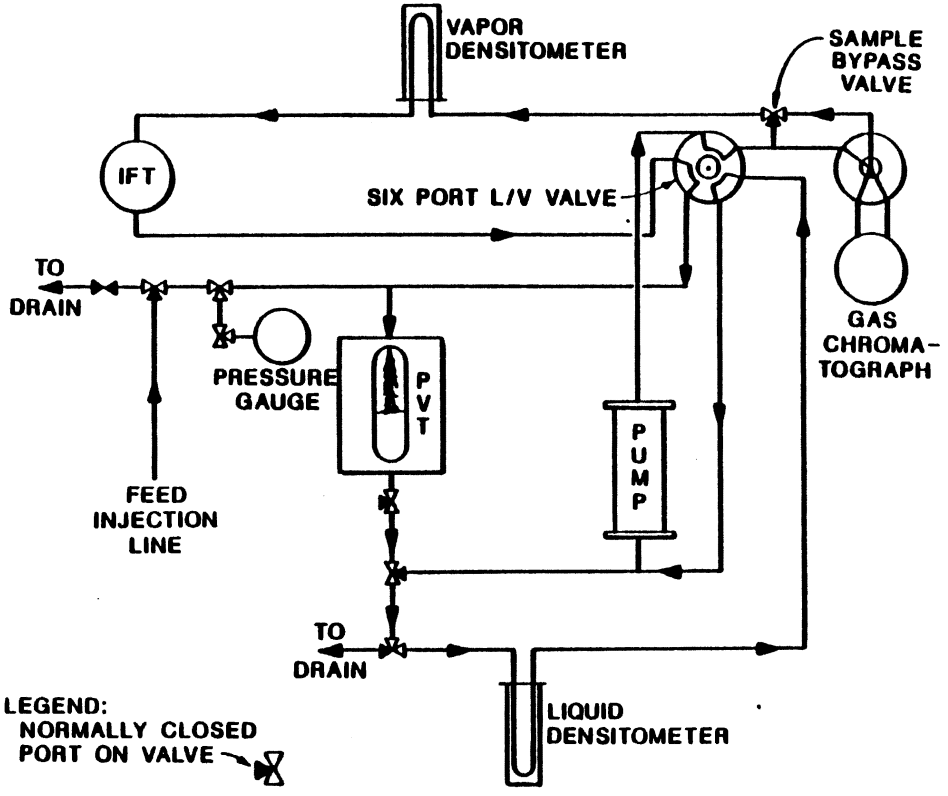

Figure 2. Liquid Circulation Pattern

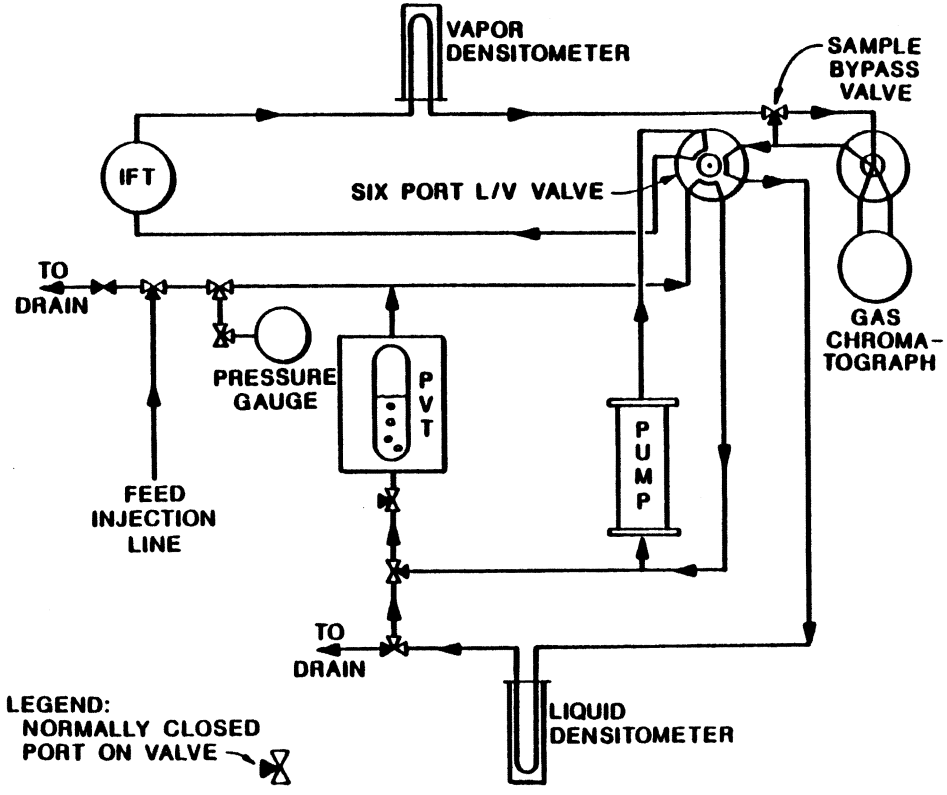

Figure 3. Vapor Circulation Pattern

brief description of the consistency tests made to ensure proper operation of the instruments used in obtaining the presented experimental measurements of this work.

Prior to each experimental run, instrumental consistency for temperature, pressure and density measuring devices is established by calibration. Temperature sensors and pressure gauges are calibrated using standards traceable to the National Bureau of Standards.

A thorough leak and pressure stability test using utility grade helium pressurized to approximately 10% above the critical pressure of the system of interest is performed before calibrations are undertaken. Once the system has been determined to be free of leaks, the instrument calibrations are performed on the following apparatus; the pressure gauges, the thermocouples, the densitometers, and the thermal conductivity detector response factor (RF). The Heise and Sensotec digital gauges are calibrated against a Ruska deadweight gauge (Catalog Number 2470-701) using nitrogen as the working fluid. The thermocouples are calibrated against an NBS certified platinum resistance temperature probe and against the freezing point of distilled water at ambient pressure.

The densitometers are calibrated at the temperature of the experimental measurements. The calibrations are performed using reference fluids of known density (air and water), where the density meter counts (the period of oscillation of the vibrating sample tube) for such fluids are fitted to the following equation:

$$\tau = A + BP + CP^2 + DP^3 \qquad (3\text{-}1)$$

where

τ = period of oscillation of the U-tube densitometer

P = fluid pressure

A,B,C,D = fitting constants

Interpolation between the reference fluid values is then used to convert the density meter count of a given sample to a measurement of density by the following equation:

$$\rho = K\ (\tau^2 - \tau_w^2) + \rho_w \qquad (3\text{-}2)$$

where

$$K = (\rho_a - \rho_w)/(\tau_a^2 - \tau_w^2)$$

τ_a, τ_w = density meter count (period of oscillation) for air and water

ρ, ρ_a, ρ_w = sample, air and water densities, respectively

Typical results of the density meter calibrations are given in Tables II and III, which show the ability of Equation 3-1 to fit the calibration data. As indicated by the tables, selection of air and water as calibration fluids provides the desired range of density (0.01 to 1.0 gm/cc) for the fluid mixtures of interest in this study.

Density measurements on pure ethane were made frequently to provide a consistency check on the operation of the density meters. Table IV presents the results of a typical density meter calibration check, including comparisons with the NBS equation of state predictions (52) and with the data of Douslin (53) and Reamer (54); results are

TABLE II

COMPARISON OF EXPERIMENTAL AND LITERATURE
PHASE DENSITIES FOR PURE AIR AT 160°F

PRESSURE	PHASE DENSITIES, GM/CC		DIFFERENCE IN MEASURED DENSITY	
psia	EXPT'L	LIT	gm/cc	%DIFFERENCE
----------VAPOR DENSITY METER----------				
216	0.01509	0.01511	-0.00002	-0.12
414	0.02885	0.02884	0.00001	0.03
812	0.05635	0.05634	0.00001	0.02
612	0.04256	0.04254	0.00001	0.04
1011	0.07008	0.06997	0.00011	0.16
1208	0.08316	0.08335	-0.00019	-0.23
1408	0.09680	0.09676	0.00004	0.04
1607	0.10999	0.10998	0.00001	0.01
1806	0.12300	0.12296	0.00004	0.03
2004	0.13573	0.13575	-0.00002	-0.01
2203	0.14841	0.14837	0.00005	0.03
2387	0.15981	0.15983	-0.00003	-0.02
----------LIQUID DENSITY METER----------				
216	0.01511	0.01511	0.00001	0.04
414	0.02889	0.02887	0.00002	0.07
612	0.04256	0.04254	0.00001	0.03
812	0.05626	0.05634	-0.00008	-0.15
1011	0.06997	0.06997	0.00000	0.00
1208	0.08331	0.08335	-0.00004	-0.05
1408	0.09687	0.09676	0.00011	0.12
1607	0.11003	0.10998	0.00005	0.04
1806	0.12301	0.12296	0.00005	0.04
2004	0.13563	0.13575	-0.00012	-0.09
2203	0.14829	0.14837	-0.00007	-0.05
2386	0.15986	0.15977	0.00009	0.05

TABLE III

COMPARISON OF EXPERIMENTAL AND LITERATURE
PHASE DENSITIES FOR PURE WATER AT 160°F

PRESSURE psia	PHASE DENSITIES, GM/CC EXPT'L	LIT	DIFFERENCE IN MEASURED DENSITY gm/cc	%DIFFERENCE
----------VAPOR DENSITY METER----------				
240	0.97614	0.97600	0.00013	0.01
412	0.97637	0.97654	-0.00017	-0.02
615	0.97709	0.97717	-0.00007	-0.01
825	0.97818	0.97782	0.00036	0.04
1016	0.97855	0.97841	0.00014	0.01
1219	0.97906	0.97903	0.00003	0.00
1403	0.97962	0.97960	0.00002	0.00
1612	0.98019	0.98024	-0.00004	0.00
1812	0.98081	0.98085	-0.00004	0.00
2010	0.98143	0.98145	-0.00002	0.00
2205	0.98205	0.98205	0.00000	0.00
2369	0.98258	0.98255	0.00003	0.00
----------LIQUID DENSITY METER----------				
242	0.97602	0.97601	0.00001	0.00
413	0.97655	0.97654	0.00000	0.00
618	0.97715	0.97718	-0.00003	0.00
826	0.97782	0.97782	0.00000	0.00
1016	0.97842	0.97841	0.00001	0.00
1219	0.97928	0.97903	0.00024	0.02
1403	0.97965	0.97960	0.00005	0.01
1612	0.98019	0.98024	-0.00005	-0.01
1812	0.98085	0.98085	0.00000	0.00
2010	0.98147	0.98145	0.00001	0.00
2205	0.98203	0.98205	-0.00002	0.00
2368	0.98256	0.98254	0.00001	0.00

TABLE IV

COMPARISON OF EXPERIMENTAL AND CALCULATED (NBS)
PHASE DENSITIES FOR PURE ETHANE AT 160°F

PRESSURE	PHASE DENSITIES,GM/CC		DIFFERENCE IN MEASURED DENSITY	
psia	EXPT'L	IUPAC	gm/cc	%DIFFERENCE
		VAPOR DENSITY METER		
215	0.01673	0.01704	-0.00031	-1.84
409	0.03456	0.03474	-0.00018	-0.52
779	0.08078	0.08203	-0.00125	-1.55
1215	0.18024	0.18044	-0.00020	-0.11
1813	0.28905	0.28665	0.00240	0.83
1997	0.30525	0.30391	0.00134	0.44
2207	0.31970	0.31865	0.00105	0.33
2396	0.33044	0.32993	0.00051	0.15
		LIQUID DENSITY METER		
215	0.01702	0.01704	-0.00002	-0.11
409	0.03475	0.03474	0.00001	0.04
778	0.08070	0.08195	-0.00125	-1.54
1215	0.17962	0.18044	-0.00082	-0.46
1813	0.28843	0.28665	0.00177	0.61
1997	0.30459	0.30391	0.00068	0.22
2207	0.31909	0.31865	0.00044	0.14
2397	0.32991	0.32998	-0.00007	-0.02

illustrated in Figure 4. In the figure, results are shown in terms of deviations from the NBS equation of state values. The comparisons cover a range of pressures up to 2400 psia. In general, the results presented in this work show very good agreement with the data of Reamer, with typical differences being 0.0004 gm/cc.

The gas chromatograph employed for compositional analyses utilized a thermal conductivity detector. In order to convert the area counts produced by the integrator to a composition, a response factor for the system of interest was determined. In the present work, the chromatograph response factor, RF, was determined in a manner identical to that employed in previous studies (36, 44). The response factor may be expressed mathematically by:

$$RF = (AR)N_2/N_1 \tag{3-3}$$

where: AR = area ratio of solute to solvent

N_1 = moles of solute in calibration mixture

N_2 = moles of solvent in calibration mixture

An estimate for the uncertainty in the RF due to uncertainties in AR, N_1 and N_2 is given by standard error propagation methods as:

$$(\varepsilon_{RF}/RF)^2 = (\varepsilon_{AR}/AR)^2 + (\varepsilon_{N_1}/N_1)^2 + (\varepsilon_{N_2}/N_2)^2 \tag{3-4}$$

where

ε_{RF} = uncertainty in RF

ε_{AR} = uncertainty in AR

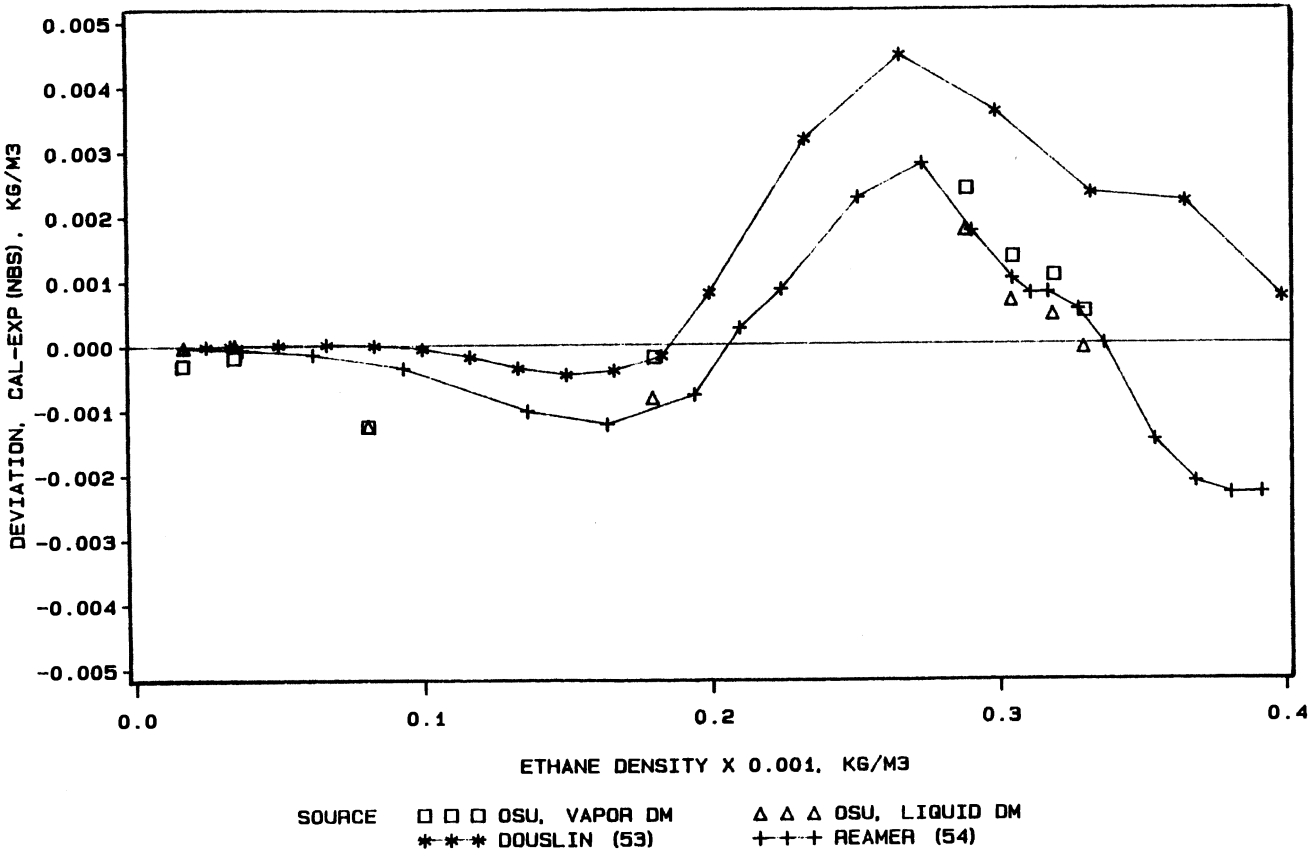

Figure 4. Predictions for Pure Ethane Densities @ 344.3 K (160°F) Using the National Bureau of Standards Equation of State (52)

ε_{N_1}, ε_{N_2} = uncertainty in N_1 and N_2, respectively

The method used to prepare a mixture for use in a chromatographic calibration employs a material balance to determine the composition of the calibration mixture, where the amount of each component in the mixture may be calculated by the following relations:

$$N_1 = \sum_{i=1}^{n_1} (\rho_1 V_1/MW_1)_i \tag{3-5}$$

$$N_2 = \sum_{i=1}^{n_i} (\rho_2 V_2/MW_2)_i \tag{3-6}$$

where

n_1, n_2 = number of solute or solvent injections, respectively

ρ_1, ρ_2 = solute or solvent density, respectively

V_1, V_2 = volume of injected solute or solvent, respectively

MW_1, MW_2 = solute or solvent molecular weight, respectively

By applying error propagation to Equations 3-5 and 3-6, the following uncertainties in N_1 and N_2 are obtained:

$$(\varepsilon_{N_1}/N_1)^2 = n_1 ((\varepsilon_{V_1}/V_1)^2 + (\varepsilon_{\rho_1}/\rho_1)^2) \tag{3-7}$$

$$(\varepsilon_{N_2}/N_2)^2 = n_2 ((\varepsilon_{V_2}/V_2)^2 + (\varepsilon_{\rho_2}/\rho_2)^2) \tag{3-8}$$

where

ε_{V_1}, ε_{V_2} = uncertainty in solute or solvent injected volumes, respectively

Figure 5 presents the results of RF determinations obtained for several mixtures of different compositions. Error bars are also given, based on the following assessment for the uncertainty in the input variables of Equation 3-4:

$$\varepsilon_{V_1} = 0.05 \text{ cc}$$
$$\varepsilon_{V_2} = 0.10 \text{ cc}$$
$$\varepsilon_{\rho_1} = \varepsilon_{\rho_2} = 0.003 \text{ gm/cc}$$
$$\varepsilon_{AR} = 0.005(AR)$$

A clear compositional dependence of the RF is indicated in Figure 5. Accordingly, weighted least squares regression was performed on these RF-x_{ethane} data. Weights for the data points were assigned according to Equations 3-4, 3-7 and 3-8. Figure 6 presents the weighted deviation plot resulting from the simple linear fit of the data given by:

$$RF = 0.431 - 0.055\ (x_{ethane}) \qquad (3\text{-}9)$$

Equation 3-9 describes the RF values with a standard deviation of 0.008 (1.3%).

Experimental Procedure

Once the measuring equipment had been calibrated and the system was

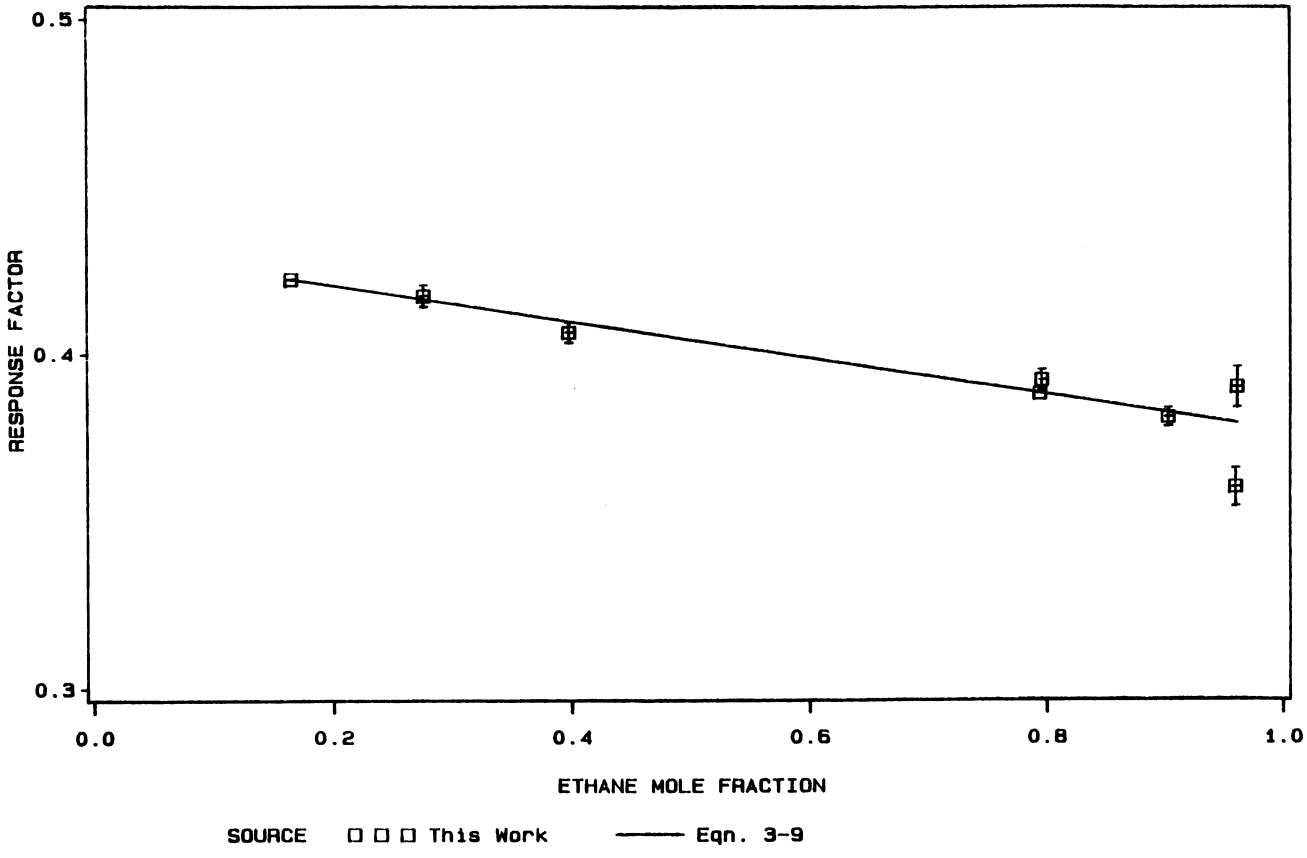

Figure 5. Response Factor Composition Dependence for the Ethane + trans-Decalin System @ 344.3 K (160°F)

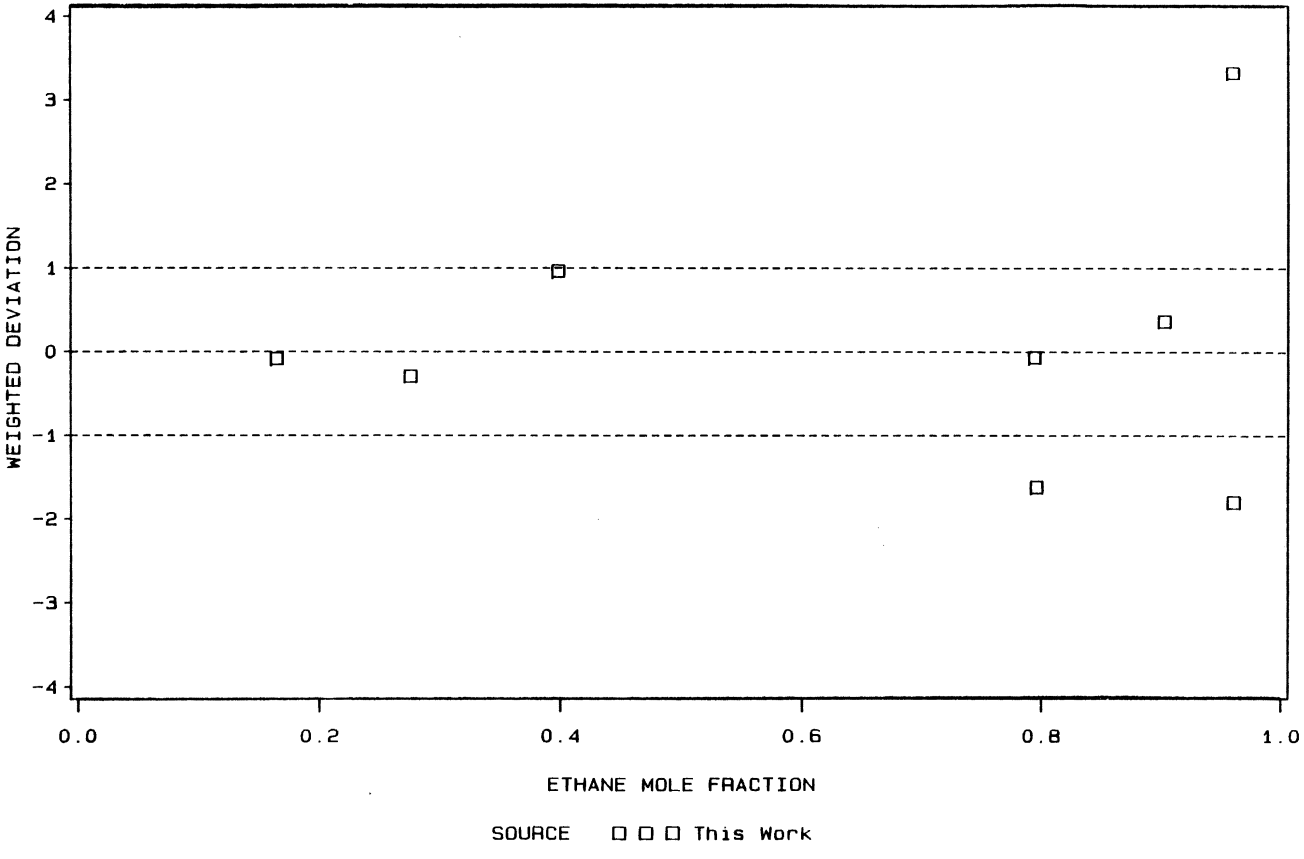

Figure 6. Response Factor Weighted Deviations for the Ethane + trans-Decalin System @ 344.3 K (160°F)

determined to be free of leaks, it was thoroughly cleaned using a solvent such as n-pentane or benzene pressurized with the solute gas, either CO_2 or ethane. After the system had been cleaned and purged with the solute gas, the system was evacuated. The system remained under vacuum until the time of injection, which was usually taken as one hour (or until the system pressure was $\leq$ 1 micrometer of mercury). The system was then heated and the appropriate temperature controllers were "fine tuned" to give a uniform temperature profile within the oven. After the desired temperature had been reached and sustained, the solvent (trans-Decalin) was injected into the system and the density and vapor pressure of the pure hydrocarbon were obtained. Usually enough hydrocarbon was injected to half-fill the 100 cc equilibrium (PVT) cell. The solute (ethane) was injected into the system using a manually operated Ruska positive displacement pump. The solute injection was used to established the desired pressure. The system was then placed in the vapor circulation pattern and allowed to reach equilibrium. The system was usually considered to be at equilibrium once the densitometer readings and system pressure became stable. This waiting period was usually 2 hours.

The current arrangement of the experimental apparatus permits adequate vapor and liquid circulation at pressures as low as 200 psia. The minimum pressure varies for each system and is related to the viscosity of the solvent. Data were gathered from the lowest pressure at which circulation was observed (209 psia) up to the critical point. For each pressure, the data acquisition sequence usually follows this order: vapor chromatograms are recorded, with the magnetic pump operating at a rate of 25 strokes/min (the stroke length is 4"), the

pump is then turned off and the vapor density is measured, circulation for the liquid is established and the liquid chromatograms are recorded, the pump is again turned off and the liquid density is recorded. Once the phase density and composition data have been recorded, a pendant drop is formed and photographed.

No effort was made to obtain densities and phase compositions at precisely the same pressure; therefore, changes in pressure between individual measurements were noted and indicated in the raw data presented, usually $\leq$ 5 psi from nominal measurement pressure. (Smoothed data are presented along with the raw data, as discussed in Chapter IV.)

The procedure for obtaining the photographs for the IFT determination begins by placing the system in the liquid circulation pattern. A low liquid level is established in the IFT cell so that a drop may be formed in the vapor atmosphere. Enough liquid is retained in the cell to ensure equilibrium between phases. By manipulating the two valves upstream of the cell, a liquid drop may be formed on the appropriate needle (or wire). The liquid is squeezed on to the tip of the needle (or wire) until the drop is pendant, meaning the drop is the largest that can be suspended on the tip of the needle (or wire). The drop is then photographed using the installed poloroid camera. Negatives from the photograph produced are then enlarged and measured, as described below.

A schematic diagram of the drop with the required measurements for analyses are shown in Figure 7, along with the contact angle, ϕ. The distance de is the equatorial diameter of the drop and the distance ds is the diameter measured a distance de up from the nadir of the drop.

The equation representing the curvature of the drop is given by

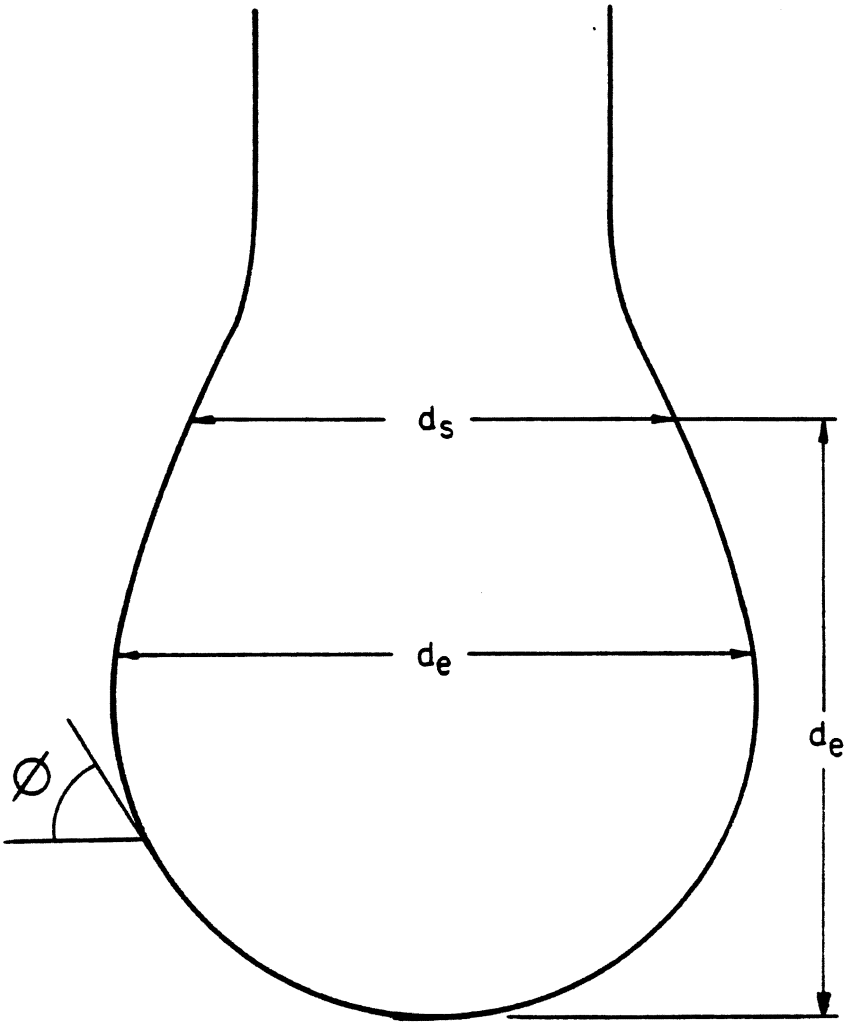

Figure 7. Profile of a Pendant Drop

Bashforth and Adams (48) and Laplace (55) as:

$$1/(R/b) + \sin(\phi)/(x/b) = 2 + (\beta)(y/b)$$

where R - radius of curvature at point (x, y)

b - radius of curvature at the vertex

ϕ - angle made by the tangent at (x, y) with the horizontal

$\beta = (\Delta\rho/\gamma)(gb^2)$

$\Delta\rho = \rho^L - \rho^V$

g - acceleration due to gravity

γ - interfacial tension

The quantity of interest is, of course, the interfacial tension, γ. The experimental method employed yeilds $\gamma/\Delta\rho$, not γ, directly from the measurements obtained in the laboratory. The $\gamma/\Delta\rho$ values may be found from the following relation:

$$\gamma/\Delta\rho = g\ (1/H)\ X_{de}^2 \qquad (3\text{-}11)$$

where $H = \beta(X_{de}/b)^2$

H is found from the relationship given by Bashforth and Adams (47):

$$1/H = f(S) = AS^{-2.644} + BS^2 + CS + D \qquad (3\text{-}12)$$

where A, B, C, D are constants and $S = x_{ds}/x_{de}$.

Since calculation of $\gamma/\Delta\rho$ requires a value for 1/H, it is convenient to use the tables presented by Mills (56) which present values for the shape parameter, H, for a given shape factor, S. Stegemeier (57) found that a plot of log (1/H) vs. log S is nearly linear. The approximate equation found by Stegemeier was:

$$1/H = 0.31270\ S^{-2.6444} \tag{3-13}$$

By implementing a method of least squares on the tabulated data presented by Mills the following equation was found during this work:

$$1/H = 0.31470\ S^{-2.62529} \tag{3-14}$$

with r^2 = correlation coefficient = 1.0000

From the standpoint of the data collected experimentally, the expression for $\gamma/\Delta\rho$ may be stated as:

$$\gamma/\Delta\rho = 308.406\ (X_{de}/X_{ds})^{-2.62529}\ X_{de}^2 \tag{3-15}$$

A comparison of the $\gamma/\Delta\rho$ values generated using a) the estimates for 1/H tabulated by Mills, b) the equation presented by Stegemeier, and c) the equation found during this work may be found in Table V.

After all required data have been gathered for a particular pressure, additional solute is injected into the system until the next desired pressure is obtained. The above procedure is repeated for all pressures of interest to the critical point. As the critical point is approached, the liquid and vapor properties approach equality and the

TABLE V

COMPARISON OF INTERFACIAL TENSION/DENSITY DIFFERENCE
CALCULATED USING 1/H FOUND FROM EQUATIONS AND
TABULATED VALUES FOR THE ETHANE +
TRANS-DECALIN SYSTEM AT 160°F

PRESSURE (PSIA)	TABULATED VALUE $\gamma/\Delta\rho$	STEGEMEIER EQ, $\gamma/\Delta\rho$	DEV.	THIS WORK EQ. $\gamma/\Delta\rho$	DEV.
486.0	15.3418	15.3161	-0.0257	15.3101	-0.0318
588.0	13.5433	13.5242	-0.0191	13.5214	-0.0219
682.0	11.4683	11.4560	-0.0123	11.4569	-0.0114
789.0	9.0759	9.0582	-0.0177	9.0623	-0.0137
837.0	7.9140	7.8972	-0.0167	7.9034	-0.0106
882.0	7.2314	7.2177	-0.0137	7.2229	-0.0085
937.0	5.9867	5.9742	-0.0125	5.9808	-0.0059
989.0	4.5058	4.4952	-0.0106	4.5036	-0.0021
1013.0	4.3136	4.3100	-0.0036	4.1051	-0.0085
1037.0	3.4838	3.4653	-0.0185	3.4621	-0.0217
1083.0	2.4042	2.4003	-0.0039	2.3999	-0.0043
1098.0	1.9367	1.8969	-0.0398	1.8974	-0.0394
1112.0	1.7685	1.7633	-0.0051	1.7635	-0.0050
1125.0	1.5812	1.5801	-0.0011	1.5799	-0.0013
1136.0	1.1706	1.1672	-0.0033	1.1681	-0.0025
1147.0	0.8454	0.8435	-0.0019	0.8447	-0.0006
1160.0	0.6010	0.5989	-0.0022	0.6000	-0.0010
1168.0	0.4998	0.4994	-0.0004	0.5004	0.0006
1177.0	0.2230	0.2224	-0.0006	0.2226	-0.0004
1182.0	0.1883	0.1872	-0.0012	0.1880	-0.0004
		AAPD = 0.0105		AAPD = 0.0096	

AAPD - ABSOLUTE AVERAGE PERCENT DEVIATION

interfacial tension tends toward zero. Thus, the distinction between the vapor and liquid phases diminishes. The visual interface in the PVT cell becomes harder to distinguish, and all data acquisition becomes difficult. Great care must be exercised during the collection of data in the near critical region, due to the increasing instability of the system. A visual observation of the critical point is always attempted. The critical point is usually characterized by a bright burst of orange to red color exhibited when the PVT cell is back-lighted with a white incandescent light bulb. Since this behavior is observed over a range as large as 5 psi, more credence is placed on the critical properties predicted by scaling law analyses. The application of scaling law analyses to the experimental data is discussed briefly in Chapter IV and in more detail by Robinson (58).

A sample of the forms used to record the data for a particular run, along with some forms used during other essential steps in the data acquisition, may be found in Appendix A.

Materials

The trans-Decalin used in this work was supplied by the Aldrich Chemical Company with a reported purity of 99+ mole %. The trans-Decalin was analyzed chromatographically in our laboratory and found to have a purity of 99.2 mole % (78). The ethane was supplied by Matheson with a stated purity of 99.9 mole %. No further purification of the chemicals was attempted.

CHAPTER IV

EXPERIMENTAL RESULTS AND DISCUSSION

Experimental data on equilibrium phase densities (ρ^L, ρ^V), phase compositions (x, y) and interfacial tensions (γ) for ethane + trans-Decalin have been measured at 160°F. The measurements cover the pressure range from approximately 200 psia to the critical point pressure (P_c = 1198 psia).

Eexperimental Data

The raw data appear in Table VI. In this table, values of $\gamma/\Delta\rho$ (rather than γ values) are presented since $\gamma/\Delta\rho$ is the quantity determined directly from the photographs obtained in the pendant drop IFT measurements. Also included in the table are equilibrium phase compositions and densities. The accuracy of the experimental data was estimated by Robinson, et al. (31, 58) as:

Composition (x, y), mole fraction:	±0.003
Densities (ρ^L,ρ^V), gm/cc:	±0.001
IFT (γ), mN/m:	±0.04 $\gamma^{0.8}$
Pressure (P), psi:	±2.0
Temperature (T), °F:	±0.1

For the IFT accuracy, multiple measurements by separate operators were

TABLE VI

EQUILIBRIUM PHASE DENSITIES, PHASE COMPOSITIONS AND INTERFACIAL TENSIONS FOR ETHANE + TRANS-DECALIN AT 344.3 K (160°F)

Phase Compositions, Mole Fraction Ethane				Phase Densities, $(kg/m^3) \times 10^{-3}$				IFT-Density Difference Ratio	
Liquid Phase		Vapor Phase		Liquid Phase					
Pressure, (psia)	x	Pressure, (psia)	y	Pressure, (psia)	ρ^L	Pressure (psia)	ρ^V	Pressure, (psia)	$\gamma/\Delta\rho \times 10^{-3}$ $(mN/m)/(kg/m^3)$
209	0.191	224	0.993	209	0.7958	209	0.0207		
298	0.263	305	0.994	298	0.7820	298	0.0275		
394	0.335	395	0.994	394	0.7644	394	0.0369		
499	0.415	499	0.994	499	0.7432	498	0.0451	499	15.6
601	0.485	601	0.994	601	0.7201	601	0.0581	601	13.2
696	0.549	694	0.993	696	0.6965	696	0.0719	695	11.1
801	0.614	802	0.993	801	0.6651	800	0.0887	801	8.79
849	0.645	850	0.993	849	0.6489	848	0.0979	849	7.92
894	0.675	893	0.993	894	0.319	893	0.1069	894	6.89
950	0.714	947	0.992	949	0.6083	948	0.1203	949	5.84
1000	0.745	998	0.991	1001	0.5825	1000	0.1351	1001	4.30
1025	0.764	1022	0.991	1024	0.5696	1023	0.1427	1024	4.17
1048	0.781	1046	0.990	1049	0.5548	1048	0.1520	1049	3.49
1071	0.799	1068	0.990	1070	0.5406	1069	0.1609	1071	2.92
1094	0.817	1092	0.989	1094	0.5232	1092	0.1711	1094	2.40
1109	0.830	1098	0.989	1109	0.5109	1107	0.1795	1109	2.07
1118	0.836	1107	0.989	1123	0.504	1116	0.1856	1123	1.85
1122	0.838	1118	0.988	1131	0.4923	1130	0.1935	1131	1.73
1130	0.844	1130	0.988	1136	0.4859	1135	0.1969	1137	1.50
1136	0.850	1138	0.988	1148	0.4729	1147	0.2061	1148	1.23
1148	0.862	1147	0.988	1158	0.4588	1157	0.2161	1158	0.966
1158	0.870	1158	0.987	1172	0.4386	1171	0.2310	1172	0.600
1172	0.884	1178	0.985	1183	0.4167	1182	0.2505	1180	0.504
1184	0.897	1182	0.987			1188	0.2623	1188	0.254
1191	0.906	1186	0.985						

performed on each pendant drop photograph, plus multiple photographs were used to calculate the maximum deviations from the mean value of the IFT for each data point. These deviations are well represented by the expression shown above for the IFT.

The experimental phase densities, phase compositions, and $\gamma/\Delta\rho$ values are illustrated in Figures 8-10, respectively. The $\gamma/\Delta\rho$ values are plotted as a function of "scaled" pressure (P_c-P/P_c) because this conveniently expands the near-critical, low-IFT region and because "scaling laws" require that this relationship become linear (log-log plot) as the critical pressure is approached. The slope of the line should be a specific, system independent universal value of $2\nu-\beta = 0.93$ (59). The data presented in this work show good agreement with scaling law behavior over the entire pressure range covered. Scaling behavior has been confirmed for fluids approaching the critical point by both experimental and theoretical investigations (60). The scaling law behavior for both mixtures and pure compounds suggests that all fluids obey certain general relationships in the near-critical region, and some of the parameters in these relationships are independent of the particular system studied. The following relationship for $\gamma/\Delta\rho$ is suggested for the near-critical region:

$$\gamma/\Delta\rho = A(P^*)^{2\nu-\beta}$$

where A is a constant for the specific system of interest and ν and β are system independent universal scaling exponents ($\nu = 0.63$ and $\beta = 0.32$ (59)).

As shown in Table VI, the experimental data (x, y, ρ^L, ρ^V, $\gamma/\Delta\rho$)

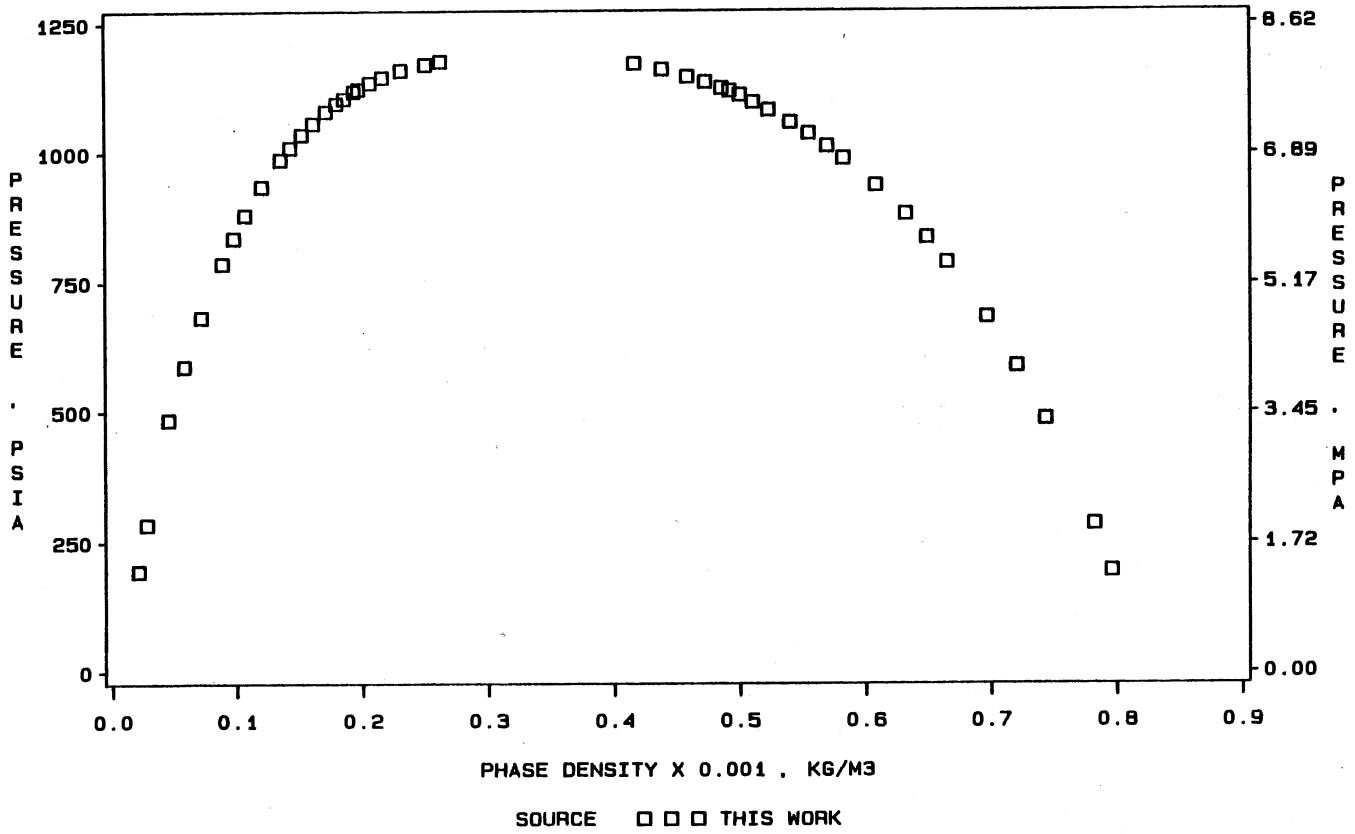

Figure 8. Phase Density Data for the Ethane + trans-Decalin System @ 344.3 K (160°F)

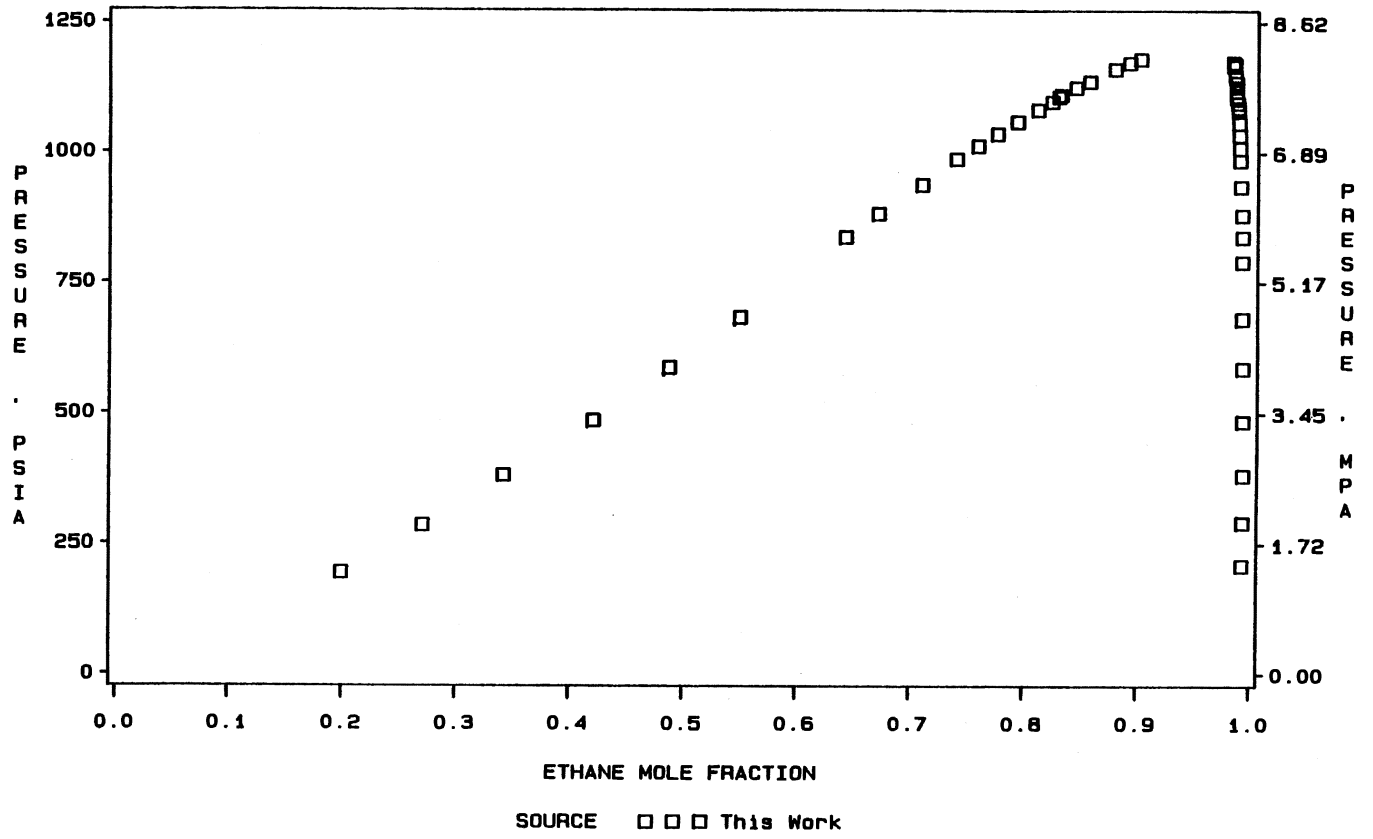

Figure 9. Phase Composition Data for the Ethane + trans-Decalin System @ 344.3 K (160°F)

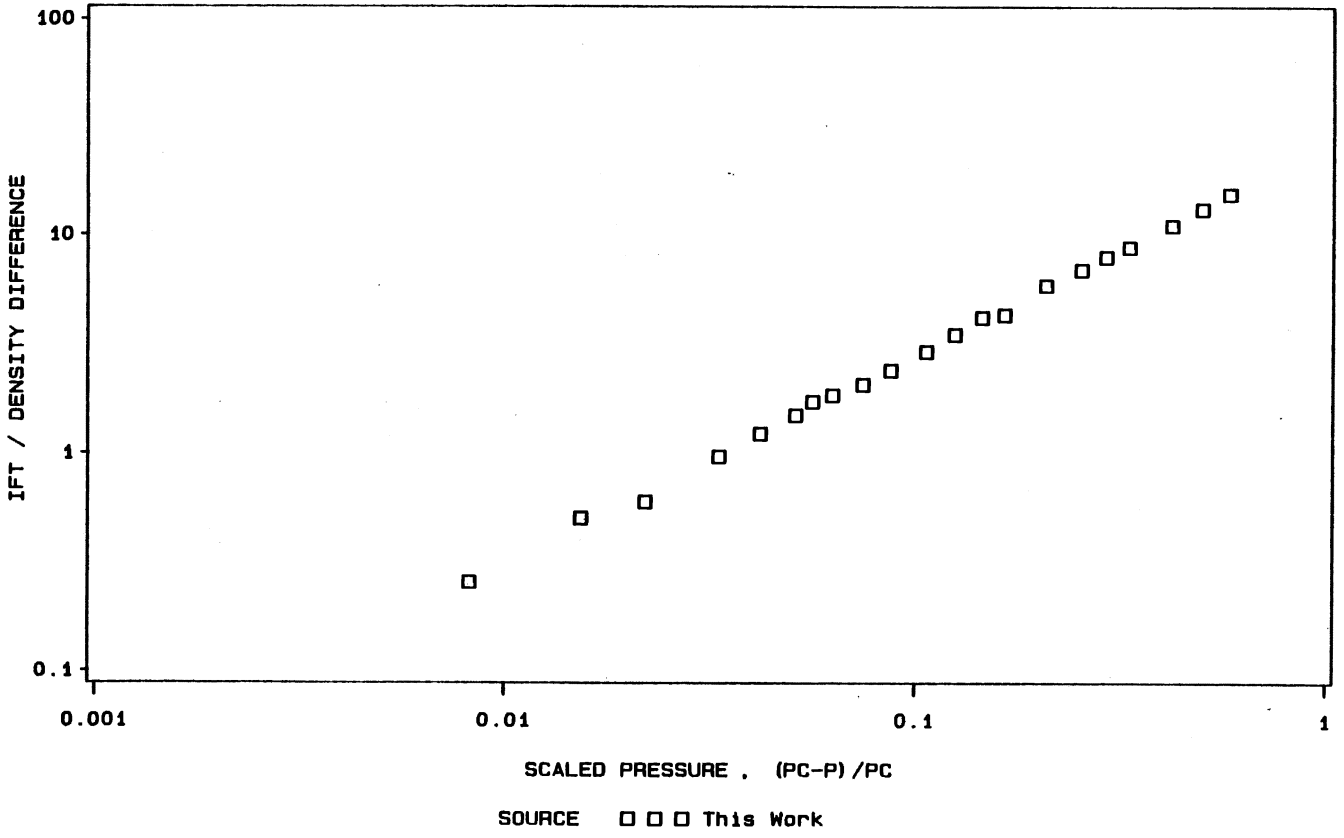

Figure 10. Pendant Drop Data for the Ethane + trans-Decalin System @ 344.3 K (160°F)

were not measured at precisely the same pressure for a given equilibrium condition. This was convenient for the operators from a practical sense. However, for the convenience of users of the data and to facilitate the use of the data, smoothed and interpolated results are presented in Table VII. The smoothed data retain the full stated accuracy of the raw data.

Table VII contains an estimate of the critical-point pressure, composition, and density for ethane + trans-Decalin at 160°F. These estimates are the values which produced optimum representation of the phase properties from the smoothing functions. The critical pressure (1198 psia) is in excellent agreement with the value from repeated visual observations in the equilibrium cell (1198 ± 5 psi). The extrapolated values (beyond the highest measured pressures) shown in parentheses in Table VII are believed to be reliable since these values are in the near-critical power-law region, which is correctly described by the formulae. However, the formulae are not suitable for extrapolations to pressures lower than those given in Table VII. The smoothing procedure is outlined below.

Smoothing Functions for Phase Properties

Experimental measurements on the subject apparatus are performed much more easily and efficiently if the individual properties (x, y, ρ^L, ρ^V and $\gamma/\Delta\rho$) are each obtained at a slightly different pressure (e.g., ± 5 psi from the "nominal" pressure of interest). Such a procedure eliminates the tedious adjustments of pressure between each individual measurement. Although this is convenient from an experimental standpoint, the resultant data are not in an optimum form for users of

TABLE VII

SMOOTHED PHASE EQUILIBRIA AND INTERFACIAL TENSIONS
FOR ETHANE + TRANS-DECALIN at 344.3 K (160°F)

Pressure		Phase Compositions, Mole Fraction Ethane		Phase Densities, $(kg/m^3) \times 10^{-3}$		Interfacial Tension,
kPa	psia	Liquid	Vapor	Liquid	Vapor	mN/m
1379	200	0.184	0.993	0.7966	0.0201	17.2
2068	300	0.264	0.994	0.7821	0.0274	15.0
2758	400	0.341	0.994	0.7631	0.0353	12.9
3447	500	0.415	0.994	0.7426	0.0456	10.8
4137	600	0.485	0.994	0.7206	0.0580	8.81
4826	700	0.551	0.993	0.6956	0.0723	6.92
5516	800	0.615	0.993	0.6658	0.0886	5.14
6205	900	0.679	0.993	0.6292	0.1087	3.50
6895	1000	0.746	0.991	0.5829	0.1354	2.03
7584	1100	0.821	0.989	0.5190	0.1755	0.792
7653	1110	0.829	0.989	0.5107	0.1810	0.686
7722	1120	0.838	0.988	0.5018	0.1870	0.584
7791	1130	0.846	0.988	0.4923	0.1936	0.486
7860	1140	0.854	0.988	0.4818	0.2009	0.393
7929	1150	0.863	0.988	0.4702	0.2093	0.306
7998	1160	0.872	0.987	0.4571	0.2190	0.224
8067	1170	0.881	0.987	0.4417	0.2309	0.148
8136	1180	0.892	0.986	0.4226	0.2463	0.082
8150	1182	0.894	0.986	0.4181	0.2500	0.070
8163	1184	0.896	0.985	(0.4133)	0.2541	0.058
8177	1186	0.899	0.985	(0.4080)	0.2586	0.047
8191	1188	0.902	0.984	(0.4023)	0.2636	0.037
8205	1190	0.905	0.983	(0.3958)	0.2692	(0.028)
8219	1192	(0.909)*	(0.982)	(0.3884)	(0.2758)	(0.019)
8232	1194	(0.913)	(0.980)	(0.3795)	(0.2840)	(0.011)
8246	1196	(0.920)	(0.976)	(0.3675)	(0.2951)	(0.004)
8260**	1198	(0.950)	(0.950)	(0.3309)	(0.3309)	(0.000)

*Numbers in parentheses are extrapolations beyond highest measured pressures.

**Estimated critical point (visual observations gave 1198 ± 5 psia for the critical pressure).

the data. Thus, formulae have been employed for interpolation and extrapolation of the measured values so that the results can be presented in a more directly usable form. Such formulae, to be of value, should (a) represent the data within their experimental uncertainties and (b) obey known power law behavior as the critical point is approached. The functions used herein (and described below) have been found to fulfill these requirements. These procedures were used in work done previously by Robinson, et al. (33, 36) and are reproduced here for the sake of completeness.

Wichterle, et al. (61) and Charoensombut-amon (62) employed functions of the type shown below to represent the difference between an "order parameter, ϕ", in two equilibrium phases (denoted by "+" and "-"):

$$\phi_+ - \phi_- = \sum_{i=0}^{N} B_i \, (P^*)^{\beta+i\Delta} \qquad (4\text{-}1)$$

where the lead (i = 0) is the limiting "power (scaling) law" behavior of the order parameter, ϕ, and the subsequent terms in the summation are corrections to the scaling behavior as given by Wegner (63).

If the above relation is coupled with an equation for the "rectilinear diameter" of the form:

$$\frac{(\phi_+ + \phi_-)}{2} = \phi_c + A_o \, (P^*)^{1-\alpha} + \sum_{j=1}^{m} A_j \, (P^*)^j \qquad (4\text{-}2)$$

then these expressions may be combined to yield ϕ_+ and ϕ_- individually as:

$$\phi_{\pm} = \phi_c + A_o (P^*)^{1-\alpha} + \sum_{j=1}^{M} A_j (P^*)^j \pm \frac{1}{2} \sum_{i=1}^{N} B_i (P^*)^{\beta+i\Delta} \qquad (4\text{-}3)$$

where $\phi_+ = \phi^L$, $\phi_- = \phi^V$. The real value of the above formalism is that the exponents α, β, and Δ are universal constants, independent of the fluid of interest. An approach similar to the above has been discussed by Nagarajan (64).

Charoensombut-amon used Equation 4-3 to fit isothermal P-x,y data ($\phi_+ = y$, $\phi_- = x$) for ethane + n-hexadecane using $\beta = 1/3$, $\alpha = 1/8$, $\Delta = 1/2$, M = 3, N = 6, for a total of 12 constants (z_c included).

In the present work, Equation 4-3 has been used to represent the P vs ρ^L, ρ^V and P vs x, y behavior with

for P - ρ^L, ρ^V : $\phi_c = \rho_c$, $\phi_+ = \rho^L$, $\phi_- = \rho^V$, M=6, N=6

for P - x, y : $\phi_c = z_c$, $\phi_+ = y$, $\phi_- = x$, M=6, N=6

The values of $\gamma/\Delta\rho$ (which are the quantities determined from measurements of the pendant drop photographs) were expressed as

$$\gamma/\Delta\rho = \sum_{K=0}^{L} G_i (P^*)^{2\nu-\beta+K\Delta} \qquad (4\text{-}4)$$

with L = 1 (i.e., one correction-to-scaling term).

In the regressions employed to fit the above expressions to the experimental data, various values of M, N and L were studied to determine the minimum number of terms required to represent the data accurately. In addition, the values for P_c and for the critical

exponents were varied. The calculations were insensitive to the exponents over their accepted ranges (e.g., 0.325 (59) to 0.355 (60) for β, so the simple values of $\beta = 1/3$ and $\alpha = 1/8$ by Charoensombut-amon were used, as was the generally accepted value of $\nu = 0.63$. Calculations were more sensitive to P_c.

Smoothed Experimental Data

The optimum (integer) value of P_c to fit all data (density, composition and IFT-density difference ratio), from the ethane + trans-Decalin system, simultaneously was found to be 1198 psia. Tables VIII, IX, and X document the abilities of the equations to all of the experimental data. The parameters used to smooth the data appear in Table XI. These results are based on weighted regressions of the data, i.e., the sum of squares of weighted residuals (SS) was minimized:

$$SS = \sum_{i=1}^{K} [(Y^{Calc} - Y^{Exp})/\sigma_Y]_i^2 = \sum_{i=1}^{K} (\Delta Y/\sigma_Y)_i^2 \qquad (4\text{-}5)$$

where K is the number of experimental observations and

$$\sigma_Y^2 = \varepsilon_Y^2 + (\partial Y/\partial P)^2 \, \varepsilon_P^2 \qquad (4\text{-}6)$$

Y denotes the compositions (x, y), densities (ρ^L, ρ^V) or IFT-to-density difference ratio ($\gamma/\Delta\rho$). The experimental uncertainties, ε, were taken to be the following in the regressions:

TABLE VIII

COMPARISON OF EXPERIMENTAL AND CALCULATED (EQN. 4-3)
PHASE DENSITIES FOR ETHANE + TRANS-DECALIN AT 160°F

PRESSURE psia	Scaled Press., (PC-P)/PC	PHASE DENSITIES, GM/CC EXPT'L	CALC'D	ERROR IN CALCULATED DENSITY GM/CC	%	WTD	WEIGHTING FACTOR, GM/CC
			LIQUID PHASE				
208.7	0.826	0.7958	0.7957	-0.00014	-0.02	-0.69	0.00021
298.4	0.751	0.7820	0.7823	0.00039	0.05	1.76	0.00022
394.1	0.671	0.7644	0.7643	-0.00016	-0.02	-0.71	0.00022
499.3	0.583	0.7432	0.7428	-0.00041	-0.05	-1.81	0.00023
601.0	0.498	0.7201	0.7204	0.00023	0.03	0.99	0.00023
695.7	0.419	0.6965	0.6967	0.00024	0.03	0.98	0.00024
801.4	0.331	0.6650	0.6653	0.00026	0.04	1.00	0.00026
849.2	0.291	0.6489	0.6487	-0.00016	-0.03	-0.61	0.00027
894.1	0.254	0.6319	0.6316	-0.00036	-0.06	-1.26	0.00028
948.9	0.208	0.6082	0.6080	-0.00021	-0.03	-0.68	0.00030
1000.7	0.165	0.5825	0.5825	0.00002	0.00	0.07	0.00033
1024.2	0.145	0.5696	0.5697	0.00003	0.01	0.08	0.00035
1049.1	0.124	0.5548	0.5548	-0.00001	0.00	-0.02	0.00037
1070.0	0.107	0.5406	0.5411	0.00053	0.10	1.33	0.00040
1094.0	0.087	0.5232	0.5237	0.00050	0.10	1.15	0.00044
1108.9	0.074	0.5109	0.5116	0.00075	0.15	1.60	0.00047
1122.9	0.063	0.5004	0.4992	-0.00122	-0.24	-2.39	0.00051
1130.8	0.056	0.4923	0.4914	-0.00088	-0.18	-1.63	0.00054
1136.3	0.051	0.4859	0.4858	-0.00015	-0.03	-0.27	0.00056
1147.8	0.042	0.4729	0.4729	0.00003	0.01	0.05	0.00063
1158.3	0.033	0.4588	0.4595	0.00070	0.15	0.97	0.00072
1171.7	0.022	0.4386	0.4388	0.00021	0.05	0.23	0.00090
1182.7	0.013	0.4167	0.4165	-0.00018	-0.04	-0.15	0.00121

TABLE VIII (continued)

PRESSURE psia	Scaled Press., (PC-P)/PC	PHASE DENSITIES, GM/CC EXPT'L	CALC'D	ERROR IN CALCULATED DENSITY GM/CC	%	WTD	WEIGHTING FACTOR, GM/CC
			VAPOR PHASE				
208.7	0.826	0.0207	0.0208	0.00009	0.43	0.44	0.00020
298.4	0.751	0.0275	0.0273	-0.00021	-0.76	-1.03	0.00020
498.3	0.584	0.0451	0.0454	0.00024	0.54	1.17	0.00021
601.0	0.498	0.0581	0.0581	0.00008	0.14	0.37	0.00021
695.7	0.419	0.0718	0.0716	-0.00025	-0.34	-1.16	0.00021
799.9	0.332	0.0887	0.0886	-0.00010	-0.11	-0.44	0.00022
848.2	0.292	0.0979	0.0977	-0.00023	-0.24	-1.05	0.00022
893.1	0.255	0.1069	0.1071	0.00028	0.26	1.23	0.00023
947.9	0.209	0.1203	0.1204	0.00011	0.09	0.4?	0.00024
999.7	0.165	0.1351	0.1353	0.00016	0.12	0.64	0.00025
1022.7	0.146	0.1427	0.1429	0.00016	0.11	0.61	0.00026
1047.6	0.126	0.1520	0.1520	-0.00001	0.00	-0.02	0.00028
1069.0	0.108	0.1609	0.1607	-0.00016	-0.10	-0.54	0.00029
1092.0	0.089	0.1711	0.1714	0.00030	0.17	0.92	0.00032
1106.9	0.076	0.1795	0.1793	-0.00028	-0.16	-0.82	0.00034
1116.4	0.068	0.1856	0.1848	-0.00086	-0.46	-2.37	0.00036
1129.8	0.057	0.1935	0.1935	-0.00005	-0.02	-0.11	0.00040
1134.8	0.053	0.1969	0.1970	0.00012	0.06	0.29	0.00042
1146.8	0.043	0.2061	0.2065	0.00033	0.16	0.70	0.00047
1157.3	0.034	0.2161	0.2162	0.00013	0.06	0.23	0.00054
1170.7	0.023	0.2310	0.2319	0.00083	0.36	1.17	0.00071
1181.7	0.014	0.2505	0.2494	-0.00108	-0.43	-1.10	0.00098
1187.7	0.009	0.2623	0.2627	0.00038	0.15	0.29	0.00131

TABLE IX

COMPARISON OF EXPERIMENTAL AND CALCULATED (EQN. 4-3) FOR PHASE COMPOSITIONS FOR ETHANE + TRANS-DECALIN AT 160° F

PRESSURE psia	Scaled Press., (PC-P)/PC	PHASE DENSITIES, GM/CC EXPT'L	CALC'D	ERROR IN CALCULATED DENSITY GM/CC	WTD	WEIGHTING FACTOR
			LIQUID PHASE			
208.7	0.826	0.1911	0.1912	0.00008	0.10	0.00081
298.4	0.751	0.2630	0.2624	-0.00059	-0.74	0.00080
394.1	0.671	0.3353	0.3366	0.00131	1.65	0.00080
499.3	0.583	0.4155	0.4144	-0.00115	-1.47	0.00079
601.0	0.498	0.4847	0.4853	0.00061	0.78	0.00078
695.7	0.419	0.5491	0.5479	-0.00122	-1.58	0.00077
801.4	0.331	0.6142	0.6154	0.00124	1.61	0.00077
849.2	0.291	0.6451	0.6459	0.00076	0.98	0.00077
894.1	0.254	0.6747	0.6749	0.00012	0.15	0.00077
949.9	0.207	0.7140	0.7119	-0.00212	-2.72	0.00078
999.7	0.165	0.7450	0.7463	0.00128	1.63	0.00078
1025.2	0.144	0.7643	0.7645	0.00020	0.25	0.00079
1047.6	0.126	0.7814	0.7810	-0.00040	-0.50	0.00079
1070.5	0.106	0.7990	0.7984	-0.00067	-0.84	0.00080
1093.5	0.087	0.8172	0.8162	-0.00095	-1.19	0.00080
1108.9	0.074	0.8296	0.8286	-0.00102	-1.26	0.00081
1117.9	0.067	0.8356	0.8359	0.00028	0.35	0.00081
1121.9	0.064	0.8376	0.8392	0.00158	1.95	0.00081
1129.8	0.057	0.8440	0.8458	0.00185	2.26	0.00082
1136.3	0.051	0.8504	0.8513	0.00093	1.13	0.00082
1147.8	0.042	0.8624	0.8611	-0.00125	-1.51	0.00082
1157.8	0.034	0.8698	0.8700	0.00019	0.23	0.00083
1171.7	0.022	0.8843	0.8831	-0.00120	-1.40	0.00086
1183.7	0.012	0.8968	0.8961	-0.00075	-0.81	0.00093
1191.2	0.006	0.9062	0.9069	0.00078	0.68	0.00115

TABLE IX (Continued)

PRESSURE psia	Scaled Press., (PC-P)/PC	PHASE DENSITIES, GM/CC EXPT'L	CALC'D	ERROR IN CALCULATED DENSITY GM/CC	WTD	WEIGHTING FACTOR GM/CC
			VAPOR PHASE			
223.7	0.813	0.9930	0.9931	0.00010	0.15	0.00070
305.4	0.745	0.9939	0.9938	-0.00014	-0.20	0.00070
394.6	0.671	0.9943	0.9942	-0.00015	-0.21	0.00070
498.8	0.584	0.9940	0.9941	0.00017	0.24	0.00070
600.5	0.499	0.9936	0.9938	0.00015	0.21	0.00070
694.2	0.421	0.9933	0.9934	0.00016	0.23	0.00070
802.4	0.330	0.9933	0.9931	-0.00023	-0.33	0.00070
849.7	0.291	0.9934	0.9929	-0.00047	-0.67	0.00070
892.6	0.255	0.9930	0.9927	-0.00027	-0.39	0.00070
947.4	0.209	0.9916	0.9922	0.00058	0.82	0.00070
997.8	0.167	0.9911	0.9915	0.00039	0.56	0.00070
1021.7	0.147	0.9908	0.9910	0.00021	0.31	0.00070
1046.1	0.127	0.9903	0.9904	0.00011	0.15	0.00070
1068.0	0.108	0.9901	0.9898	-0.00024	-0.35	0.00070
1091.5	0.089	0.9895	0.9891	-0.00039	-0.56	0.00070
1097.9	0.084	0.9894	0.9889	-0.00045	-0.64	0.00070
1106.9	0.076	0.9889	0.9887	-0.00021	-0.30	0.00070
1117.9	0.067	0.9878	0.9884	0.00053	0.76	0.00070
1129.8	0.057	0.9879	0.9880	0.00009	0.13	0.00070
1137.8	0.050	0.9877	0.9878	0.00009	0.13	0.00070
1146.8	0.043	0.9882	0.9876	-0.00056	-0.79	0.00070
1157.6	0.034	0.9869	0.9873	0.00049	0.69	0.00070
1178.2	0.017	0.9854	0.9863	0.00092	1.31	0.00070
1182.2	0.013	0.9866	0.9858	-0.00074	-1.05	0.00070
1185.7	0.010	0.9853	0.9851	-0.00021	-0.29	0.00071

TABLE X

COMPARISON OF EXPERIMENTAL AND CALCULATED (EQN. 4-3) IFT-TO-DENSITY DIFFERENCE RATIO FOR ETHANE + TRANS-DECALIN AT 160°F

PRESSURE PSIA	P* (PC-P)/PC	IFT-TO-DENSITY RATIO EXPT'L	IFT-TO-DENSITY RATIO CALC'D	ERROR IN CALCULATED IFT RATIO DEV	ERROR IN CALCULATED IFT RATIO %DEV	ERROR IN CALCULATED IFT RATIO WTD	WEIGHTING FACTOR,
499.3	0.583	15.605	15.520	-0.0853	-0.55	-0.25	0.343
601.0	0.498	13.239	13.281	0.0414	0.31	0.14	0.300
694.7	0.420	11.072	11.222	0.1503	1.36	0.58	0.260
801.4	0.331	8.787	8.884	0.0973	1.11	0.45	0.215
849.2	0.291	7.923	7.835	-0.0878	-1.11	-0.44	0.198
894.1	0.254	6.890	6.852	-0.0377	-0.55	-0.21	0.177
948.9	0.208	5.844	5.649	-0.1946	-3.33	-1.26	0.155
1000.7	0.165	4.296	4.509	0.2127	4.95	1.76	0.121
1024.2	0.145	4.171	3.992	-0.1794	-4.30	-1.52	0.118
1049.1	0.124	3.485	3.440	-0.0447	-1.28	-0.44	0.102
1071.0	0.106	2.921	2.953	0.0318	1.09	0.36	0.089
1094.0	0.087	2.403	2.441	0.0381	1.59	0.50	0.076
1108.9	0.074	2.070	2.106	0.0356	1.72	0.53	0.068
1122.9	0.063	1.850	1.790	-0.0593	-3.21	-0.96	0.062
1130.8	0.056	1.727	1.609	-0.1176	-6.81	-2.00	0.059
1136.8	0.051	1.500	1.473	-0.0266	-1.78	-0.51	0.053
1147.8	0.042	1.231	1.222	-0.0094	-0.76	-0.21	0.045
1158.3	0.033	0.966	0.979	0.0135	1.39	0.36	0.038
1171.7	0.022	0.600	0.663	0.0635	10.58	2.33	0.027
1179.7	0.015	0.504	0.472	-0.0316	-6.28	-1.29	0.024
1188.2	0.008	0.254	0.264	0.0099	3.88	0.58	0.017

TABLE XI

PARAMETERS USED IN EQUATIONS 4-3 and 4-4 TO GENERATE SMOOTHED PROPERTIES IN TABLES VII, VIII, IX AND X

PHASE COMPOSITIONS
Units: Mole Fraction Ethane

ZC	0.94950718
A0	-0.52458749
A1	0.18719338
A2	-0.20708827
A3	0.87582785
A4	-1.84897196
A5	1.45940788
A6	-0.38128969
B0	0.56625465
B1	-2.65276972
B2	11.68046473
B3	-20.63394725
B4	17.06352645
B5	-4.36393238
B6	-0.70023962

PHASE DENSITIES
Units: $(kg/m^3) \times 10^{-3}$ or (gm/cc)

RHOC	0.33090589
A0	-0.00794199
A1	0.26125975
A2	-0.81394605
A3	2.80572393
A4	-5.97227830
A5	6.35288321
A6	-2.58254408
B0	0.52102724
B1	2.61035460
B2	-11.41815060
B3	29.32312098
B4	-42.46822502
B5	31.84874738
B6	-9.62279970

IFT-DENSITY DIFFERENCE RATIO
Units: $[(mN/m)/(kg/m^3)] \times 10^{-3}$ or [(mN/m)/(gm/cc)]

G0	22.18905052
G1	4.43956953

$$\varepsilon_x = \varepsilon_y = 0.0007$$

$$\varepsilon_\rho^L = \varepsilon_\rho^V = 0.0002 \text{ gm/cc}$$

$$\varepsilon_{\gamma/\Delta\rho} = 0.037\ (\gamma/\Delta\rho)^{0.8}$$

$$\varepsilon_p = 0.5 \text{ psi}$$

(Note: The above are measures of precision, rather than accuracy, of the measurements. Estimated inaccuracies are generally larger than these values.)

The final values for the properties given in Tables VIII, IX, and X were determined as follows. First, regressions were performed with all measured data points included and the results were analyzed. Next, those data points having weighted deviation, $\Delta Y/\sigma_Y$ larger than 2.5 were discarded, and the final regressions were performed on the reduced data sets.

This procedure resulted in deletion of two data points: one vapor density (394 psia) and one liquid composition (950 psia).

If the assigned values for the experimental uncertainties are correct, the weighted-root-mean-square deviations, (WRMS) should be near 1.0. For the present cases, the WRMS values are 1.0 for density, 1.0 for composition and 1.0 for $\gamma/\Delta\rho$. This suggests that reasonable values for uncertainties have been used in the regressions. The final RMS residuals (unweighted) are 0.00042 gm/cc for densities, 0.00079 in mole fraction for compositions and 0.096 (mN/m)/(gm/cc) or 2.8% for $\gamma/\Delta\rho$. The residuals in Tables VIII, IX, and X retain some systematic behavior; however, the magnitudes of these residuals are generally within the experimental expectations. Figure 11 shows the fit of Equation 4-4 to the pendant drop data, using the parameters from Table XI. The weighted residuals for each of the measured properties are illustrated in Figures

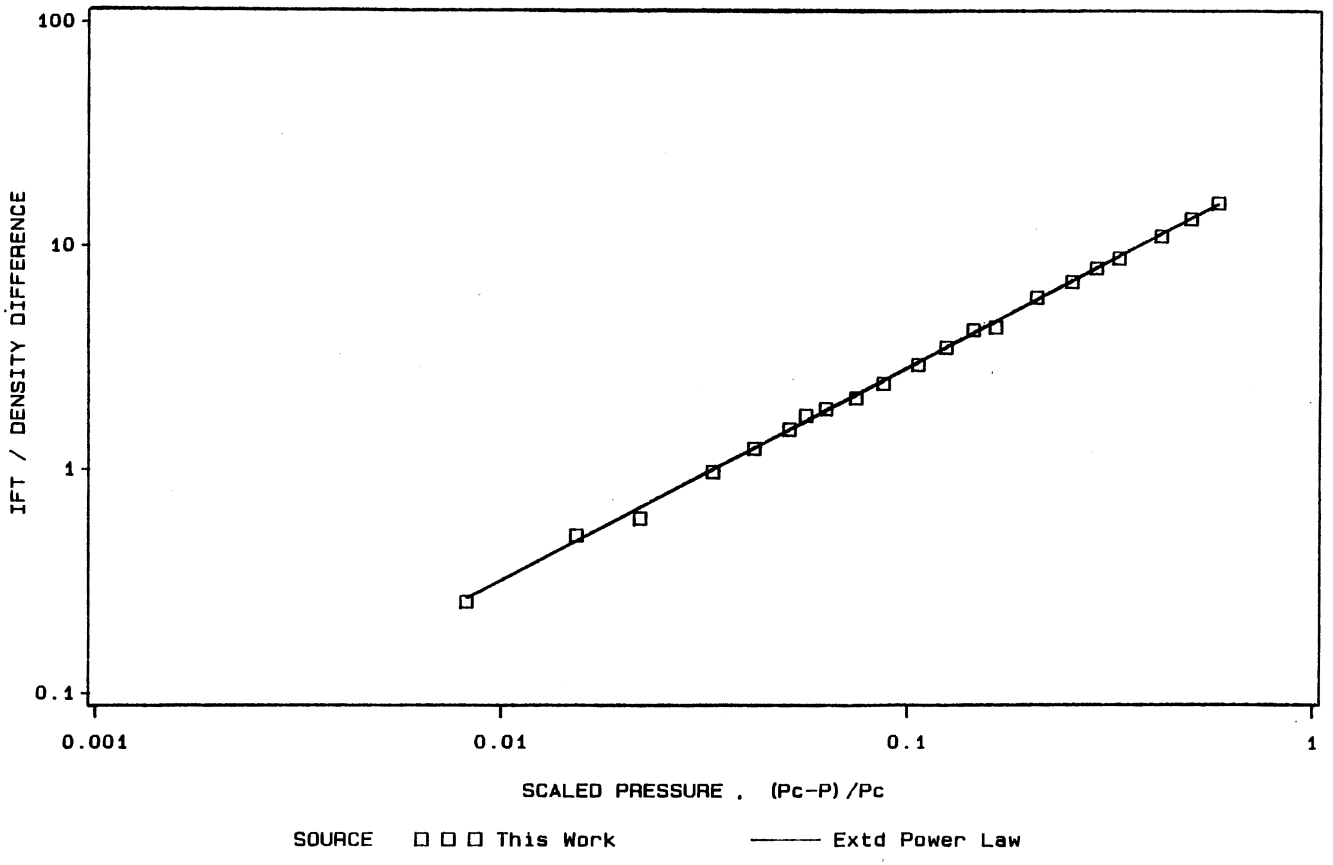

Figure 11. Extended Power Law Behavior of Pendant Drop Data for Ethane + trans-Decalin @ 344.3 K (160°F)

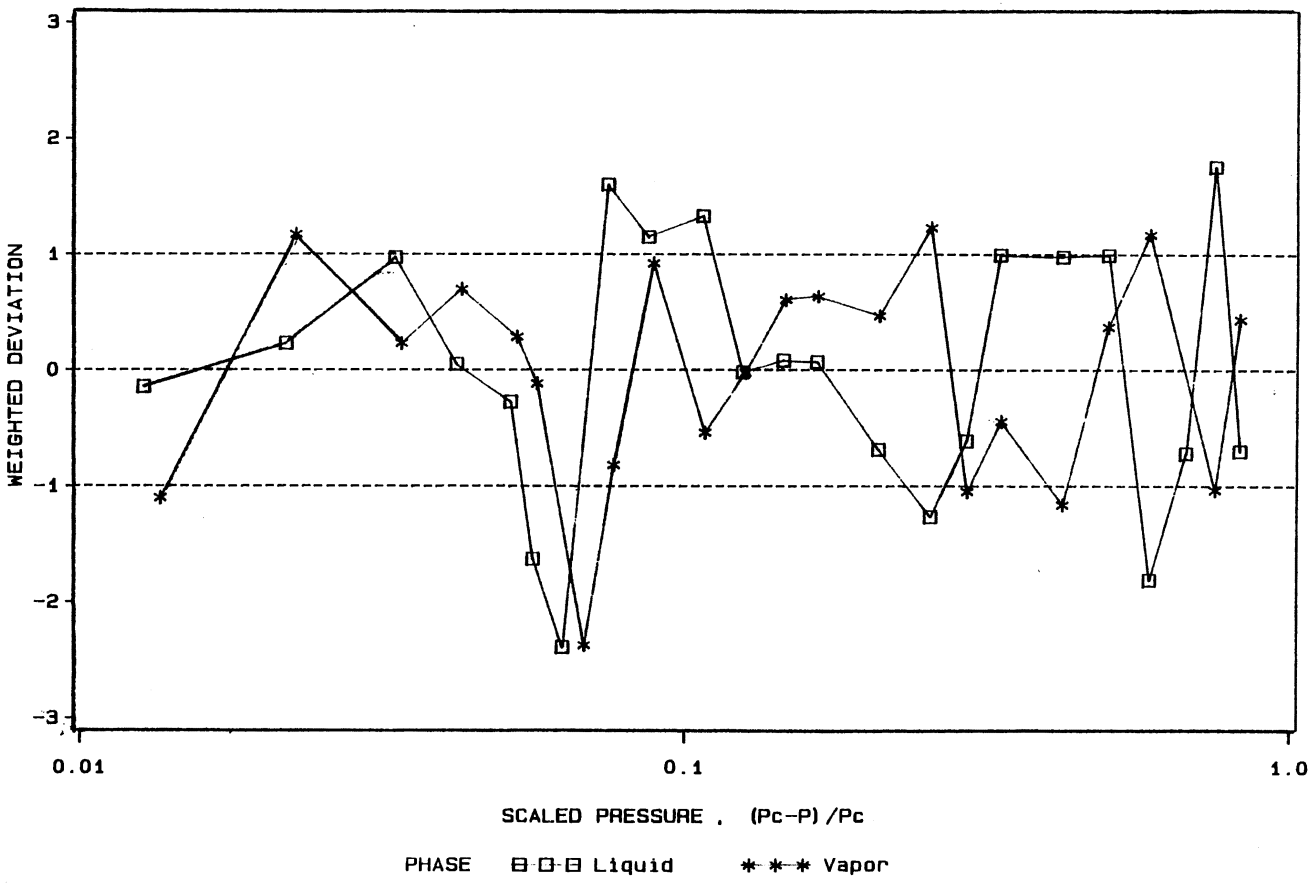

Figure 12. Extended Power Law Fit to Density Data for Ethane + trans-Decalin @ 344.3 K (160°F)

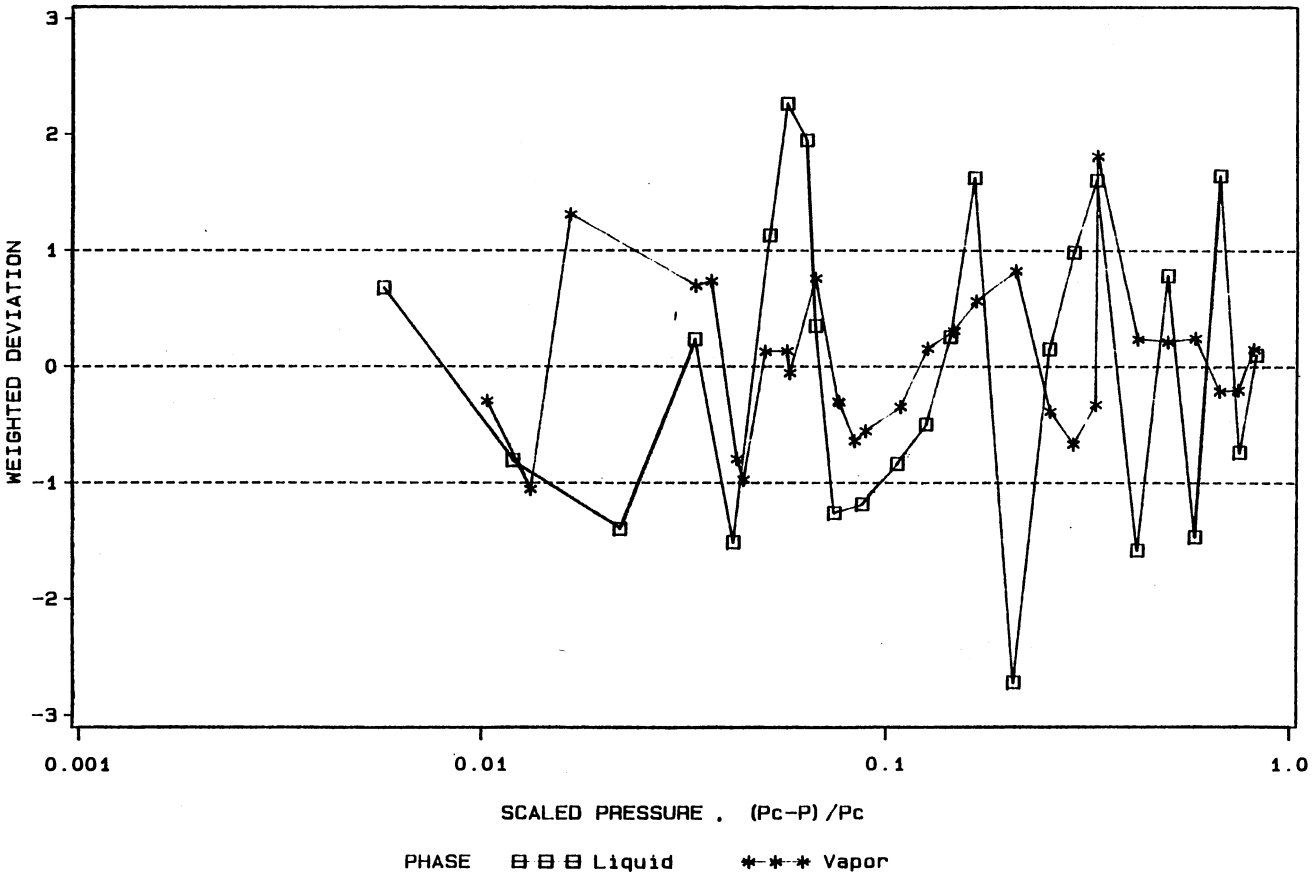

Figure 13. Extended Power Law Fit to Composition Data for Ethane + trans-Decalin @ 344.3 K (160°F)

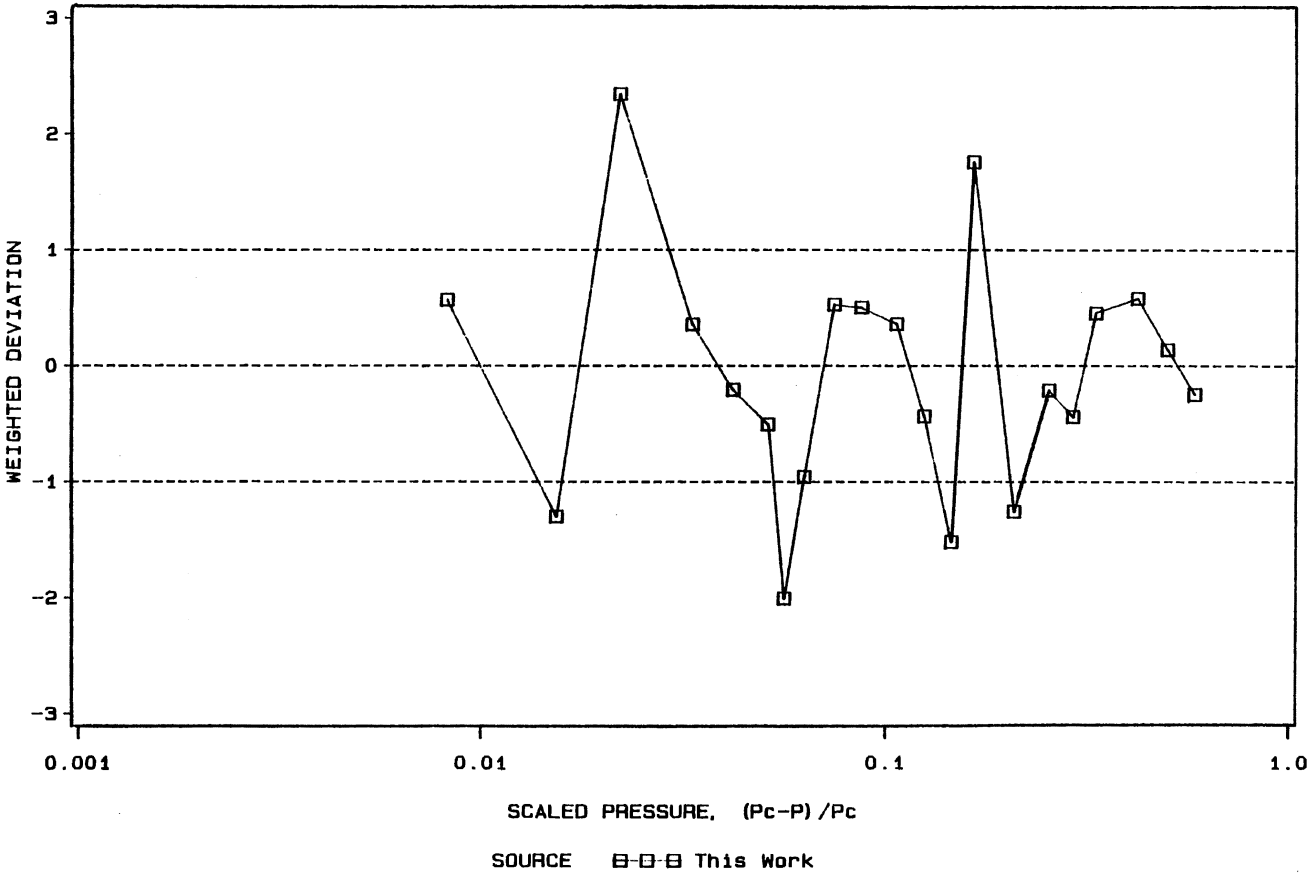

Figure 14. Extended Power Law Fit to Pendant Drop Data for Ethane + trans-Decalin @ 344.3 K (160°F)

12, 13, and 14.

The parameters in Table XI have been used to generate the smoothed data which appear in Table VII. The extrapolated values (beyond the highest measured pressures) shown in parentheses in Table VII are believed to be reliable since these values are in the near-critical power-law region, which is described correctly by the formulae. However, these formulae are not suitable for extrapolations to pressures lower than those given in Table VII.

The formulae described above was also used to smooth other data taken at the Oklahoma State University, details of those results appear in Appendix B.

Comparison of Experimental Results

No previous experimental data have been reported in the literature for this system at 160°F. However, Bufkin (65) has presented liquid phase composition and density data at 50, 100 and 150°C. In addition, Mapes (66) has performed bubble point measurements in an apparatus of the type used by Anderson, et al. (67). Comparison of the data obtained in this work for liquid compositions to those reported by Mapes indicates disagreement as large as 0.019 in the ethane mole fraction at higher pressures. No explanation for these differences is evident. However, bubble point measurements were performed at three different compositions as part of this study, and these results agree with the compositional data collected from the gas chromatograph to within 0.002 mole fraction ethane.

Comparison of the liquid composition data of the present work with those reported by Mapes appear in Table XII and Figure 15. To

TABLE XII

COMPARISON OF LIQUID COMPOSITION DATA
FOR ETHANE + TRANS-DECALIN

Source	Pressure, psia	Liquid Composition, Mole Fraction Ethane EXP'TL	Calc'd	Dev.
This Work (160°F)	209	0.1911	0.1899	-0.0012
	298	0.2630	0.2637	0.0007
	394	0.3353	0.3380	0.0027
	499	0.4160	0.4151	-0.0009
	601	0.4847	0.4856	0.0009
	696	0.5491	0.5483	-0.0008
	801	0.6142	0.6154	0.0012
	849	0.6451	0.6449	-0.0002
	894	0.6747	0.6724	-0.0023
This Work (160°F, Bubble point)	165	0.1505	0.1523	0.0018
	300	0.2629	0.2650	0.0021
	915	0.6830	0.6851	0.0021
Mapes (160°F)	205	0.1801	0.1870	0.0069
	261	0.2204	0.2336	0.0132
	391	0.3227	0.3353	0.0126
	576	0.4500	0.4685	0.0185
	682	0.5201	0.5394	0.0193
	842	0.6379	0.6530	0.0151

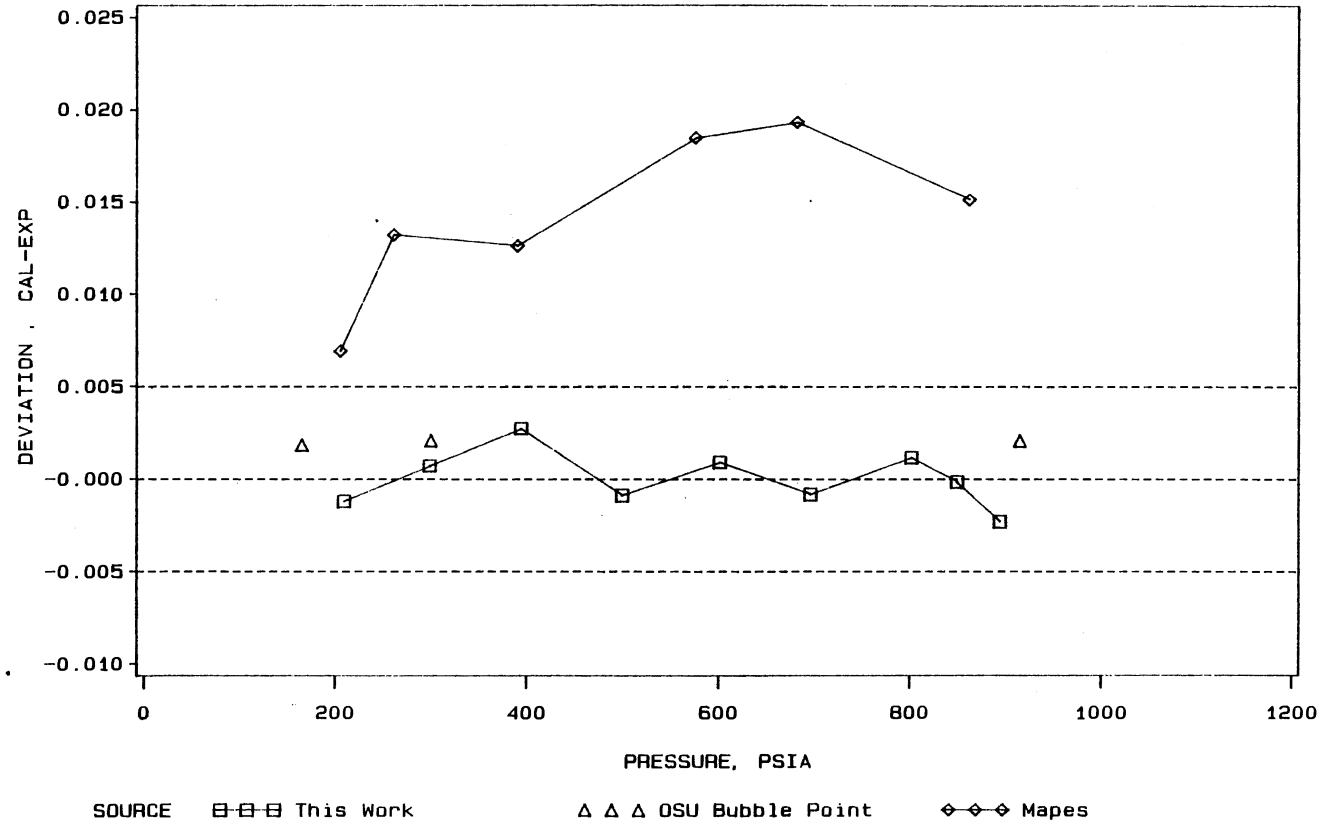

Figure 15. SRK Equation of State Predictions for Ethane + trans-Decalin @ 344.3 K (160°F)

facilitate these comparisons, the Soave-Redlich-Kwong (SRK) equation of state (68) was fit to the present data at pressures below 900 psia using two interaction parameters (C_{ij}, D_{ij}) in the SRK equation. Using the optimum values of the parameters (C_{ij} = 0.030, D_{ij} = -0.038) produced a fit to the present data having a standard deviation in predicted ethane mole fraction of 0.0014 and a maximum deviation of 0.0023 at 894 psia.

The SRK equation was used to generate the values shown as "Calc'd." in Table XII and the deviations shown in the table are deviations of the SRK representation from the experimental measurements. Obviously, the deviations from the data presented in this work are small, since the parameters were optimized to represent this data. The deviations shown from the data reported by Mapes should be viewed as essentially the difference between his data and the data collected in this study. As can be seen from Table XII, these differences are as large as 0.0195 at a pressure of 682 psia. Although the direction of these differences is typical (higher bubble point pressures from the solubility apparatus than from the apparatus used in this work), no obvious explanation for these differences is known.

As part of the work presented here, three bubble point measurements were made during the determination of the response factor for the gas chromatograph. For these measurements, a known amount of trans-Decalin was metered into the constant volume equilibrium cell, then known quantities of ethane were added to the cell. After each ethane addition, the system was equilibrated, and the system pressure was determined. A plot of pressure versus moles of ethane added showed a clear break at the point at the bubble point pressure where the cell contents passed from the two-phase to the single-phase state. These

data also appear in Table XII and Figure 15 and are in good agreement with the P-T-x-y data, the differences being essentially constant at 0.002 mole fraction ethane.

In addition to the composition comparisons described above, measurements were also made of the densities of pure ethane and trans-Decalin for comparison with literature results. For trans-Decalin, the measured saturated liquid density was found to be 0.8290 gm/cc, which is in good agreement with the literature value of 0.829 (69) and the previous value presented by Robinson, et al. of 0.8284 (36). For pure ethane, the values obtained in this work agree with those of Reamer (54) over a wide range of pressures. These measurements are described in detail in Chapter III.

CHAPTER V

INTERFACIAL TENSION MODEL EVALUATIONS

In order to properly evaluate the models chosen for study in this work, a search of the literature for currently available correlations and data to test the models of interest was performed. Once the available data had been accumulated and the models to be studied had been chosen, attention was turned to the various scenarios that might be investigated for each model. Three interfacial tension correlations were chosen and evaluated in this work. The three correlations are:

1) the Weinaug-Katz (WK) correlation (Equation 2-25)
2) the Hugill and Van Welsenes (HVW) correlation (Equation 2-30)
3) the Lee and Chien (LC) mixed parachor correlation (Equation 2-26)

These three correlations were chosen because of their ease of application. The input data required for the correlations may be obtained through widely known data bases such as the National Bureau of Standards, and/or predictive equations, such as the Soave-Redlich-Kwong equation of state. The simplicity of the correlations makes their use desirable in the application of computer models such as petroleum reservoir simulators.

The input variables used in evaluating the three different interfacial tension models came from data available in the literature and data obtained at the Oklahoma State University. Physical properties

for the pure substances were obtained from the National Bureau of Standards (NBS) publications and are presented in Appendix C. The parachors, which are required in all three correlations, can be obtained from published tables such as those of Quayle (70) or predicted by various correlations. A brief discussion of pure property parachors appears in Appendix D. The references for the equilibrium phase compositions, densities, and interfacial tensions used in this work are tabulated in Table I.

The models used to predict interfacial tension were evaluated by performing regressions to optimize various parameters for each correlation. This type of evaluation tested the frameworks of the correlations and their ability to predict interfacial tension. During the regressions for the various input variables used in the correlations, the performance of the "raw" model was tested. The progression in the model evaluations went from (a) the ability of the raw model to predict interfacial tensions through, (b) the regression for the parameters using experimental data, to (c) a model with generalized parameters.

During the evaluation of the three models studied, the parachors and the scaling exponent were obtained using a Marquart (71) nonlinear regression procedure on the experimental data and from sources available in the literature. These cases were then compared. The cases which use the values found in the literature may be considered the nominal or "raw potential" cases and those containing the regressed values may be considered to be optimum. By studing the regressed values, a trend may become obvious which may lead to the determination of generalized input parameters. From the observations made during the regressions of the

data using the three models studied, there is some indication that generalization of the results may be feasible. However, due to the limited data base available for this investigation, a full determination of the fully generalized parameters could not be done. The generalization of a correlation to predict IFT could provide a much needed tool for industrial applications. Evaluations of the ability of these models has been previously studied by Dickson (8) for carbon dioxide + hydrocarbon systems. The present study expands the work of Dickson to ethane and methane binary systems.

The "parameters" in the Weinaug-Katz correlation which may be regressed are the solute and solvent parachors and the scaling exponent, k. In addition to the study of cases which involved regressing the parachors for the individual components of a binary mixture, cases were also considered in which the parachors were held constant at the literature values (70). The parameters which may be optimized in the Hugill-Van Welsenes correlation include the parachors, an interaction parameter, C_{ij}, and the scaling exponent, k. The HVW model was also tested using the parachors suggested in their work (6). The parameters which may be regressed for the Lee-Chien correlation include the "density coexistence curve parameter", B, and the scaling exponent, k. The parachor is inversely proportional to the density coexistence curve parameter in the LC model (refer to equation 2-28).

The parameters for each model were optimized by performing a non-linear regression to minimize the objective function, SS:

$$SS = \sum_{i=1}^{K} [(Y^{calc} - Y^{exp})/W]_i^2 \qquad (5\text{-}1)$$

K is the number of experimental observations, Y is the value of the interfacial tension (or interfacial tension/density difference), and W is the weighting factor:

$$W = \sigma_Y$$

In this work: $\sigma_Y = Y^{exp}$. This minimizes the fractional (%) errors in the predictions.

Evaluation of the Weinaug-Katz IFT Model

The first model chosen for evaluation was the model suggested by Weinaug and Katz (5) in 1943. The WK model expands the Macleod and Sugden (26, 27) correlations for pure compounds to mixtures. The input data required by the WK model are: phase compositions (x, y), phase densities (ρ^L, ρ^V), and pure component parachors. All phase data used in this work were experimental values. These experimental data were obtained both from the Oklahoma State University work and from the literature. The carbon dioxide and ethane solute systems were obtained from the Oklahoma State University and the methane binaries were obtained from the literature. References to all the data appear in Chapter I. The parameters which are regressed are the scaling scaling exponent, k, and the solute and solvent parachors.

Evaluation of the WK model was carried out for a series of cases in which various combinations of the parameters were held constant or regressed to determine both the effectiveness and sensitivity of the correlation to the parameters in the model. The cases were assigned specific numbers, as summarized in Table XIII. These cases range from

TABLE XIII

DESCRIPTION OF CASES STUDIED FOR THE WEINAUG-KATZ IFT MODEL

CASE NO.	REGRESSED PARMS	FIXED PARAMETERS	CASE DESCRIPTION
1	NONE	P1 and P2 are from Quayle, k = 4.0	This case tests the raw potential of the Weinaug-Katz equation. The parachors are those tabulated by Quayle (70). The exponent is set to the suggested value of 4.0.
2	k	P1 and P2 are from Quayle	The parachors are those tabulated by Quayle, as in Case 1. The effect of the exponent, k, is found by regression.
3	P1, P2, k	NONE	This case has both the parachors and the exponent, k, are regressed.
4	P1, P2, k	NONE, Pr < 0.99	This case has both the parachors and the exponent, k, regressed; however, this case restricted the data set to reduced pressures of 0.99 or less.
5	P1, k	P2 are from Quayle	The solute (CO_2, ethane, or methane) parachor and the exponent, k, are regressed. The solvent parachor is that given by Quayle.
6	k	P1 and P2 are generalized values	This case introduces the idea of a fitted parachor. The parachors used are adjusted values of Quayles work. These generalized parachors, P(A), are found by reducing the solute parachor found in Quayles work by 15% and increasing the solvent parachor by 5%. The exponent, k, is regressed.

TABLE XIII (Continued)

7	NONE	P1 and P2 are generalized values	This case generalizes the parameters in the model for all k = 3.6 systems studied (carbon dioxide, ethane, and methane binaries and the pure compounds). The parachor is set equal to the adjusted or generalized parachor, P(A), and the exponent, k, is set to the value which fits all the data best and that is a value of 3.6.
8	P1	P2 are from Quayle, k = 3.6	The solute (CO_2, ethane, or methane) parachor for each system is regressed. The exponent, k, is set equal to 3.6. The solvent parachor is that given by Quayle.

the "raw" model as presented by Weinaug and Katz (Case 1) to a case in which all parameters (P_1, P_2, and k) are regressed simultaneously (Case 3) and include a case in which the parameters are set to generalized values obtained in this work (Case 7). These generalized values were determined through observation of the values obtained through regressions for the three models and the three solutes studied. These values are not specific to the models studied but are values obtained for the available data using the models relevant to this work. A discussion concerning the values used for the generalized parachors appears in Appendix D.

Besides the parachor, the other parameter in the WK model which may be regressed is the scaling exponent, k. In the original work of Weinaug and Katz, a value of 4.0 was used for k. However, as the critical pressure for a pure compound or binary is approached the scaling exponent begins to favor a lower value than 4.0; a value near 3.6 appears to be optimum and is in good agreement with the experimental value ($k = 2\nu/\beta = 3.55$) suggested by Sengers, Greer, and Sengers (60). In order to quantify this observation, the idea of an "effective scaling exponent" was also investigated; this effective scaling exponent was defined as:

$$k(\rho^*) = k' + k'' \, e^{(\Delta\rho/\rho_c)} \qquad (5\text{-}2)$$

where k' and k" are regressed parameters. This relation was selected from observing the values obtained for the scaling exponent through regressions. The scaling exponent preferred a value close to 4.0 for data sets restricted to pressures below a reduced pressure of 0.70,

however, the scaling exponent preferred a value of 3.6 near the critical point (reduced pressure of almost 1.0). This behavior led to attempts to find a correlation for a scaling exponent that would depend on either the scaled pressure ($P^* = (P_c-P)/P_c$) or the scaled density ($\rho^* = (\rho^L-\rho^V)/\rho_c$). Both relations were investigated and after some deliberation the above expression was pursued. However, the use of such a parameter led to little improvement for the systems studied and was abandoned.

The parameters which influence the performance of the WK model are the solute parachor (P_1), the solvent parachor (P_2), and the scaling exponent, k. Figures 16 and 17 show the results of sensitivity analyses performed on the parameters of the WK model. Figure 16 shows the influence that the solute (P_1) and the solvent (P_2) parachors have on the ability of the model to predict the experimental data presented in this work (ethane + trans-Decalin at 160°F). The axes of the figures correspond to the absolute average percent deviation (AAPD) as a function of deviations from regressed values for the solute parachor, the solvent parachor or the scaling exponent. The parachors corresponding to a deviation of 0.0% are 62.8 for the ethane solute) parachor and 406.0 for the trans-Decalin (solvent) parachor. The values given by Quayle for the ethane and trans-Decalin parachors are 110.5 and 371.0, respectively. Figure 16 shows that the WK model is much less sensitive to the value for the solute parachor, which is why the solute parachor can vary a large amount without affecting the predictive power of the WK model. However, the solvent parachor affects the predicted value for the IFT a large amount for a small change in the parachor. Figure 17 examines the models sensitivity to the solute parachor and the scaling exponent, k. Again, the solute parachor exhibits a small

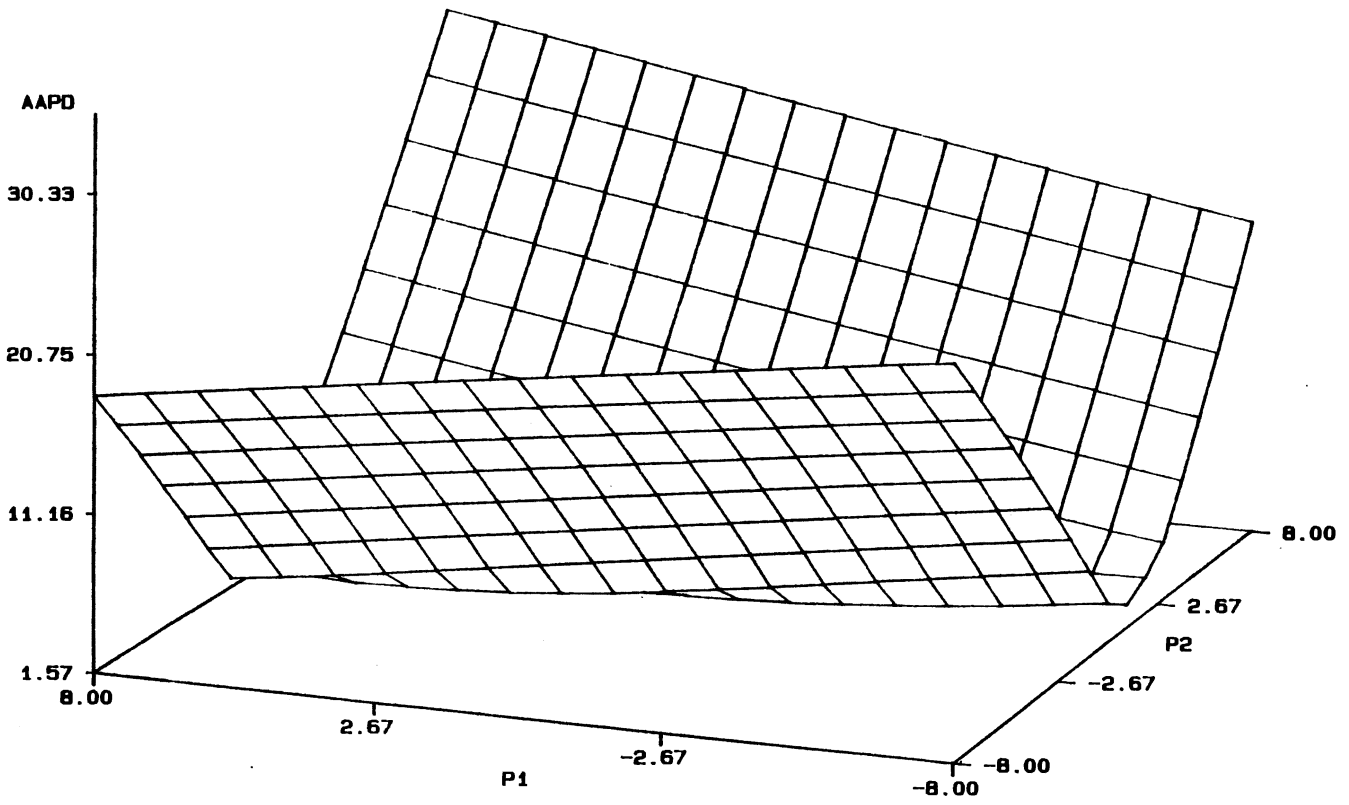

Figure 16. Sensitivity of the Weinaug-Katz IFT Model to the Solute and Solvent Parachors for Ethane + trans-Decalin @ 344.3 K (160°F)

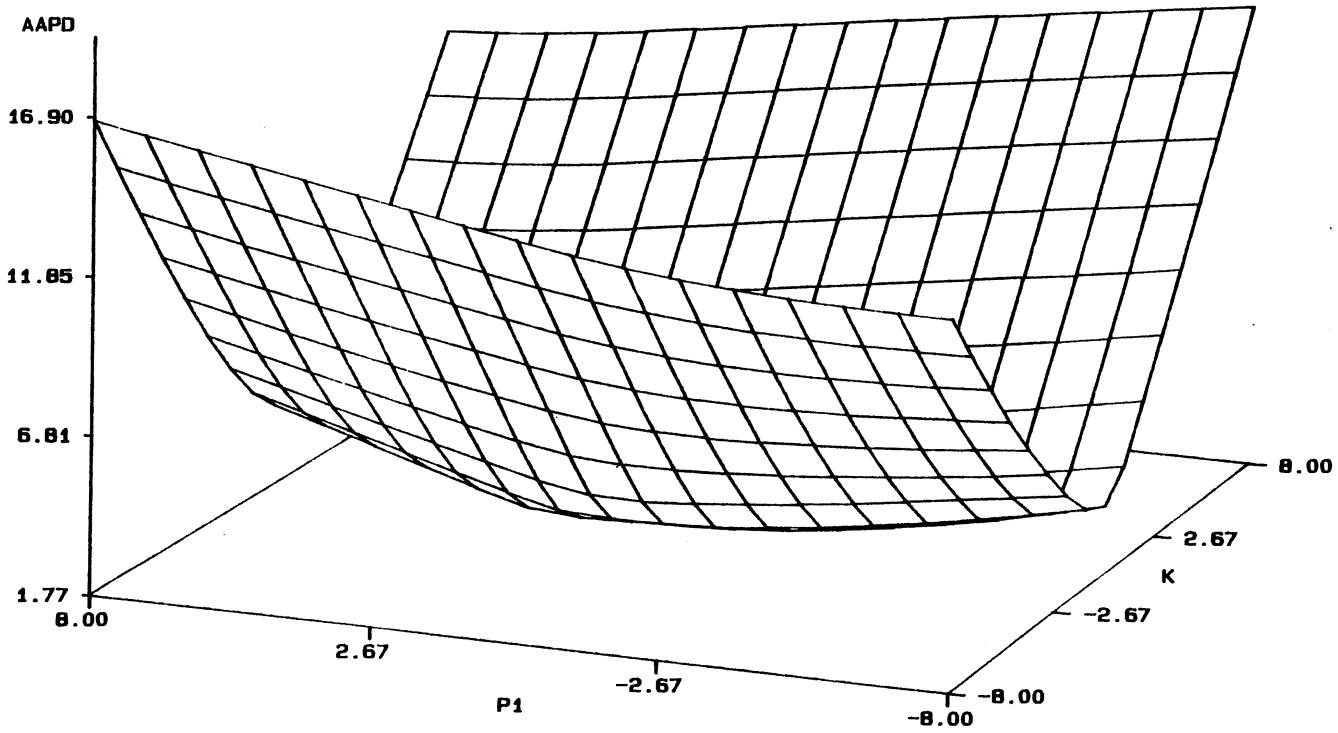

Figure 17. Sensitivity of the Weinaug-Katz IFT Model to the Solute Parachor and the Scaling Exponent for Ethane + trans-Decalin @ 344.3 K (160°F)

influence, in whereas the scaling exponent affects the predicted values by 16.9% for an 8% change in the scaling exponent. This implies that the flexibility of the model is limited to small variations in the solvent parachor and the scaling exponent.

In the course of evaluating the WK model, eight separate cases were investigated. Tables XIV, XV, and XVI contain statistics regarding the predictions of interfacial tensions for the carbon dioxide, ethane and methane binaries, respectively. Included in the statistics given in these tables are the root-mean-square error (RMSE), the absolute average percent deviation (AAPD), and the bias (BIAS). As can be seen from the tables, the WK model with parameters generalized using only the available data set is able to predict interfacial tension within an AAPD of 11.6%. For each of the solutes, the same cases were executed in order to compare the performance of the model for each solute. Table XVII gives such a comparison. The WK model is able to predict interfacial tensions of the simpler paraffin solute systems better than the systems containing the more complex molecule of carbon dioxide.

A graphical representation of the AAPD from the experimental IFT values as a function of solvent molecular weight may be seen in Figures 18, 19, and 20. The figures present the statistical information for each solute separatly. Figure 18 corresponds to the carbon dioxide systems, Figure 19 to ethane, and Figure 20 to the methane binaries. From these figures the variation in the ability of the model to predict the different solvents may be scrutinized. The trans-Decalin systems for both the carbon dioxide and the ethane solutes have the largest AAPD for each case investigated (MW = 138.254), the n-decane system for the methane solute has the larger AAPD for all solutes and cases. (A

TABLE XIV

SUMMARY OF CASES STUDIED USING THE WEINAUG-KATZ IFT MODEL FOR THE CARBON DIOXIDE + HYDROCARBON SYSTEMS

CASE NO.	REGRESSED PARMS	FIXED PARAMETERS	RMSE	AAPD	BIAS	k
1	NONE	P1 and P2 = Quayle, k = 4.0	0.2537	25.51	-0.0770	4.0
2	k	P1 and P2 = Quayle	0.3353	15.11	-0.1636	3.468
3	P1, P2, k	NONE	0.2635	9.07	-0.0086	3.568
4	P1, P2, k	NONE, Pr < 0.99	0.2426	7.20	-0.0301	3.486
5	P1, k	P2 = Quayle	0.3494	14.53	-0.1759	3.468
6	k	P1 and P2 = gen. values	0.2534	10.77	0.0662	3.637
7	NONE	P1 and P2 = gen. values, k = 3.6	0.2318	10.89	0.0508	3.6
8	P1	P2 = Quayle, k = 3.6	0.2752	15.47	-0.1386	3.6

TABLE XV

SUMMARY OF CASES STUDIED USING THE WEINAUG-KATZ IFT MODEL FOR THE ETHANE + HYDROCARBON SYSTEMS

CASE NO.	REGRESSED PARMS	FIXED PARAMETERS	RMSE	AAPD	BIAS	k
1	NONE	P1 and P2 = Quayle, k = 4.0	0.8023	15.55	0.4313	4.0
2	k	P1 and P2 = Quayle	0.5021	14.91	0.2770	3.822
3	P1, P2, k	NONE	0.4558	4.51	-0.0708	3.560
4	P1, P2, k	NONE, Pr < 0.99	0.5223	4.04	-0.0965	3.550
5	P1, k	P2 = Quayle	0.4029	5.36	-0.0897	3.638
6	k	P1 and P2 = gen. values	0.3764	8.58	0.1885	3.615
7	NONE	P1 and P2 = gen. values, k = 3.6	0.3452	8.60	0.1698	3.6
8	P1	P2 = Quayle, k = 3.6	0.4921	5.74	-0.1394	3.6

TABLE XVI

SUMMARY OF CASES STUDIED USING THE WEINAUG-KATZ IFT MODEL FOR THE METHANE + HYDROCARBON SYSTEMS

CASE NO.	REGRESSED PARMS	FIXED PARAMETERS	RMSE	AAPD	BIAS	k
1	NONE	P1 and P2 = Quayle, k = 4.0	0.7019	22.26	-0.3149	4.0
2	k	P1 and P2 = Quayle	0.8568	20.20	-0.5525	3.769
3	P1, P2, k	NONE	0.2109	6.50	-0.0508	3.647
4	P1, P2, k	NONE, Pr < 0.99	0.2001	5.96	-0.0442	3.658
5	P1, k	P2 = Quayle	0.5873	12.66	-0.3266	3.776
6	k	P1 and P2 = gen. values	0.3220	10.73	-0.0746	3.666
7	NONE	P1 and P2 = gen. values, k = 3.6	0.4372	11.59	-0.1714	3.6
8	P1	P2 = Quayle, k = 3.6	0.9464	14.39	-0.5385	3.6

TABLE XVII

CASE COMPARISONS FOR THE WEINAUG-KATZ IFT MODEL

CASE NO.	ABSOLUTE AVERAGE PERCENT DEVIATION, AAPD Carbon Dioxide	Ethane	Methane
1	25.51	15.55	22.26
2	15.11	14.91	20.20
3	9.07	4.51	6.50
4	7.20	4.04	5.96
5	14.53	5.36	12.66
6	10.77	8.58	10.73
7	10.89	8.60	11.59
8	15.47	5.74	14.39

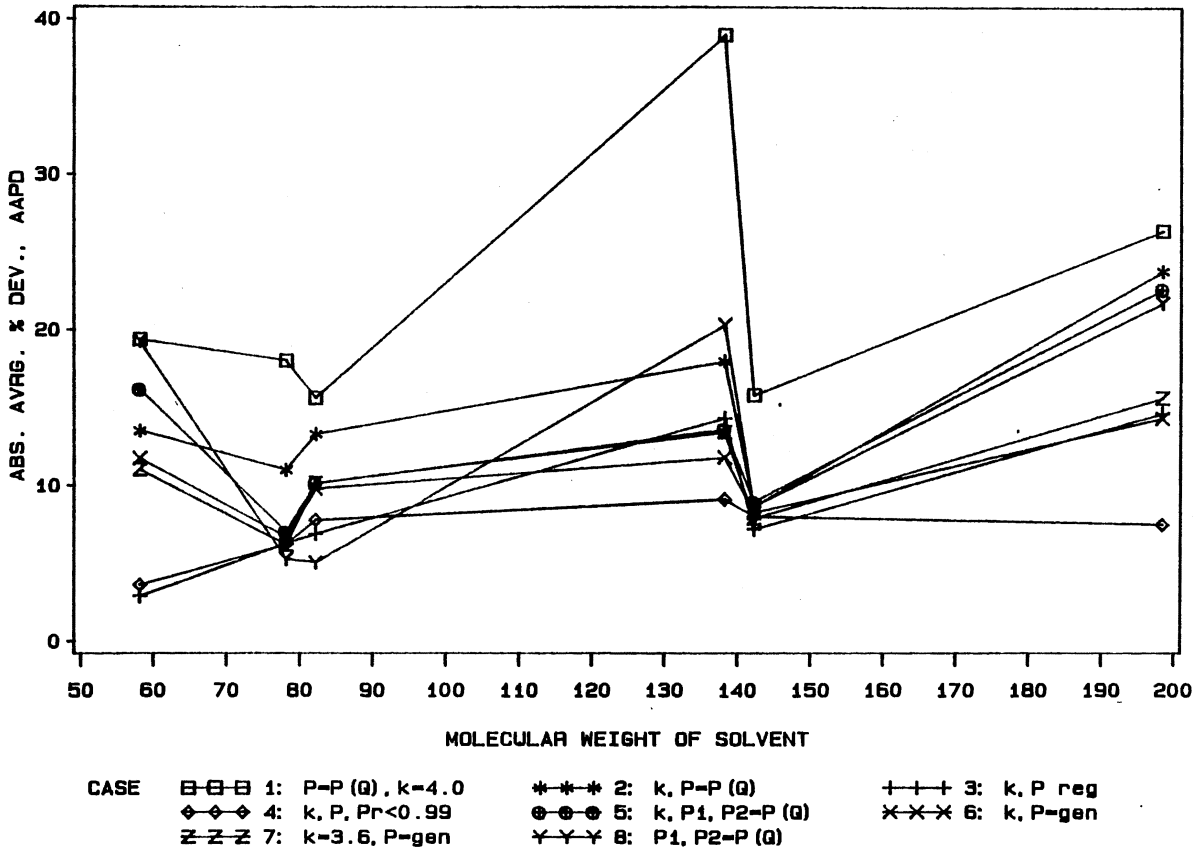

Figure 18. Case Profile of the Weinaug-Katz Model for the Carbon Dioxide + Hydrocarbon Systems

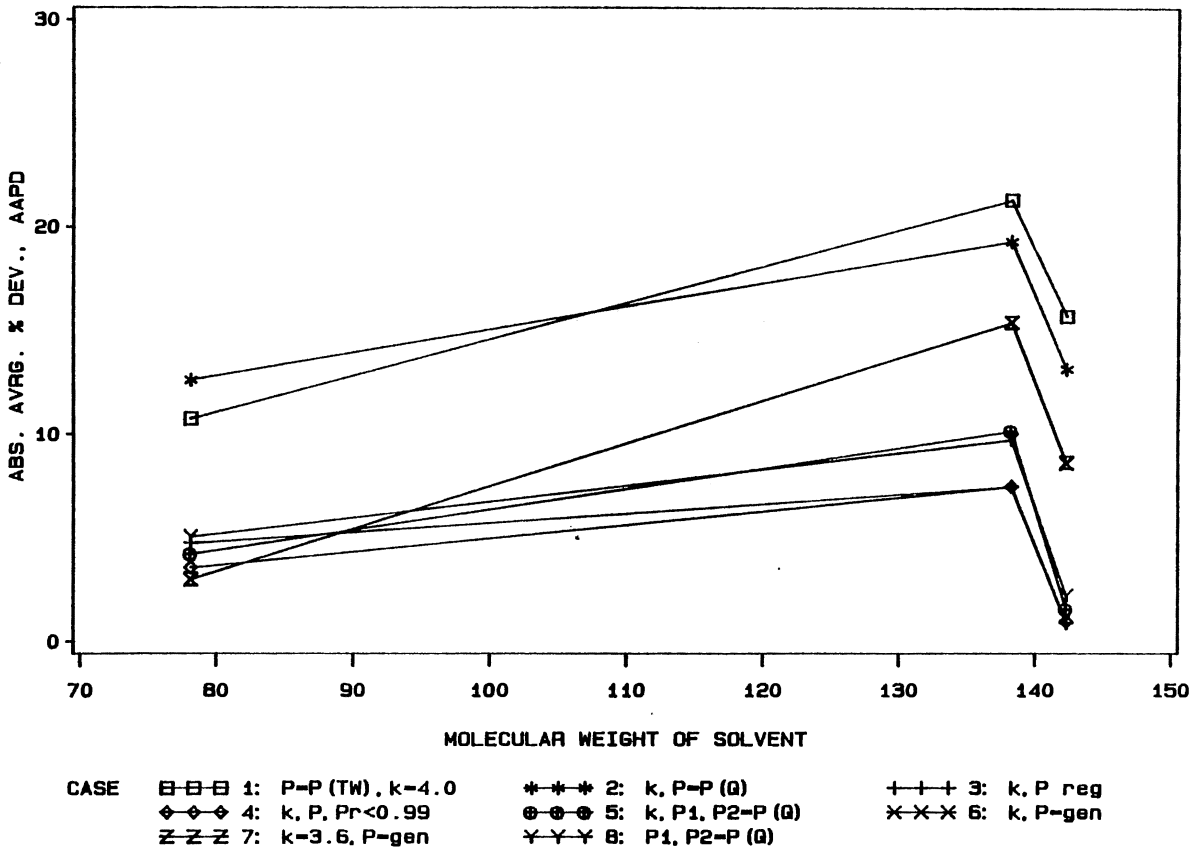

Figure 19. Case Profile of the Weinaug-Katz Model for the Ethane + Hydrocarbon Systems

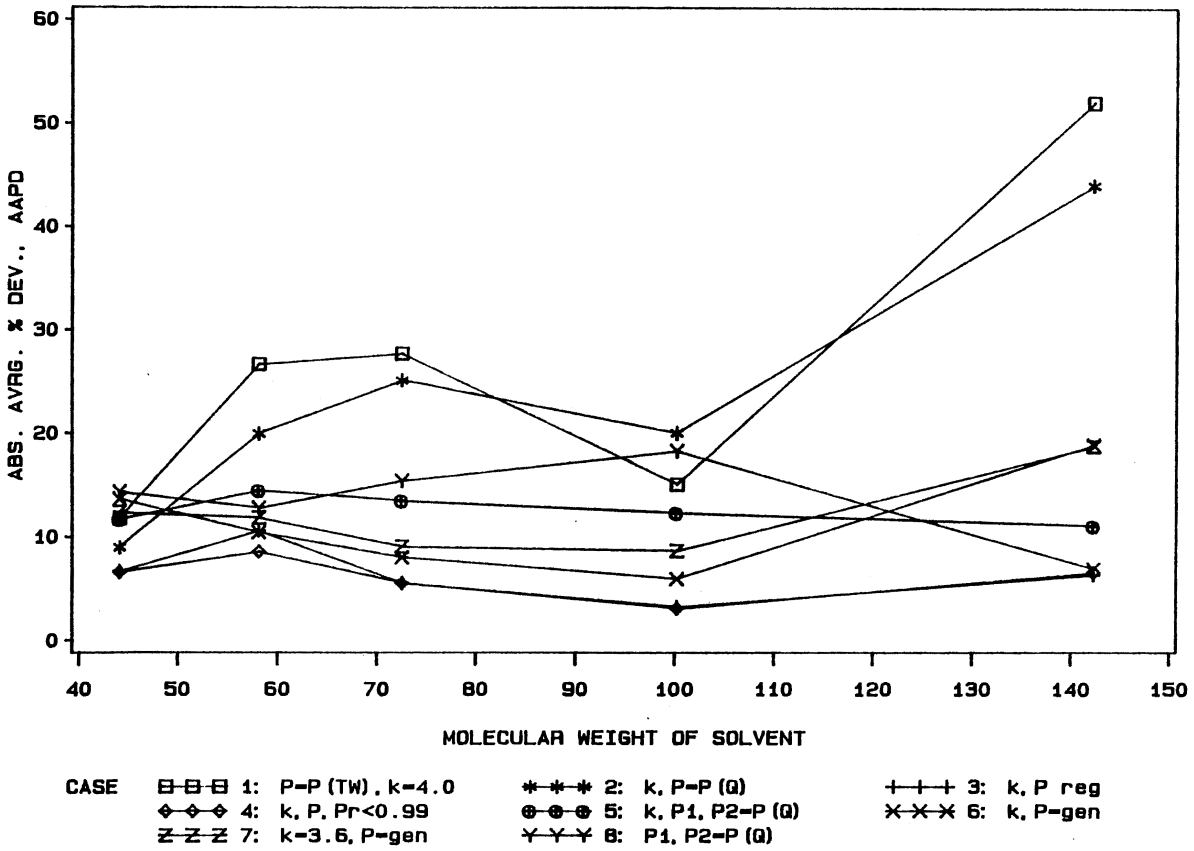

Figure 20. Case Profile of the Weinaug-Katz Model for the Methane + Hydrocarbon Systems

complete summary of the statistics for each system presented on an isotherm-by-isotherm basis is available through the School of Chemical Engineering at the Oklahoma State University (72).)

The best performance of the model is Case 3 (this case includes all the data, whereas Case 4 limits the data to values with a reduced pressure less than 0.99). The "best" implies that this case produced the lowest AAPD and RMSE of all cases for each solute. Tables XVIII, XIX, and XX show the fit of the data for each system investigated for Case 3. The WK model predicts the data within 10%. The model is less accurate for the carbon dioxide systems than for the paraffinic solutes ethane and methane. Each table presents information concerning each isotherm; at the bottom of each table the overall statistics for the case of interest are given. Among the information tabulated for each case are the isotherm number for a particular case, ISO, the temperature of the system, T(°F), the system of interest, the parachor of the solute, PAR(1), the parachor of the solvent, PAR(2), the value for the scaling exponent, k, the value for the Hugill - Van Welsenes interaction parameter, C_{ij} (the value of 0 for C_{ij} in model summaries other than the HVW is meaningless), and the minimum and maximum value for the reduced pressure, EMIN and EMAX, respectively. The statistics for each case investigated include the root-mean-square error (RMSE), the weighted root-mean-square error (WRMS), the bias (BIAS), the absolute average percent deviation (AAPD), the weighted absolute average percent deviation (AAWPD), and the number of points used in the determination of each statistical value (NO PT). The results for Case 3 appear in Figures 21, 22, and 23.

Figure 24 presents the experimental data obtained in this work (the

TABLE XVIII

SUMMARY OF THE OVERALL STATISTICS FOR THE WEINAUG-KATZ MODEL, CASE 3
USING DATA FOR THE CARBON DIOXIDE + HYDROCARBON SYSTEMS

ISO	T(F)	SYSTEM	PAR(1)	PAR(2)	K	C(I,J)	EMIN	EMAX	RMSE	WRMS	BIAS	AAPD	AAWPD	NO PT
1	160.	CO2 + BENZENE	79.2	200.4	3.568	0.000	0.6297	0.9975	0.3678	2.09	-0.1293	6.30	3.73	15
2	115.	CO2 + n-BUTANE	79.2	199.7	3.568	0.000	0.2857	0.9901	0.2682	3.43	0.1123	11.42	3.39	18
3	160.	CO2 + n-BUTANE	79.2	199.7	3.568	0.000	0.3947	0.9805	0.0620	0.87	-0.0276	2.88	3.60	12
4	220.	CO2 + n-BUTANE	79.2	199.7	3.568	0.000	0.3807	0.9636	0.0291	1.15	-0.0129	4.55	3.55	12
5	160.	CO2 + CYCLOHEXANE	79.2	234.9	3.568	0.000	0.6270	0.9975	0.3476	2.32	-0.1440	6.90	3.73	14
6	160.	CO2 + n-DECANE	79.2	445.8	3.568	0.000	0.5449	0.9930	0.1819	2.31	0.0010	7.20	3.31	17
7	220.	CO2 + n-DECANE	79.2	445.8	3.568	0.000	0.6274	0.9979	0.1178	2.25	-0.0723	8.60	4.00	23
8	160.	CO2 + t-DECALIN	79.2	391.3	3.568	0.000	0.6530	0.9856	0.4563	4.28	0.1965	14.36	4.34	20
9	160.	CO2 + TETRADECANE	79.2	621.1	3.568	0.000	0.6742	0.9952	0.0959	3.55	-0.0664	14.67	4.07	17

RMSE= 0.2635, AAPD = 9.07, BIAS = -0.0086, DMIN= -24.93, EMIN=0.2857
WRMS= 2.61, AAWPD= 3.78, WBIAS= -0.3894, DMAX= 38.41, EMAX=0.9979, NPIS = 148

TABLE XIX

SUMMARY OF THE OVERALL STATISTICS FOR THE WEINAUG-KATZ MODEL, CASE 3
USING DATA FOR THE ETHANE + HYDROCARBON SYSTEMS

ISO	T(F)	SYSTEM	PAR(1)	PAR(2)	K	C(I,J)	EMIN	EMAX	RMSE	WRMS	BIAS	AAPD	AAWPD	NO PT
1	160.	C2H6 + n-DECANE	91.0	447.7	3.560	0.000	0.3490	0.9860	0.0471	0.31	0.0027	0.90	3.25	20
2	160.	C2H6 + t-DECALIN	91.0	376.0	3.560	0.000	0.1669	0.9917	0.7846	2.70	-0.2828	7.49	3.33	22
3	160.	C2H6 + BENZENE	91.0	223.0	3.560	0.000	0.4907	0.9971	0.1661	1.30	0.0476	4.75	4.24	27

RMSE= 0.4558, AAPD = 4.51, BIAS = -0.0708, DMIN= -16.01, EMIN=0.1669
WRMS= 1.46, AAWPD= 3.66, WBIAS= -0.1535, DMAX= 12.64, EMAX=0.9971, NPIS = 69

TABLE XX

SUMMARY OF THE OVERALL STATISTICS FOR THE WEINAUG-KATZ MODEL, CASE 3
USING DATA FOR THE METHANE + HYDROCARBON SYSTEMS

ISO	T(F)	SYSTEM	PAR(1)	PAR(2)	K	C(I,J)	EMIN	EMAX	RMSE	WRMS	BIAS	AAPD	AAWPD	NO PT
1	100.	CH4 + n-BUTANE	29.0	194.2	3.647	0.000	0.5230	0.9937	0.1699	3.25	-0.0918	14.45	3.64	11
2	130.	CH4 + n-BUTANE	29.0	194.2	3.647	0.000	0.5330	0.9861	0.1106	3.15	-0.0428	12.67	3.75	10
3	160.	CH4 + n-BUTANE	29.0	194.2	3.647	0.000	0.5525	0.9945	0.0668	2.12	-0.0283	8.40	4.33	9
4	190.	CH4 + n-BUTANE	29.0	194.2	3.647	0.000	0.5889	0.9717	0.0183	1.00	-0.0136	4.48	4.13	7
5	100.	CH4 + n-DECANE	29.0	427.3	3.647	0.000	0.3766	0.9887	0.2008	2.28	0.1286	6.68	3.32	9
6	160.	CH4 + n-DECANE	29.0	427.3	3.647	0.000	0.3855	0.9638	0.2751	2.02	-0.1279	6.04	3.01	8
7	100.	CH4 + n-HEPTANE	29.0	327.3	3.647	0.000	0.0554	0.6234	0.4848	1.68	-0.1979	3.27	2.01	10
8	160.	CH4 + n-HEPTANE	29.0	327.3	3.647	0.000	0.0564	0.7749	0.3082	1.81	-0.0413	3.97	2.18	12
9	220.	CH4 + n-HEPTANE	29.0	327.3	3.647	0.000	0.0606	0.8338	0.1981	1.42	-0.0536	3.35	2.28	12
10	280.	CH4 + n-HEPTANE	29.0	327.3	3.647	0.000	0.0683	0.7687	0.1619	0.99	-0.0759	2.25	2.31	10
11	100.	CH4 + n-PENTANE	29.0	241.8	3.647	0.000	0.4073	0.9165	0.1224	1.87	0.0960	5.25	2.71	6
12	160.	CH4 + n-PENTANE	29.0	241.8	3.647	0.000	0.2566	0.9624	0.0675	1.43	-0.0175	5.75	2.84	8
13	5.	CH4 + n-PROPANE	29.0	155.9	3.647	0.000	0.1481	0.5160	0.1998	3.32	0.0930	8.98	2.45	5
14	50.	CH4 + n-PROPANE	29.0	155.9	3.647	0.000	0.1145	0.6895	0.2085	1.86	-0.1554	4.71	2.56	7
15	86.	CH4 + n-PROPANE	29.0	155.9	3.647	0.000	0.1215	0.6796	0.1845	3.10	-0.1562	8.93	2.68	12
16	113.	CH4 + n-PROPANE	29.0	155.9	3.647	0.000	0.1972	0.5564	0.0638	1.28	-0.0579	3.55	2.74	11
17	149.	CH4 + n-PROPANE	29.0	155.9	3.647	0.000	0.3074	0.6608	0.0888	2.53	0.0767	8.14	3.10	6

RMSE= 0.2109, AAPD = 6.50, BIAS = -0.0508, DMIN= -83.10, EMIN=0.0554
WRMS= 2.05, AAWPD= 2.92, WBIAS= -0.3492, DMAX= 30.31, EMAX=0.9945, NPIS = 153

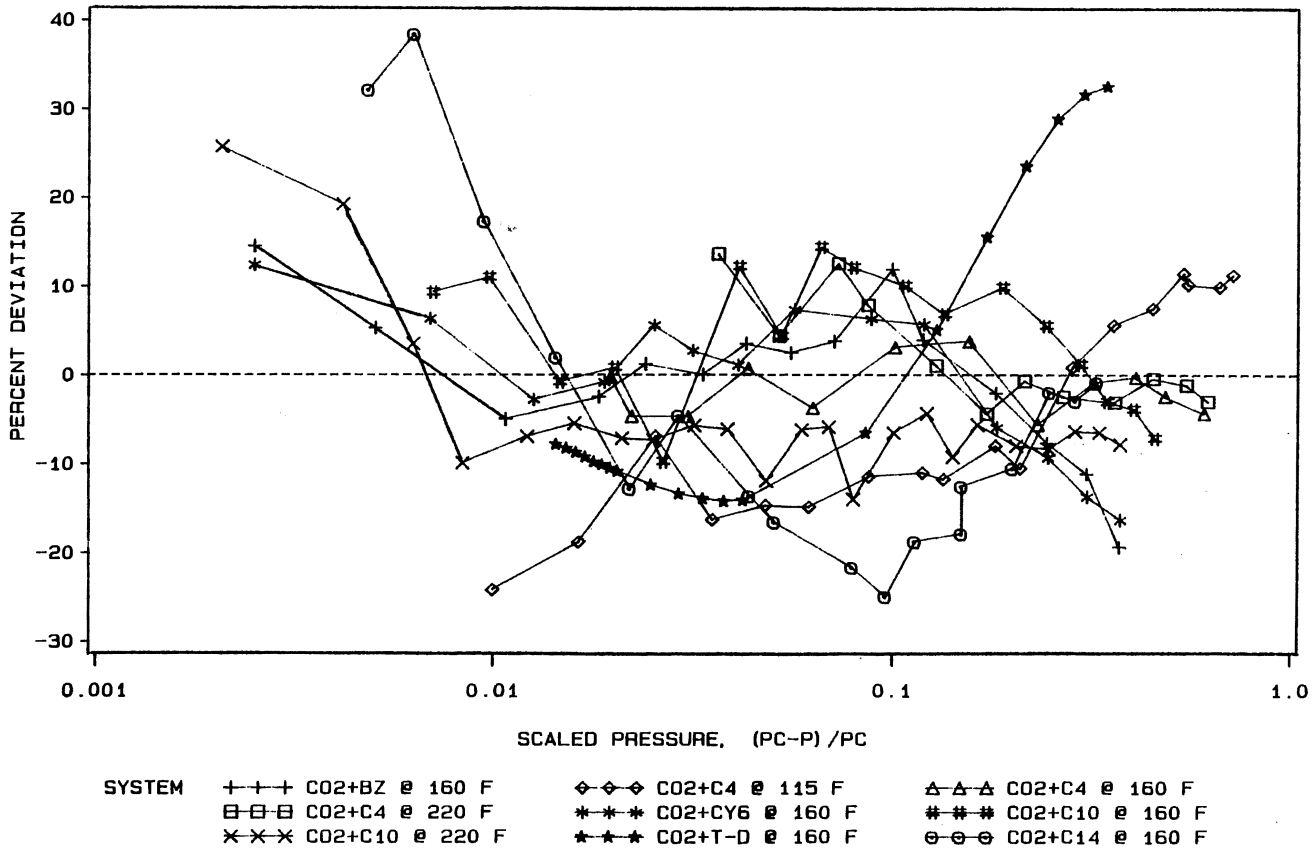

Figure 21. Evaluation of the Weinaug-Katz Model, Case #3, for the Carbon Dioxide + Hydrocarbon Systems. The Solute and Solvent Parachors and the Scaling Exponent are Regressed

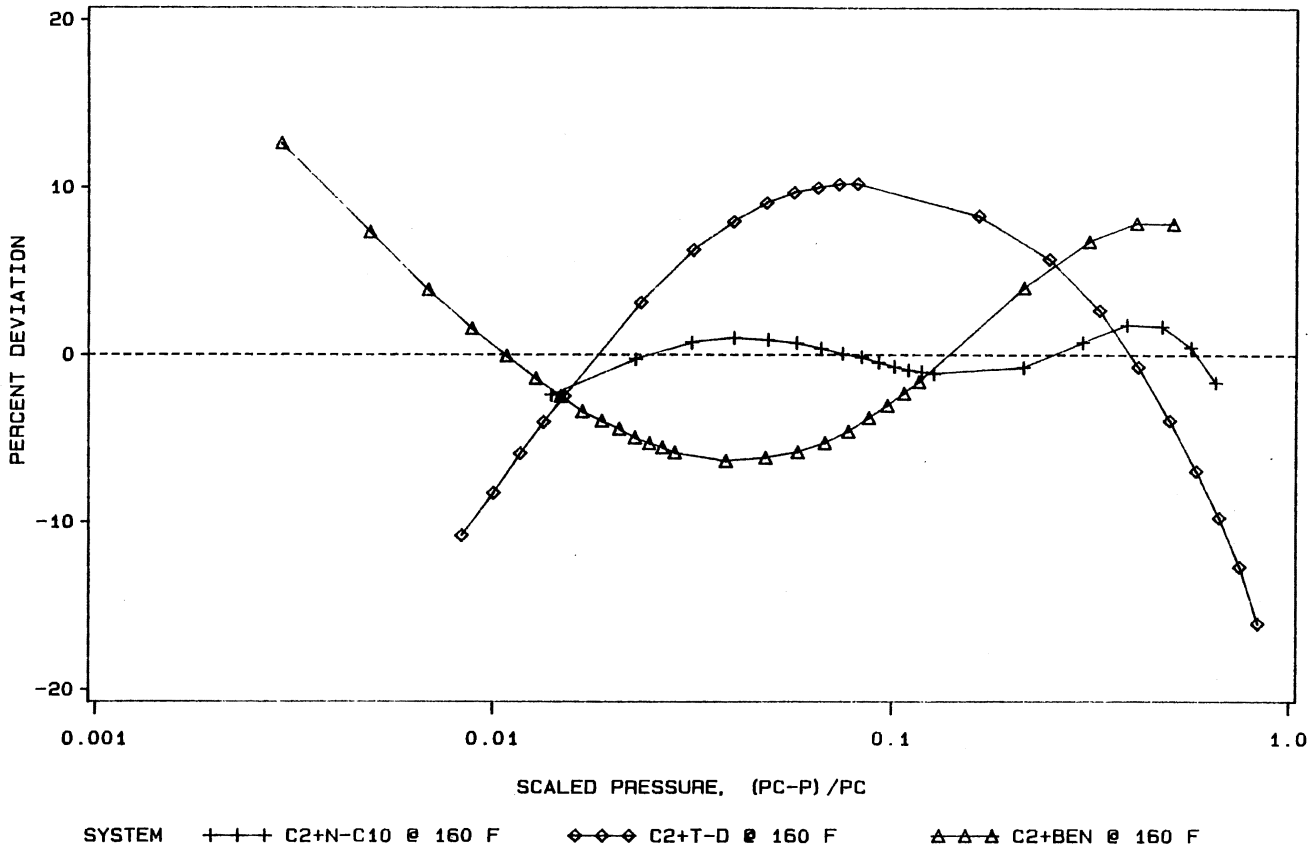

Figure 22. Evaluation of the Weinaug-Katz Model, Case #3, for the Ethane + Hydrocarbon Systems. The Solute and Solvent Parachors and the Scaling Exponent are Regressed

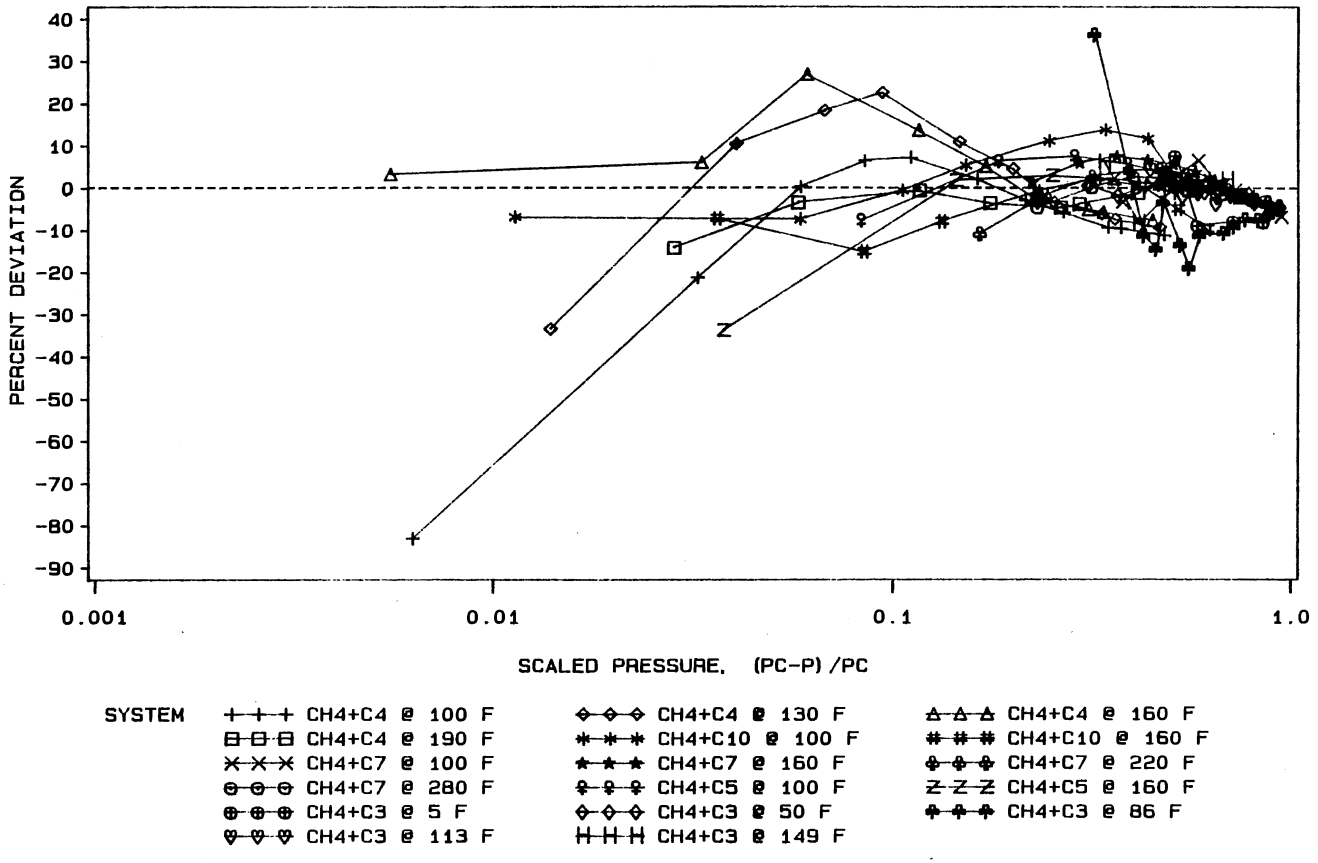

Figure 23. Evaluation of the Weinaug-Katz Model, Case #3, for the Methane + Hydrocarbon Systems. The Solute and Solvent Parachors and the Scaling Exponent are Regressed

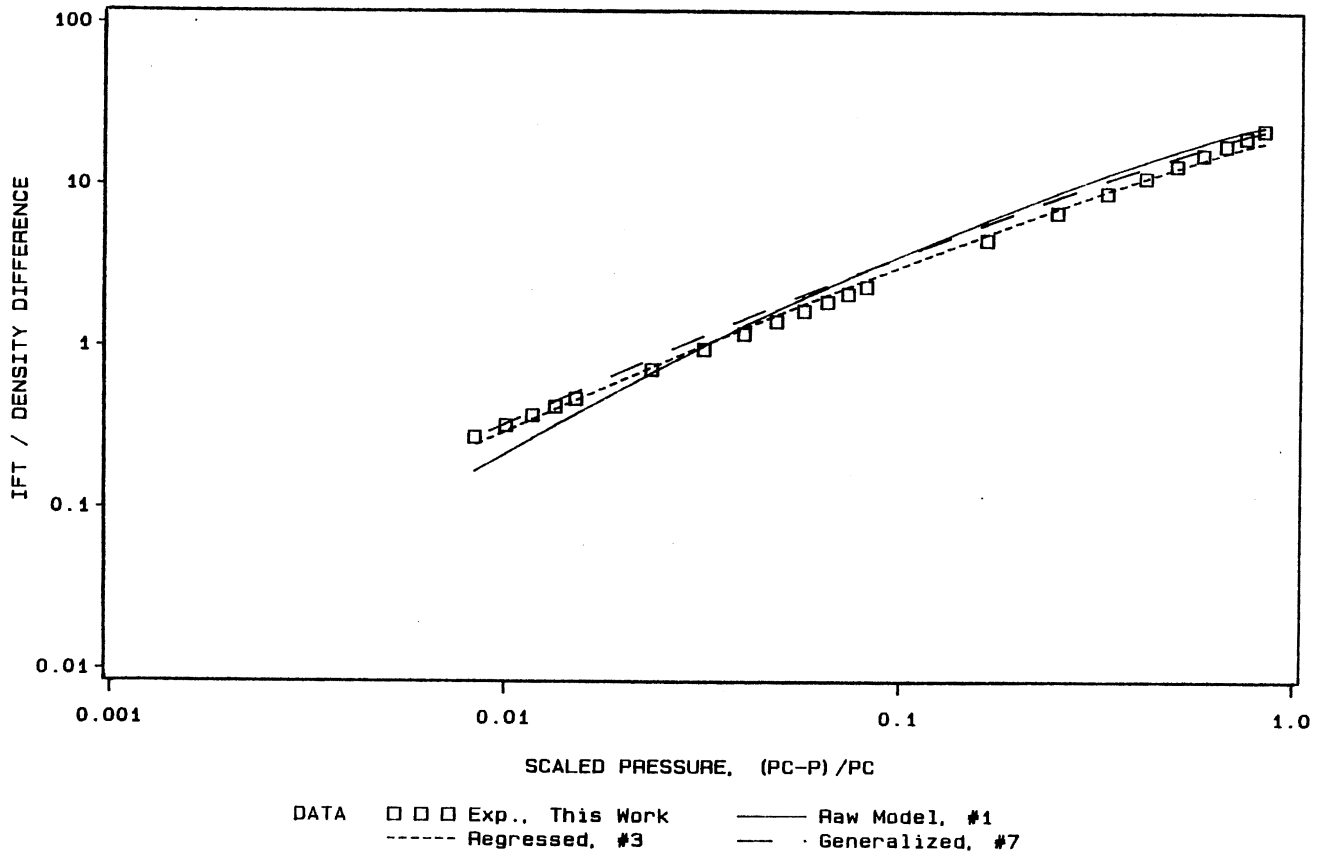

Figure 24. Comparison of the Ability of the Weinaug-Katz Model to Predict Experimental Data for Ethane + trans-Decalin @ 344.3 K (160°F)

ethane + trans-Decalin system) along with predictions for three of the cases investigated in the evaluation of the Weinaug-Katz model. As can be seen from the figure, the case with regressed parameters is the best, as might be expected. The generalized case performs better closer to the critical point than does the nominal case (Case 1). However, based on the evaluations in this work, and with regard to the limited number of solute systems available, the reason for the improved performance cannot be totally attributed to the parachor values chosen as "generalized". The ability of the generalized case to predict the data in the critical region may rest more heavily on the value of 3.6 used for the scaling exponent. The generalized case was determined by varying parachors from the literature (70) by -15% for the solute parachor and +5% for the solvent parachor, k was held equal to 3.6. The generalized case fit the data almost as well as the regressed case, especially in the high-pressure near-critical regions, which may be largely attributed to the value chosen for the scaling exponent; k = 3.6. As stated earlier, the general validity of the generalized parachors must be investigated further, but the potential for the use of generalized values is noted.

Evaluation of the Hugill-Van Welsenes IFT Model

The Hugill-Van Welsenes (HVW) model introduces the idea of a generalized "mixing rule" for the parachor which may be used in the Weinaug-Katz model. The parameters which may be evaluated through regression techniques are the solute and solvent parachors, the scaling exponent, k, and the interaction parameter, C_{ij}. The parachors labeled as "HVW" throughout the following discussion correspond to parachors

from methods described in thier work (6) and are summarized in Appendix D.

During the evaluation of the effectiveness of the HVW model, an attempt was made to find a useful correlation for the interaction parameters. Presented in Figures 25 and 26 are ideas which were investigated in this work. In Figure 25 the dependence of the interaction parameter on temperature is explored. The carbon dioxide systems show only a small dependence on temperature, and tend to favor a value near 1.0; the same is true for the methane-propane and methane-n-heptane binaries. The other methane binaries exhibit strange behavior which perhaps may be attributed to the fact that the data used were from a number of different sources. That is, the interfacial tension data, composition data and density data were not all obtained by the same investigators using the same apparatus. Figure 26 has the same theme as Figure 25; the difference is that the interaction parameter in Figure 26 is plotted against the molecular weight/carbon number ratio. This type of plot was investigated to find if the interaction parameter was specie dependent. The values for the carbon dioxide and ethane systems were for the 160°F isotherm. The values for the methane systems were obtained from averaging the values for all isotherms. The values of the interaction parameter for the carbon dioxide systems are approximately 1.0 and do not vary as a function of the molecular weight/carbon number ratio. The methane systems, upon further investigation, show that the methane + propane system with a MW/CN ratio = 14.7 and the methane + n-heptane system with a MW/CN ratio = 14.3 also have values near 1.0 for the interaction parameter at all isotherms investigated.

The HVW model was investigated in a series of cases similar to

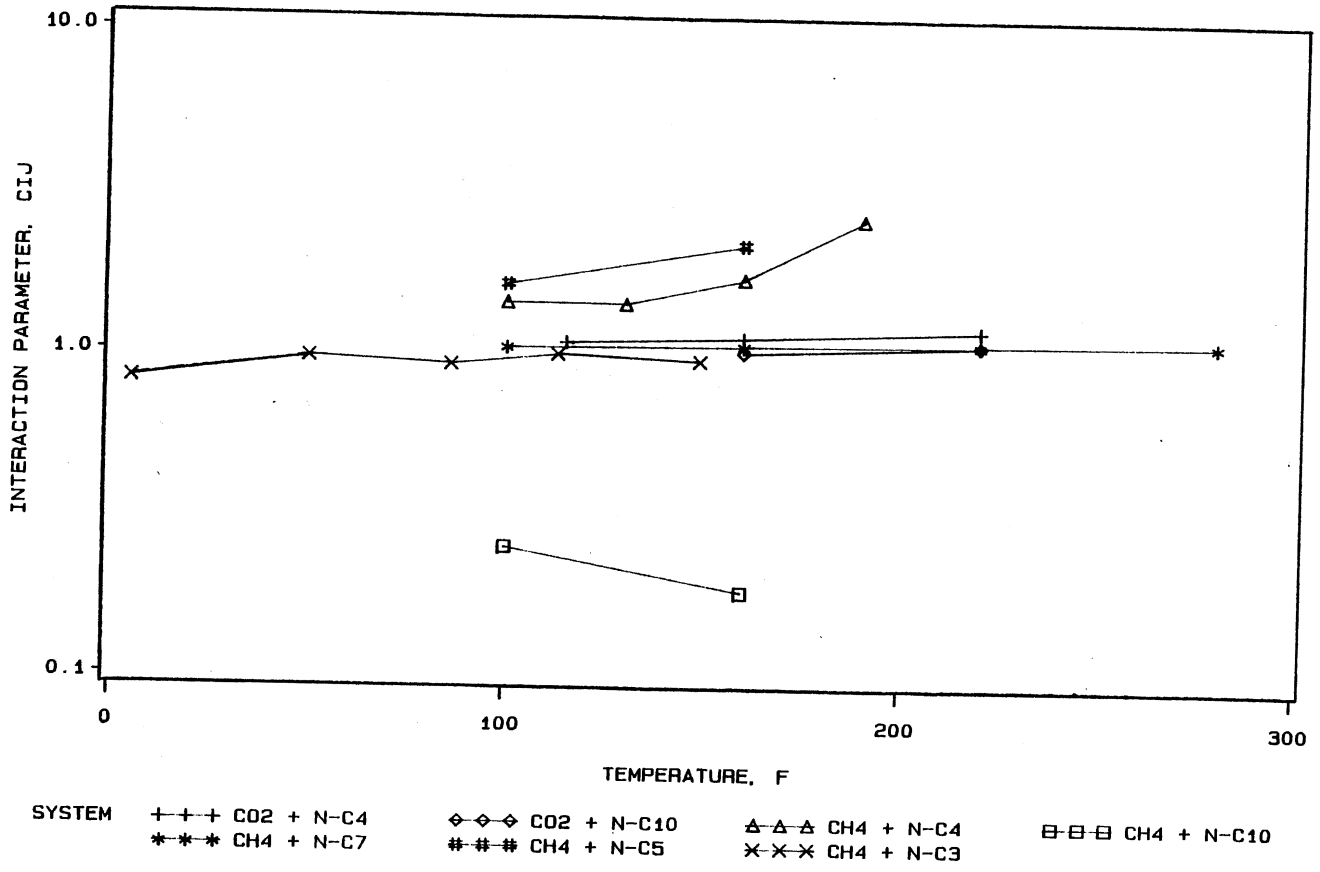

Figure 25. Dependence of the Interaction Parmeter, Cij, on Temperature for the Hugill-Van Welsenes Model, Case #2

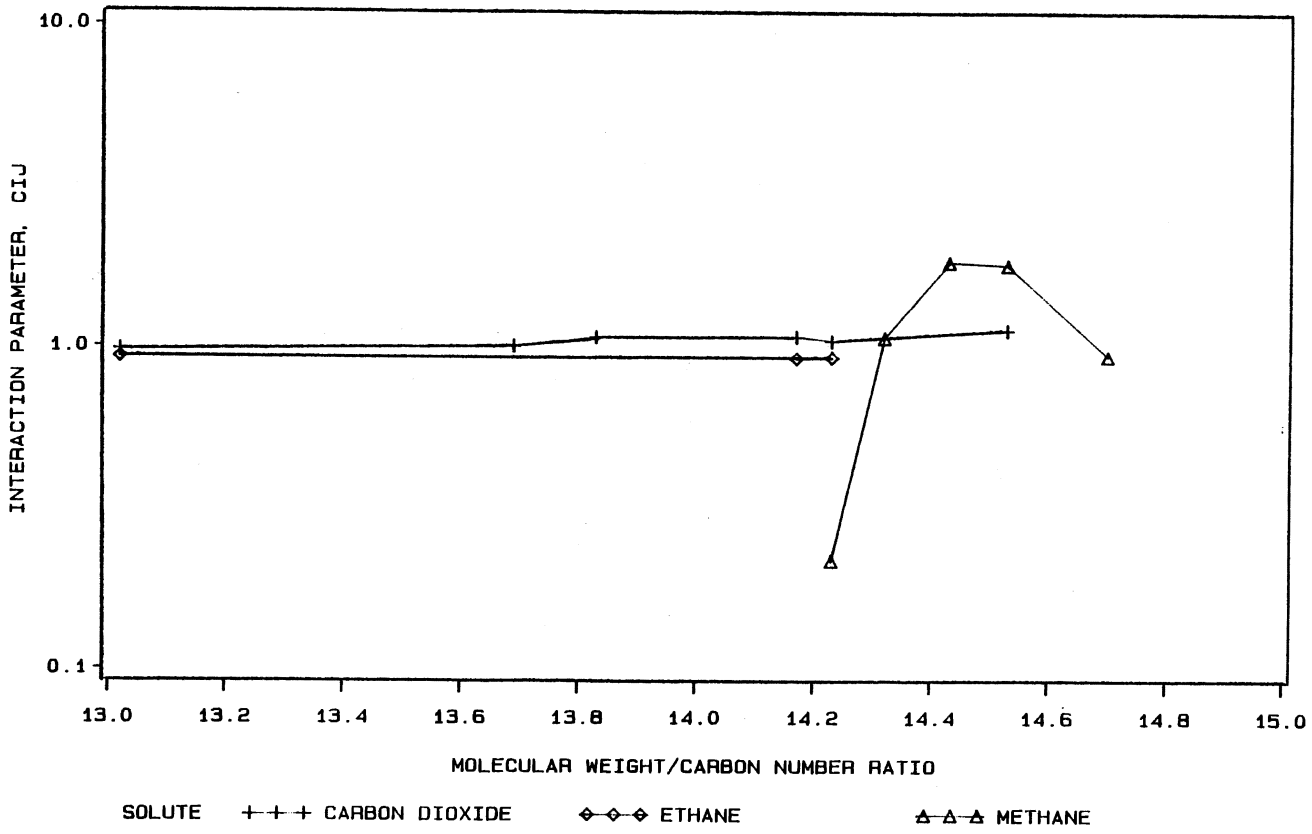

Figure 26. Dependence of the Interaction Parmeter, Cij, on the Molecular Weight to Carbon Number Ratio for the Hugill-Van Welsenes Model, Case #2

those for the Weinaug-Katz model. Table XXI present a description of each of thirteen cases investigated for the HVW model.

A sensitivity analysis of the parameters in the HVW model was performed. The effect the parachors have on the HVW model are very similar to the effect portrayed by the WK model as shown in Figure 16. The same is true for the sensitivity the model has for the solute parachor, P_1, and the scaling exponent, k, as shown in Figure 17. Figure 27 presents the sensitivity of the model to the interaction parameter, C_{ij}, and the scaling exponent, k. Both parameters have a substantial influence on the performance of the HVW model. The value which corresponds to a value of 0.0% on the C_{ij} axis is the the regressed value for the interaction parameter of 0.9237. (Incidently a value of 1.0 corresponds to an adjustment of 8.3% and an AAPD of 27%.) The regressed value for the scaling exponent is 3.40. Figure 28 shows the insensitivity of the model to the solute parachor; the solute parachor may be varied by ± 8% without greatly affecting the results. The parachors obtained through regression (which correspond to a deviation value of 0.0%) have values of 73.96 for ethane and 419.5 for trans-Decalin. The parachor values predicted using the method described by Hugill and Van Welsenes gives values of 112.6 for ethane and 377.9 for trans-Decalin. Because the predictions are reasonably insensitive to the solute parachor, variations of the solute parachor have a small effect on the performance of the model.

A summary of results for the cases explored, as described in Table XXI, is presented for the three solute (carbon dioxide, ethane, and methane) binaries in Tables XXII, XXIII, and XXIV. As can be seen from the tables, the HVW using generalized parameters is able to predict the

TABLE XXI

DESCRIPTION OF CASES STUDIED FOR THE HUGILL-VAN WELSENES IFT MODEL

CASE NO.	REGRESSED PARMS	FIXED PARAMETERS	CASE DESCRIPTION
1	NONE	P1 and P2 are from HVW, C_{ij} = 1.0, k = 4.0	The raw potential of the predicting capabilities of the model are tested in this case. The parachors are those suggested by Hugill and Van Welsenes; that is, the parachor is found from the reduced parachor as a function of the acentric factor. The interaction parameter, C_{ij}, is set to 1.0 and the value of the exponent, k, is set to 4.0.
2	$C_{ij}(T)$	P1 and P2 are from HVW, k = 4.0	This case tests the influence of the interaction parameter, C_{ij}. C_{ij} is regressed for each isotherm in the data set. The parachors are those of Hugill and Van Welsenes and the exponent, k, is 4.0.
3	$C_{ij}(T)$, k	P1 and P2 are from HVW	Both the interaction parameter for each isotherm, $C_{ij}(T)$, and the exponent, k, are regressed. The parachors are those of Hugill and Van Welsenes.
4	P1, p2, $C_{ij}(T)$, k	NONE	All three parameters are regressed, the the parachor, the interaction parameter for each iso- therm, $C_{ij}(T)$, and the exponent, k.

TABLE XXI (Continued)

5	$C_{ij}(MW)$	P1 and P2 are from HVW, k = 4.0	This case is similar to Case 2 in that both the parachor and the exponent are fixed and the inter- action parameter is regressed. The difference is that the interaction parameter regressed is for each system instead of each isotherm. (This case does not apply to the ethane systems since there is only one isotherm of data for each system.)
6	$C_{ij}(T)$, k	P1 and P2 are from HVW, Pr < 0.99	Both the interaction parameter at each temperature, $C_{ij}(T)$, and the exponent, k, are regressed. The parachors are those of Hugill and Van Welsenes. The only difference between this case and case 3 is that the data set is restricted reduced pressures of 0.99 or less.
7	$C_{ij}(T)$, k	P1 and P2 are generalized values	This case introduces the fitted parachors. The parachors are adjusted values of Quayles work. The adjusted parachors or generalized values , P(A), are found by reducing the solute parachor found in Quayles work by 15% and increasing the solvent parachor by 5%. The interaction parameter for each isotherm, $C_{ij}(T)$, and the exponent, k, are regressed.

TABLE XXI (Continued)

8	NONE	P1 and P2 are generalized values, C_{ij}=0.98	The parameters are are set to values generalized for each system. For all the systems (carbon dioxide, ethane, and methane) the parachor is set to the adjusted values discussed in Case 7 and the exponent, k, is set to 3.6. The interaction parameter, C_{ij}, was found for each solute system: $C_{ij}(CO_2$ systems) = 0.98, C_{ij}(ethane systems) = 0.96, C_{ij}(methane systems) = 0.97.
9	NONE	P1 and P2 are generalized values, C_{ij}=0.97	The parameters are are set to values generalized for all systems (carbon dioxide, ethane, and methane) the parachor is set to the adjusted values discussed in Case 7, the exponent, k, is set to 3.6, and the interaction parameter, C_{ij}, is set to 0.98.
10	NONE	P1 and P2 are generalized values, C_{ij}=1.00	The parameters are are set to values generalized for all systems (carbon dioxide, ethane, and methane) the parachor is set to the adjusted values discussed in Case 7, the component, k, is set to 3.6, and the interaction parameter, C_{ij}, is set to 1.00.
11	$C_{ij}(T)$, k	P1 and P2 are from Quayle	Both the interaction parameter for each isotherm, $C_{ij}(T)$, and the exponent, k, are regressed. The parachors are those of Quayle.

TABLE XXI (Continued)

12	$C_{ij}(T)$, k, P1	P2 is from HVW	The solute (CO_2, ethane, or methane) parachor, the exponent, k, and the interaction parameter for each isotherm, $C_{ij}(T)$ are regressed. The solvent parachors are those of Hugill and Van Welsenes.
13	$C_{ij}(T)$, k, P1	P2 is from Quayle	The solute (CO_2, ethane, or methane) parachor, the exponent, k, and the interaction parameter for each isotherm, $C_{ij}(T)$ are regressed. The solvent parachors are those of Quayle.

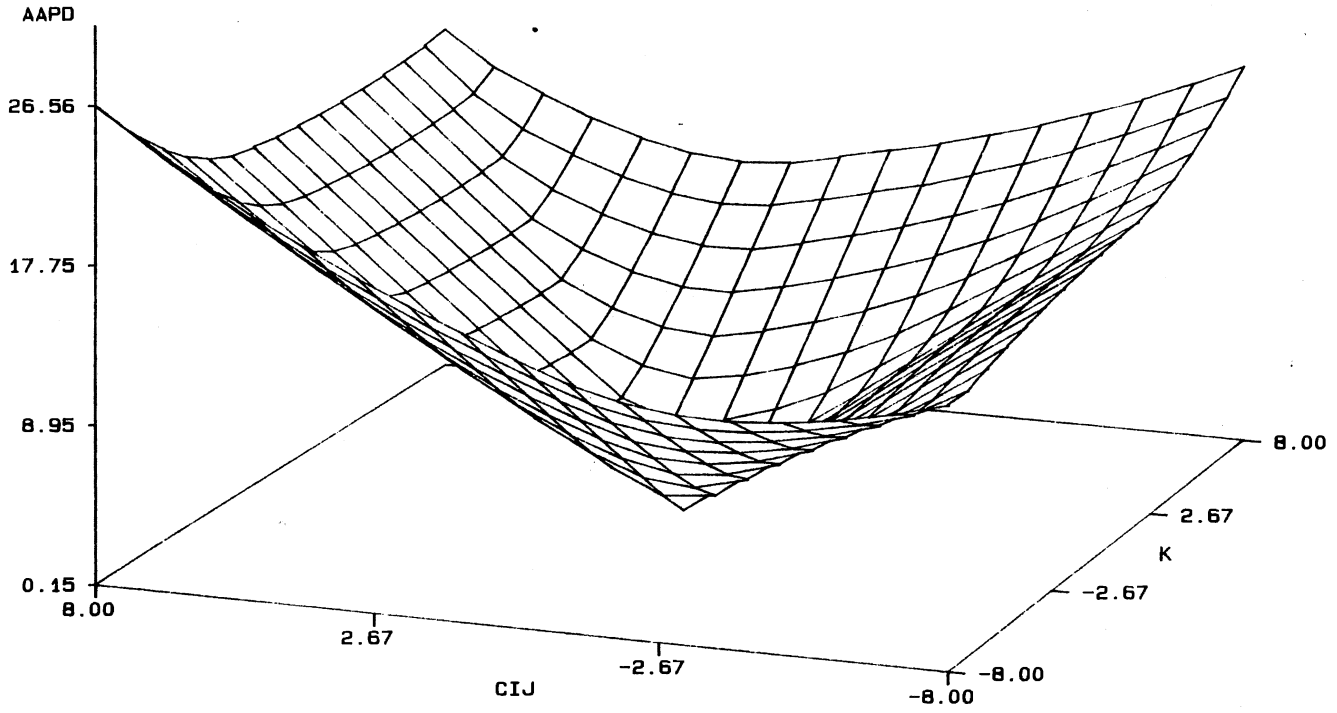

Figure 27. Sensitivity of the Hugill-Van Welsenes IFT Model to the Interaction Parameter, Cij, and the Scaling Exponent, k, for Ethane + trans-Decalin @ 344.3 K (160°F)

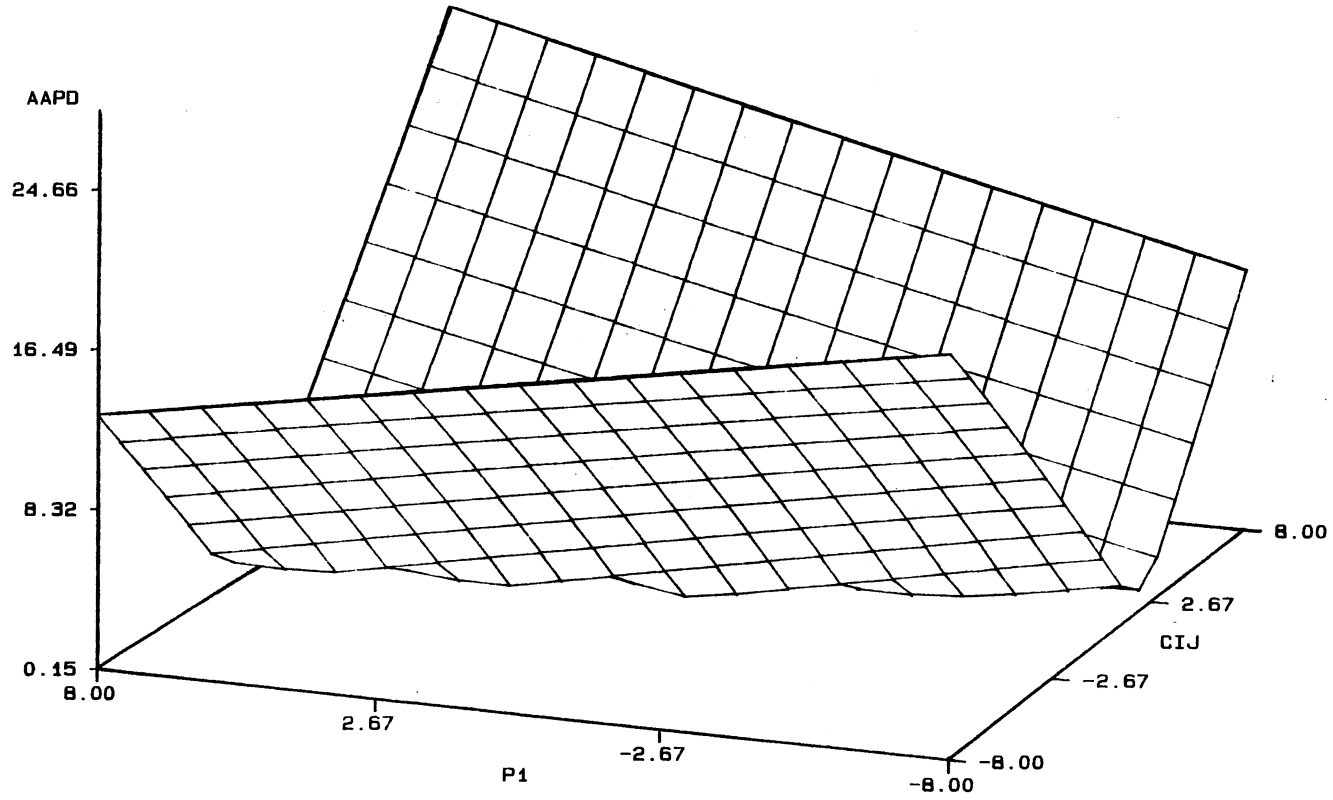

Figure 28. Sensitivity of the Hugill-Van Welsenes IFT Model to the Solute Parachor and the Interaction Parameter, Cij, for Ethane + trans-Decalin @ 344.3 K (160°F)

TABLE XXII

SUMMARY OF CASES STUDIED USING THE HUGILL-VAN WELSENES IFT MODEL FOR THE CARBON DIOXIDE + HYDROCARBON SYSTEMS

CASE NO.	REGRESSED PARMS	FIXED PARAMETERS	RMSE	AAPD	BIAS	k
1	NONE	P1 and P2 = HVW, C_{ij} = 1.0, k = 4.0	0.3712	23.08	0.0980	4.0
2	$C_{ij}(T)$	P1 and P2 = HVW, k = 4.0	0.5312	17.55	0.2313	4.0
3	$C_{ij}(T)$, k	P1 and P2 = HVW	0.2409	7.96	-0.0045	3.589
4	P1, p2, $C_{ij}(T)$, k	NONE	0.1192	4.94	-0.0044	3.689
5	C_{ij}(MW)	P1 and P2 = HVW, k = 4.0	0.2299	8.55	-0.0048	3.585
6	$C_{ij}(T)$, k	NONE, Pr < 0.99	0.2503	6.31	-0.0326	3.511
7	$C_{ij}(T)$, k	P1 and P2 = gen. values	0.2444	8.35	0.0130	3.550
8	NONE	P1 and P2 = gen. values, C_{ij}=0.98	0.1993	10.49	-0.0031	3.6
9	NONE	P1 and P2 = gen. values, C_{ij}=0.97	0.1966	11.34	-0.0336	3.6
10	NONE	P1 and P2 = gen. values, C_{ij}=1.00	0.2318	10.89	0.0508	3.6
11	$C_{ij}(T)$, k	P1 and P2 = Quayle	0.2444	7.96	-0.0114	3.606
12	$C_{ij}(T)$, k, P1	P2 = HVW	0.2446	7.93	-0.0056	3.590
13	$C_{ij}(T)$, k, P1	P2 = Quayle	0.2449	7.95	-0.2570	3.606

TABLE XXIII

SUMMARY OF CASES STUDIED USING THE HUGILL-VAN WELSENES IFT MODEL FOR THE ETHANE + HYDROCARBON SYSTEMS

CASE NO.	REGRESSED PARMS	FIXED PARAMETERS	RMSE	AAPD	BIAS	k
1	NONE	P1 and P2 = HVW, C_{ij} = 1.0, k = 4.	1.4081	22.74	0.7263	4.0
2	$C_{ij}(T)$	P1 and P2 = HVW, k = 4.0	0.6191	11.17	0.2788	4.0
3	$C_{ij}(T)$, k	P1 and P2 = HVW	0.2309	5.67	-0.0505	3.734
4	P1, p2, $C_{ij}(T)$, k	NONE	0.1468	3.47	-0.0062	3.536
5	Same as Case 2, one isotherm per binary.					
6	$C_{ij}(T)$, k	NONE, Pr < 0.99	0.2632	5.12	-0.0717	3.727
7	$C_{ij}(T)$, k	P1 and P2 = gen. values	0.1701	4.01	-0.0133	3.597
8	NONE	P1 and P2 = gen. values, C_{ij}=0.96	0.1623	5.63	0.0051	3.6
9	NONE	P1 and P2 = gen. values, C_{ij}=0.97	0.1826	5.59	0.0436	3.6
10	NONE	P1 and P2 = gen. values, C_{ij}=1.00	0.3452	8.60	0.1698	3.6
11	$C_{ij}(T)$, k	P1 and P2 = Quayle	0.3343	5.57	-0.0817	3.736
12	$C_{ij}(T)$, k, P1	P2 = HVW	0.4275	3.88	-0.0725	3.553
13	$C_{ij}(T)$, k, P1	P2 = Quayle	0.5056	4.01	-0.0950	3.570

TABLE XXIV

SUMMARY OF CASES STUDIED USING THE HUGILL-VAN WELSENES IFT MODEL FOR THE METHANE + HYDROCARBON SYSTEMS

CASE NO.	REGRESSED PARMS	FIXED PARAMETERS	RMSE	AAPD	BIAS	k
1	NONE	P1 and P2 = HVW, C_{ij} = 1.0, k = 4.	0.4579	15.97	-0.0516	4.0
2	$C_{ij}(T)$	P1 and P2 = HVW, k = 4.0	0.5899	11.98	0.0441	4.0
3	$C_{ij}(T)$, k	P1 and P2 = HVW	0.5881	9.99	-0.2257	3.706
4	P1, p2, $C_{ij}(T)$, k	NONE	0.1476	5.11	-0.0272	3.515
5	C_{ij}(MW)	P1 and P2 = HVW, k = 4.0	2.9126	48.12	-1.8584	3.542
6	$C_{ij}(T)$, k	NONE, Pr < 0.99	0.5668	9.26	-0.2049	3.734
7	$C_{ij}(T)$, k	P1 and P2 = gen. values	0.3321	7.16	-0.1147	3.613
8	k, C_{ij}	P1 and P2 = HVW	0.4992	11.83	-0.2350	3.6
9	NONE	P1 and P2 = gen. values, C_{ij}=0.97	0.5049	11.85	-0.2402	3.6
10	NONE	P1 and P2 = gen. values, C_{ij}=1.00	0.4372	11.59	-0.1714	3.6
11	$C_{ij}(T)$, k	P1 and P2 = Quayle	0.7000	11.24	-0.2748	3.755
12	$C_{ij}(T)$, k, P1	P2 = HVW	0.2973	5.99	-0.0975	3.745
13	$C_{ij}(T)$, k, P1	P2 = Quayle	0.3481	6.58	-0.1196	3.809

data within 11.9%. Using the model with parachors calculated using methods described by the authors and an interaction parameter of 1.0, the model is able to predict data within 23% of the experimental data. By regressing the interaction parameter the model is then able to predict within 17.6% for all systems and within 12% for the ethane and methane binary systems. Table XXV compares the various cases for the HVW model. As seen for the WK model the methane and ethane binaries are more readily predicted using the HVW model for all cases. From this table the observation may be made that the interaction parameter based on molecular species (Case 5) is not suitable for the methane binaries as was seen from Figure 26.

A case-by-case profile for the HVW model for the three solutes appears in Figures 29, 30, and 31. The trans-Decalin systems are seen again to be the most difficult to fit using the models at hand. These figures present the absolute average percent deviation (AAPD) between the predicted values and the experimental values for IFT as a function of the molecular weight of the solvent in the binary.

As with the Weinaug-Katz model, the case which presents the lowest AAPD and lowest RMSE for all systems is the regressed case (Case 4). Tables XXVI, XXVII, and XXVIII show the values obtained for the interaction parameter at each isotherm, the scaling exponent, k, and the two parachors. The percent deviation for Case 4 as a function of scaled pressure is shown in Figures 32, 33, and 34. The scatter of the percent deviation using both the WK and HVW model suggest that the error associated with the data is rather random.

As a final comparison of the different cases, Figure 35 presents a comparison of predicted values for three of the cases with the

TABLE XXV

CASE COMPARISONS FOR THE HUGILL-VAN WELSENES IFT MODEL

CASE NO.	ABSOLUTE AVERAGE PERCENT DEVIATION, AAPD		
	Carbon Dioxide	Ethane	Methane
1	23.08	22.74	15.97
2	17.55	11.17	11.98
3	7.96	5.67	9.99
4	4.94	3.47	5.11
5	8.55	11.17	48.12
6	6.31	5.12	9.26
7	8.35	4.01	7.16
8	10.49	5.63	11.83
9	11.34	5.59	11.85
10	10.89	8.60	11.59
11	7.96	5.57	11.24
12	7.93	3.88	5.99
13	7.95	4.01	6.58

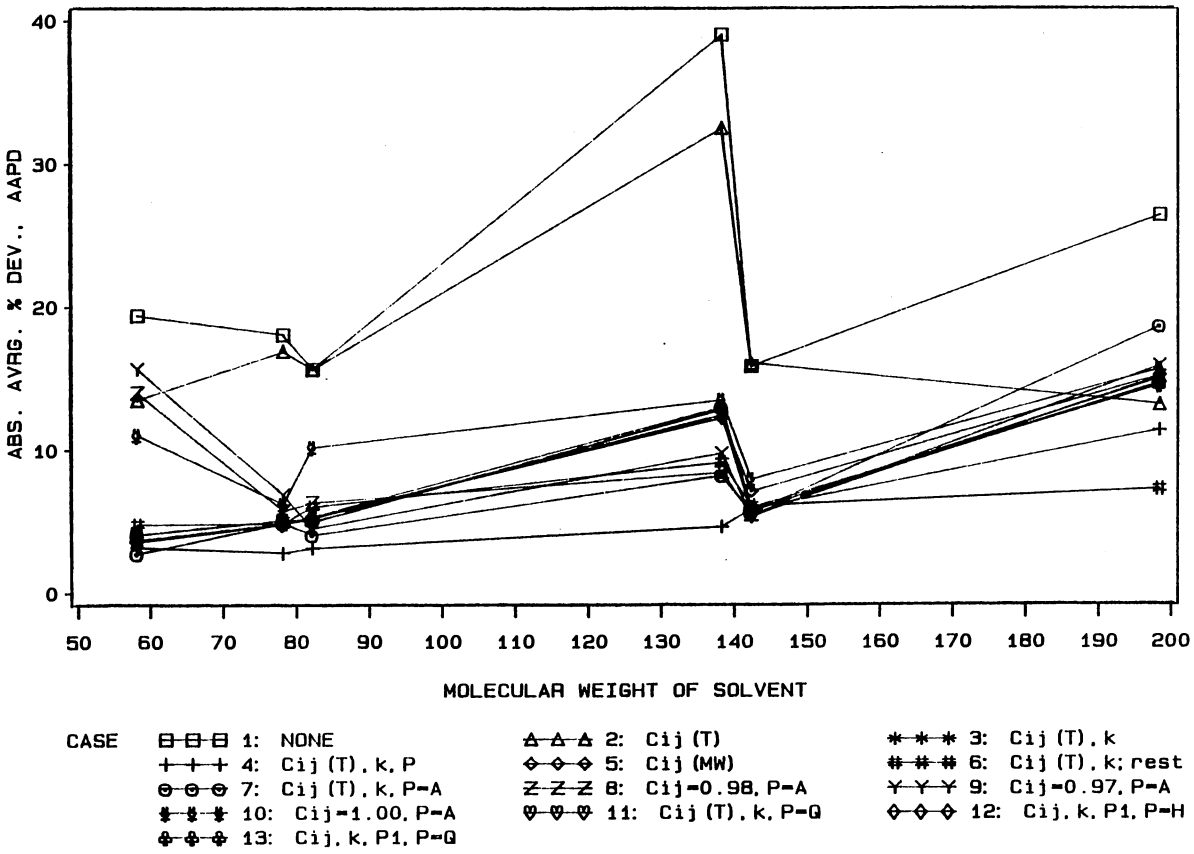

Figure 29. Case Profile of the Hugill-Van Welsenes Model for the Carbon Dioxide + Hydrocarbon Systems

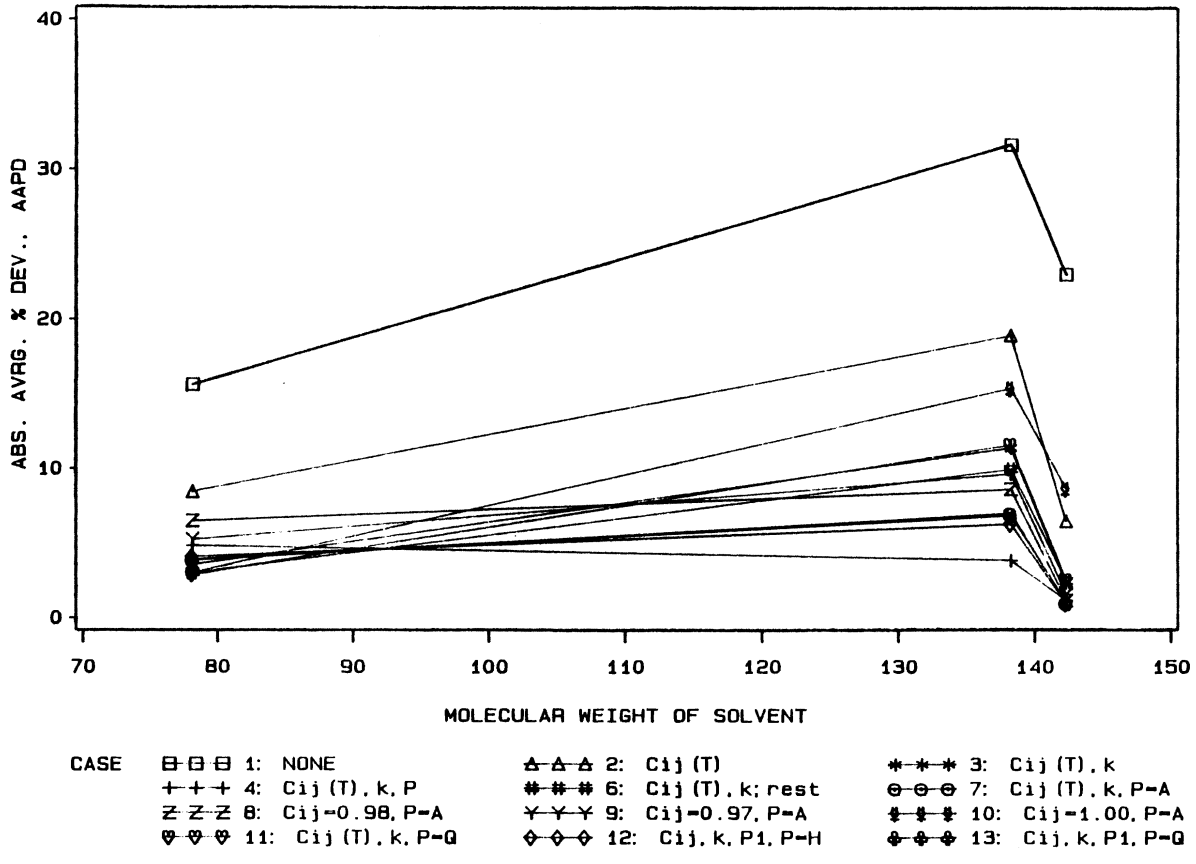

Figure 30. Case Profile of the Hugill-Van Welsenes Model for the Ethane + Hydrocarbon Systems

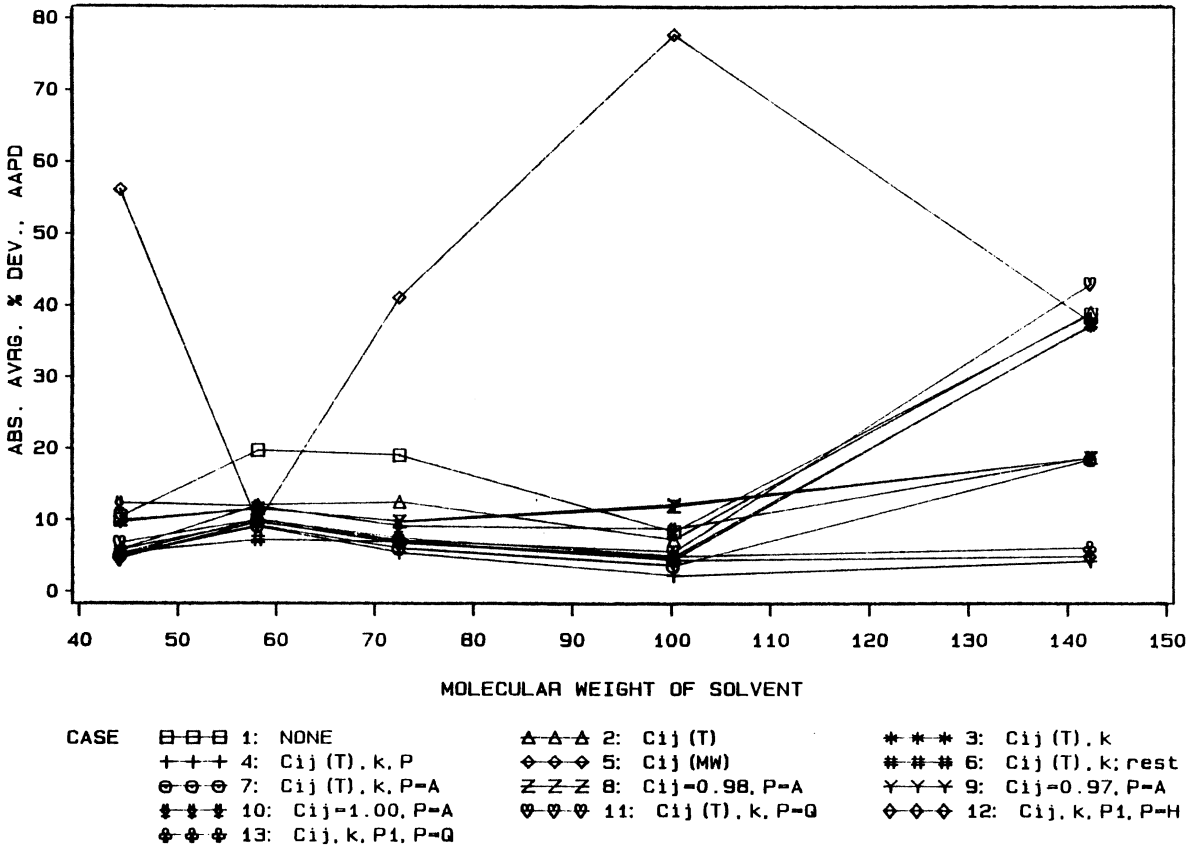

Figure 31. Case Profile of the Hugill-Van Welsenes Model for the Methane + Hydrocarbon Systems

TABLE XXVI

SUMMARY OF THE OVERALL STATISTICS FOR THE HUGILL-VAN WELSENES MODEL, CASE 4, USING DATA FOR THE CARBON DIOXIDE + HYDROCARBON SYSTEMS

ISO	T(F)	SYSTEM	PAR(1)	PAR(2)	K	C(I,J)	EMIN	EMAX	RMSE	WRMS	BIAS	AAPD	AAWPD	NO PT
1	160.	CO_2 + BENZENE	105.8	247.7	3.689	0.679	0.6297	0.9975	0.0560	0.59	-0.0059	2.79	5.04	15
2	115.	CO_2 + n-BUTANE	105.8	198.0	3.689	0.843	0.2857	0.9901	0.1108	0.84	0.0278	3.65	4.57	18
3	160.	CO_2 + n-BUTANE	105.8	198.0	3.689	0.924	0.3947	0.9805	0.0483	0.68	-0.0122	3.18	4.86	12
4	220.	CO_2 + n-BUTANE	105.8	198.0	3.689	0.958	0.3807	0.9636	0.0259	0.63	-0.0155	3.09	4.78	12
5	160.	CO_2 + CYCLOHEXANE	105.8	275.6	3.689	0.752	0.6270	0.9975	0.0469	0.67	-0.0053	3.14	5.05	14
6	160.	CO_2 + n-DECANE	205.8	434.9	3.689	0.987	0.5449	0.9930	0.2245	1.45	-0.0609	5.85	4.45	17
7	220.	CO_2 + n-DECANE	105.8	434.9	3.689	1.061	0.6274	0.9979	0.0547	0.91	0.0227	5.20	5.44	23
8	160.	CO_2 + t-DECALIN	105.8	79.8	3.689	3.808	0.6530	0.9856	0.1803	1.14	-0.0162	4.62	5.92	20
9	160.	CO_2 + TETRADECANE	105.8	400.7	3.689	1.679	0.6742	0.9952	0.1065	2.13	0.0101	11.40	5.53	17

RMSE= 0.1192, AAPD = 4.94, BIAS = -0.0044, DMIN= -21.10, EMIN=0.2857
WRMS= 1.04, AAWPD= 5.12, WBIAS= -0.0932, DMAX= 27.47, EMAX=0.9979, NPIS = 148

TABLE XXVII

SUMMARY OF THE OVERALL STATISTICS FOR THE HUGILL-VAN WELSENES MODEL, CASE 4, USING DATA FOR THE ETHANE + HYDROCARBON SYSTEMS

ISO	T(F)	SYSTEM	PAR(1)	PAR(2)	K	C(I,J)	EMIN	EMAX	RMSE	WRMS	BIAS	AAPD	AAWPD	NO PT
1	160.	C_2H_6 + n-DECANE	80.7	427.1	3.536	1.108	0.3490	0.9860	0.1114	0.34	-0.0008	1.15	4.36	20
2	160.	C_2H_6 + T-DECALIN	80.7	395.5	3.536	0.974	0.1669	0.9917	0.2110	0.90	-0.0166	3.84	4.48	22
3	160.	C_2H_6 + BENZENE	80.7	193.5	3.536	1.258	0.4907	0.9980	0.0999	0.82	-0.0020	4.83	5.99	28

RMSE= 0.1468, AAPD = 3.47, BIAS = -0.0062, DMIN= -9.18, EMIN=0.1669
WRMS= 0.71, AAWPD= 5.05, WBIAS= -0.0197, DMAX= 20.28, EMAX=0.9980, NPIS = 70

TABLE XXVIII

SUMMARY OF THE OVERALL STATISTICS FOR THE HUGILL-VAN WELSENES MODEL, CASE 4, USING DATA FOR THE METHANE + HYDROCARBON SYSTEMS

ISO	T(F)	SYSTEM	PAR(1)	PAR(2)	K	C(I,J)	EMIN	EMAX	RMSE	WRMS	BIAS	AAPD	AAWPD	NO PT
1	100.	CH_4 + n-BUTANE	43.1	210.9	3.515	0.477	0.5230	0.9937	0.0382	1.77	-0.0073	12.41	4.93	11
2	130.	CH_4 + n-BUTANE	43.1	210.9	3.515	-0.118	0.5330	0.9861	0.0737	1.69	-0.0393	9.49	5.07	10
3	160.	CH_4 + n-BUTANE	43.1	210.9	3.515	-1.065	0.5525	0.9945	0.0725	1.55	-0.0487	8.22	5.92	9
4	190.	CH_4 + n-BUTANE	43.1	210.9	3.515	-1.251	0.5889	0.9717	0.0647	0.87	0.0310	4.17	5.62	7
5	100.	CH_4 + n-DECANE	43.1	447.2	3.515	1.065	0.3766	0.9887	0.1204	1.02	0.0278	4.16	4.47	9
6	160.	CH_4 + n-DECANE	43.1	447.2	3.515	1.115	0.3855	0.9638	0.2454	1.17	-0.1184	4.35	4.02	8
7	100.	CH_4 + n-HEPTANE	43.1	340.0	3.515	0.975	0.0554	0.6234	0.3188	0.98	-0.1049	2.56	2.63	10
8	160.	CH_4 + n-HEPTANE	43.1	340.0	3.515	0.952	0.0564	0.7749	0.1620	0.65	-0.0737	1.84	2.86	12
9	220.	CH_4 + n-HEPTANE	43.1	340.0	3.515	0.961	0.0606	0.8338	0.0912	0.73	0.0453	2.44	3.00	12
10	280.	CH_4 + n-HEPTANE	43.1	340.0	3.515	0.947	0.0683	0.7687	0.0630	0.53	0.0420	1.69	3.03	10
11	100.	CH_4 + n-PENTANE	43.1	244.0	3.515	1.071	0.4073	0.9165	0.1212	0.94	-0.0306	3.42	3.60	6
12	160.	CH_4 + n-PENTANE	43.1	244.0	3.515	1.349	0.2566	0.9624	0.1508	1.56	-0.0332	6.74	3.78	8
13	5.	CH_4 + n-PROPANE	43.1	161.4	3.515	0.836	0.1481	0.5160	0.2475	1.68	-0.1585	5.28	3.24	5
14	50.	CH_4 + n-PROPANE	43.1	161.4	3.515	0.926	0.1145	0.6895	0.0625	0.51	-0.0071	1.86	3.39	7
15	86.	CH_4 + n-PROPANE	43.1	161.4	3.515	0.835	0.1215	0.6796	0.1602	2.25	-0.1095	8.91	3.56	12
16	113.	CH_4 + n-PROPANE	43.1	161.4	3.515	0.854	0.1972	0.5564	0.0730	0.47	0.0256	1.58	3.64	11
17	149.	CH_4 + n-PROPANE	43.1	161.4	3.515	0.403	0.3074	0.6608	0.1497	1.90	0.0881	7.20	4.14	6

RMSE= 0.1476, AAPD = 5.11, BIAS = -0.0272, DMIN= -79.56, EMIN=0.0554
WRMS= 1.18, AAWPD= 3.90, WBIAS= -0.1786, DMAX= 30.09, EMAX=0.9945, NPIS = 153

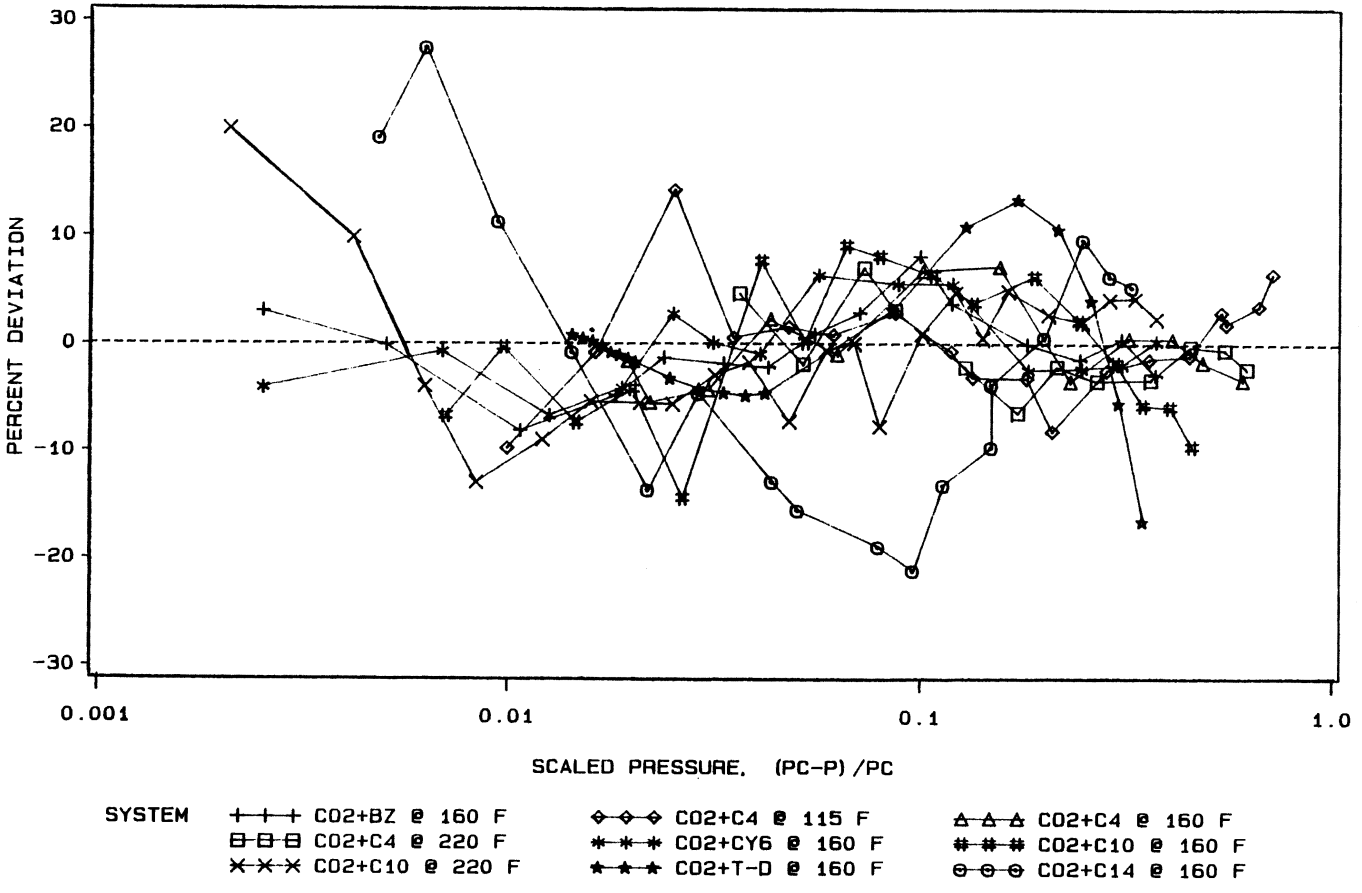

Figure 32. Evaluation of the Hugill-Van Welsenes Model, Case 4, for the Carbon Dioxide + Hydrocarbon Systems. The Interaction Parameter, Scaling Exponent, and the Solute and Solvent Parachors are Regressed

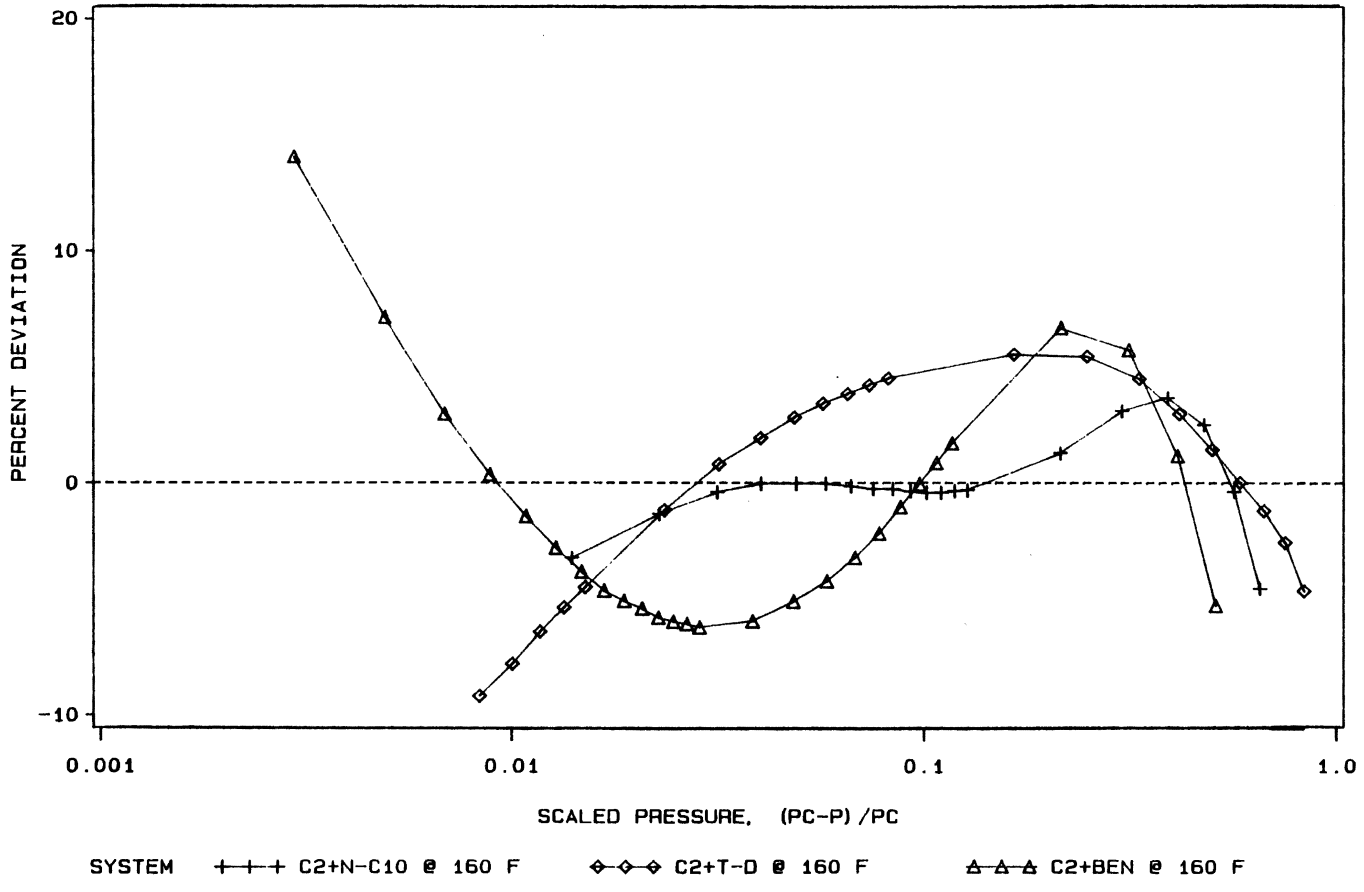

Figure 33. Evaluation of the Hugill-Van Welsenes Model, Case 4, for the Ethane + Hydrocarbon Systems. The Interaction Parameter, Scaling Exponent, and the Solute and Solvent Parachors are Regressed

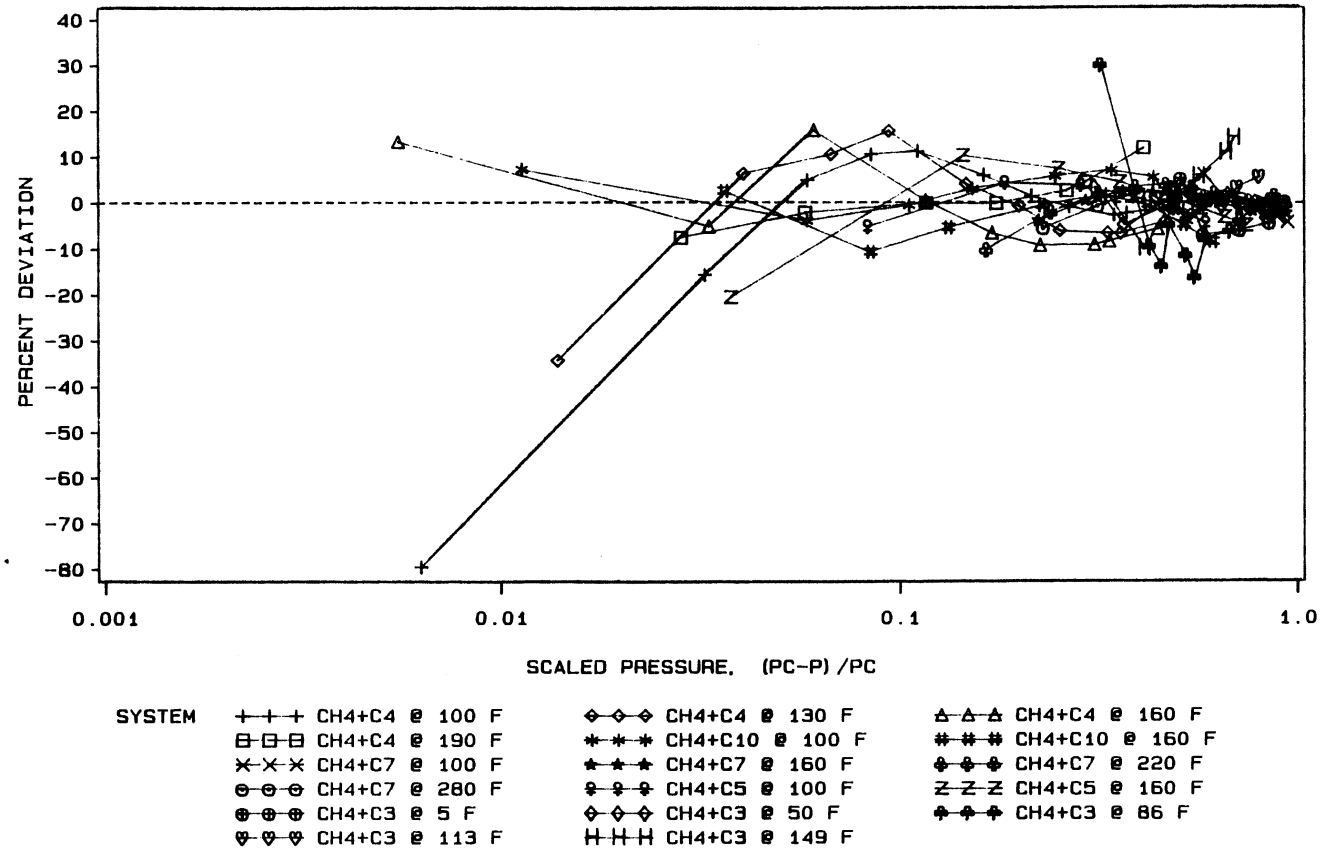

Figure 34. Evaluation of the Hugill-Van Welsenes Model, Case 4, for the Methane + Hydrocarbon Systems. The Interaction Parameter, Scaling Exponent, and the Solute and Solvent Parachors are Regressed

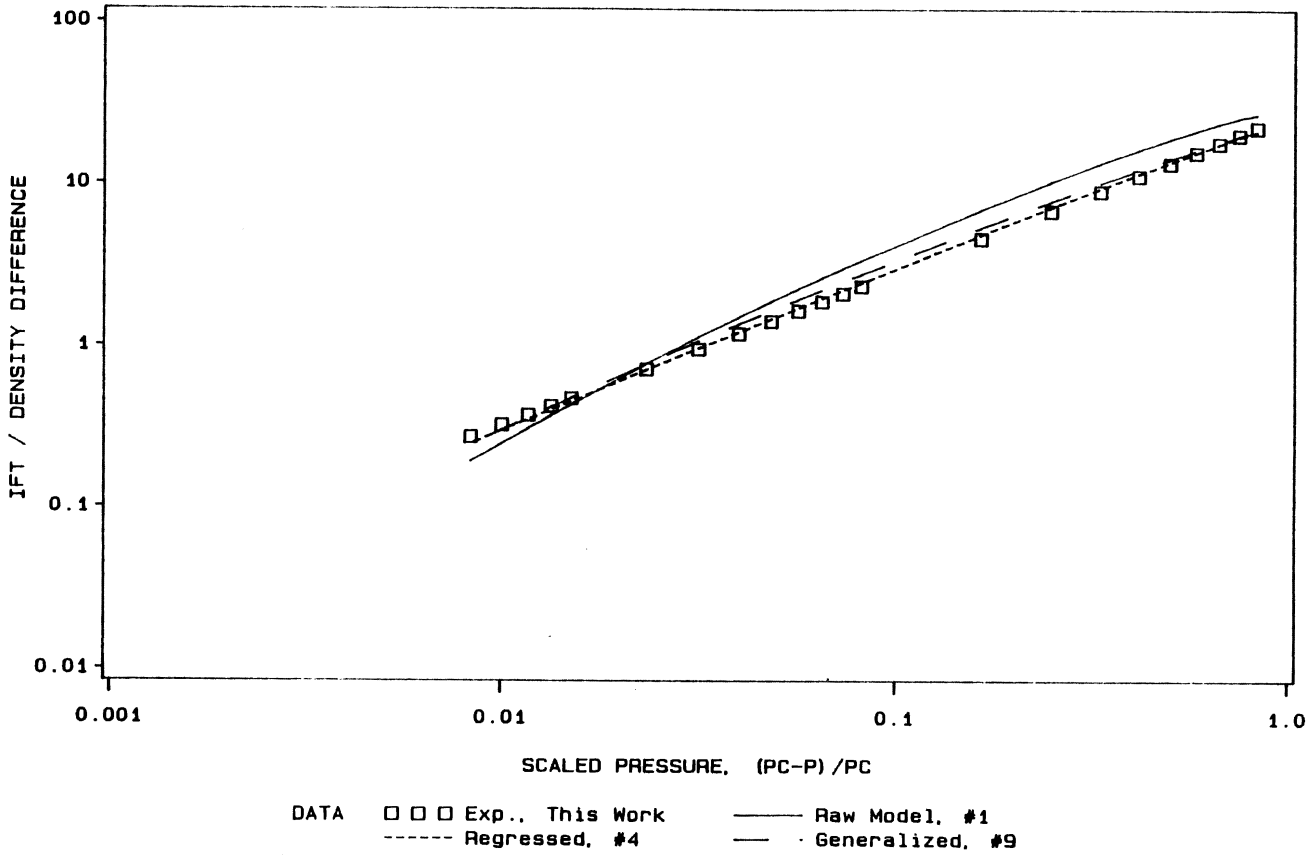

Figure 35. Comparison of the Ability of the Hugill-Van Welsenes IFT Model to Predict Experimental Data for Ethane + trans-Decalin @ 344.3 K (160°F)

experimental values for $\gamma/\Delta\rho$. The three cases plotted are similar to the those for Weinaug-Katz model shown in Figure 24. Case 1 represents the ability of the HVW model as presented originally. Case 4 uses the HVW model with all parameters (P1, P2, C_{ij}, and k) regressed. Case 9 is the generalized case in which the values from Quayle are varied by -15% for the solute parachor and +5% for the solvent parachor, k is held equal to 3.6, and the interaction parameter is held equal to 0.97 for all solutes and isotherms. The generalized case fits the data almost as well as the regressed case, especially in the high-pressure near-critical regions, which may be largely attributed to the value chosen for the scaling exponent; k = 3.6.

Evaluation of the Lee-Chien IFT Model

The Lee-Chien (LC) correlation is based on scaling theory and contains two major features: (1) a method to predict pure component parachors which is consistent with the theory of corresponding states and (2) an approach is proposed to calculate the parachors of mixtures.

The case descriptions for the four cases investigated for the LC model are presented in Table XXIX. The model parameter, B, was investigated instead of the parachor. However, the influence B has on the model is similar to the effect the parachor has on the WK and HVW models. The sensitivity of the regressed parameters (B1, B2, and k) in the LC model is similar to the Weinaug-Katz model. The effect the solute density coexistence curve parameter, B, has on the absolute average percent deviation of the predicted value for the interfacial tension is relatively small in comparison to the solvent density coexistence curve parameter and the scaling exponent, as was shown for

TABLE XXIX

DESCRIPTION OF CASES STUDIED FOR THE LEE-CHIEN IFT MODEL

CASE NO.	REGRESSED PARMS	FIXED PARAMETERS	CASE DESCRIPTION
1	NONE	B1 and B2 are from LC mixing rules, k = 3.911	The raw potential of the predicting capabilities of the model are tested in this case. The parachors used are obtained using the method outlined in the work of Lee and Chien, as discused in Appendix E. The value for the exponent is the value suggested by scaling law theory, k = 176/45 or 3.911.
2	B1, B2	k = 3.911	The density coexistence curve parameter, B, is regressed and the value of the exponent, k, is held constant and equal to 3.911.
3	B, k	NONE	This case regresses for both the density coexistence curve parameter, B, and the exponent, k.
4	B1, k	B2 is from LC mixing rules	The solute (CO_2, ethane, or methane) density coexistence curve parameter and the exponent, k are regressed. The solvent density coexistence curve parameters are held constant and equal to the values found through the methods described by Lee and Chien.

the solute parachor in the WK and HVW models.

Summaries of the statistics produced for the various cases explored during the evaluation of the LC model appear in Tables XXX, XXXI, and XXXII. Each table presents the cases for a particular solute of interest. Table XXX contains the case summaries for carbon dioxide, table XXXI has the summaries for ethane and the methane case summaries are in Table XXXII. The LC model is able to predict the IFTs for the light hydrocarbon/hydrocarbon systems far better than for the carbon dioxide systems. The LC model is able to predict the ethane systems within 4% (Case 3) but only manages to predict the carbon dioxide systems within 10.2% (same case). The generalized approach obtained for the WK and HVW models are not compatible with the LC model. The comparisons of the three solutes appear in Table XXXIII, in this table the three solutes may be compared for each case investigated. Again the carbon dioxide systems pose the most difficulty for prediction using the LC model; similar results were obtained for the WK and HVW models. (A complete compendium for the cases studied are available through Oklahoma State University (72).)

The results of each case for the LC model are shown in Figures 36, 37, and 38, which correspond to the carbon dioxide, ethane and methane solutes. From the figures the observation may be made that the regressed case (Case 3) fits the data the best for all solvents. As with the WK and HVW models, the fully regressed case (Case 3) is presented for each isotherm, these are shown in Tables XXXIV, XXXV, and XXXVI. A graphical comparison of the percent deviation of experimental and predicted values for each data point acquired is presented for Case 3 in Figures 39, 40, and 41.

TABLE XXX

SUMMARY OF CASES STUDIED USING THE LEE-CHIEN IFT MODEL
FOR THE CARBON DIOXIDE + HYDROCARBON SYSTEMS

CASE NO.	REGRESSED PARMS	FIXED PARAMETERS	RMSE	AAPD	BIAS	k
1	NONE	B1 and B2 = LC mix rules, k = 3.911	1.0624	30.50	0.5268	3.911
2	B1, B2	k = 3.911	0.3916	14.10	0.0738	3.911
3	B1, B2, k	NONE	0.3003	10.18	-0.0237	3.627
4	B1, k	B2 = LC mix rules	0.2825	13.02	0.0759	3.587

TABLE XXXI

SUMMARY OF CASES STUDIED USING THE LEE-CHIEN IFT MODEL
FOR THE ETHANE + HYDROCARBON SYSTEMS

CASE NO.	REGRESSED PARMS	FIXED_PARAMETERS	RMSE	AAPD	BIAS	k
1	NONE	B1 and B2 = LC mix rules, k = 3.91	0.9325	20.19	0.4897	3.911
2	B1, B2	k = 3.911	0.4721	8.45	-0.0401	3.911
3	B1, B2, k	NONE	0.0630	3.92	0.0138	3.548
4	B1, k	B2 = LC mix rules	0.2056	4.80	0.0078	3.510

TABLE XXXII

SUMMARY OF CASES STUDIED USING THE LEE-CHIEN IFT MODEL
FOR THE METHANE + HYDROCARBON SYSTEMS

CASE NO.	REGRESSED PARMS	FIXED PARAMETERS	RMSE	AAPD	BIAS	k
1	NONE	B1 and B2 = LC mix rules, k = 3.91	0.3670	13.39	-0.1134	3.911
2	B1, B2	k = 3.911	0.3422	9.38	0.1075	3.911
3	B1, B2, k	NONE	0.2320	7.12	-0.0024	3.628
4	B1, k	B2 = LC mix rules	0.3123	9.81	0.0021	3.745

TABLE XXXIII

CASE COMPARISONS FOR THE LEE-CHIEN IFT MODEL

CASE NO.	ABSOLUTE AVERAGE PERCENT DEVIATION, AAPD		
	Carbon Dioxide	Ethane	Methane
1	30.50	20.19	13.39
2	14.10	8.45	9.38
3	10.18	3.92	7.12
4	13.02	4.80	9.81

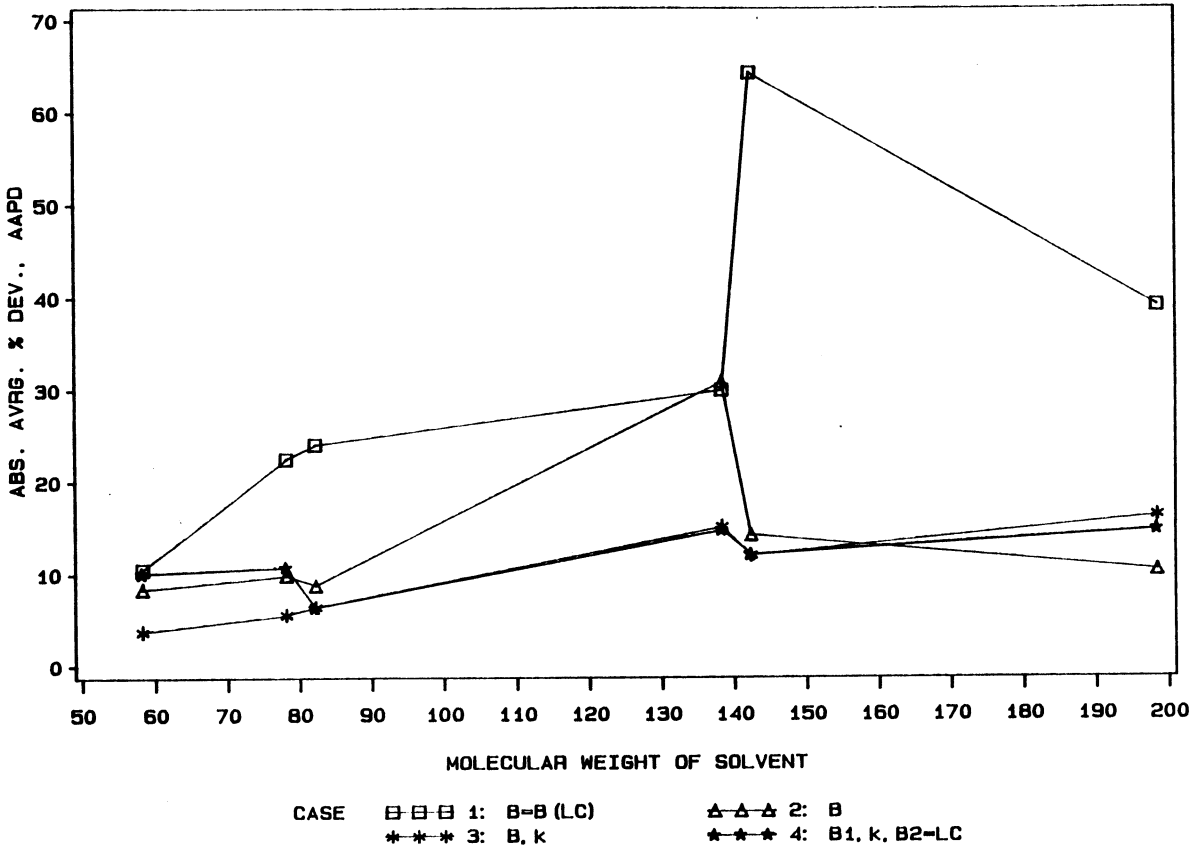

Figure 36. Case Profile of the Lee-Chien Model for the Carbon Dioxide + Hydrocarbon Systems

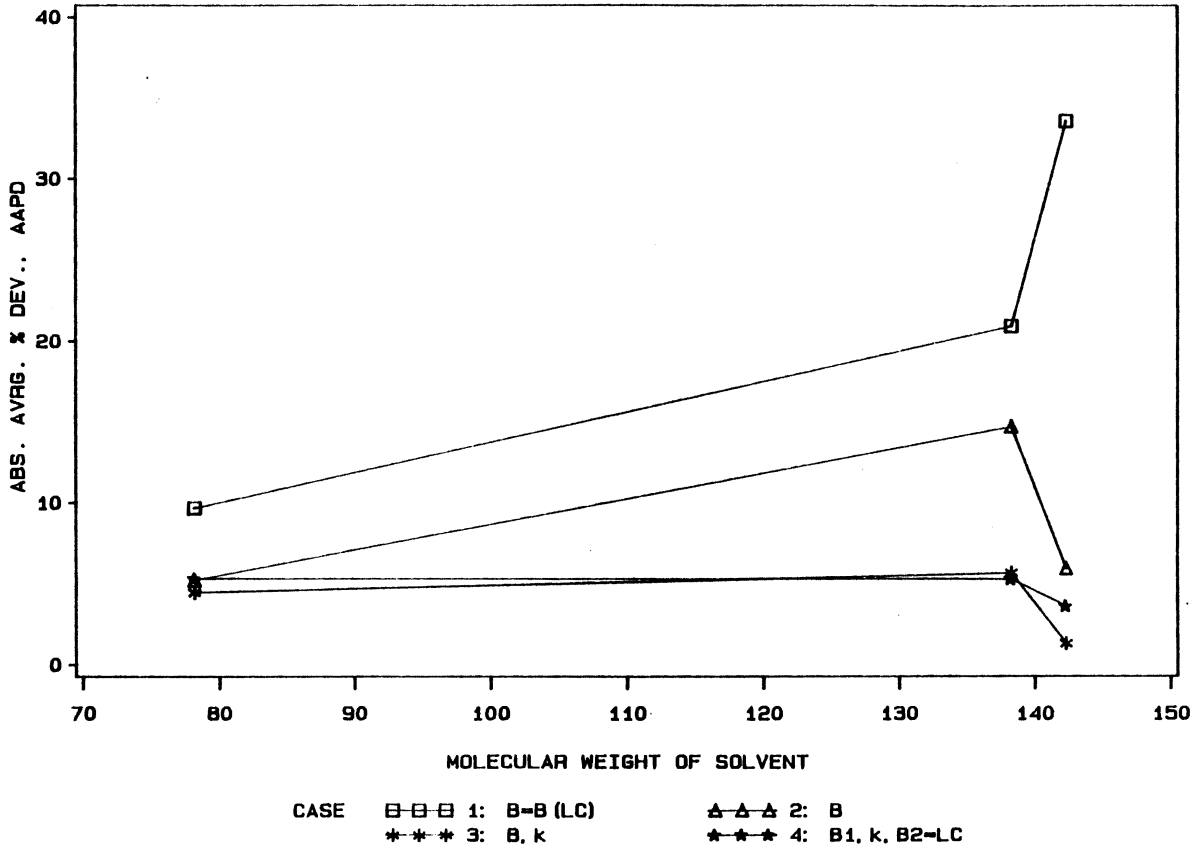

Figure 37. Case Profile of the Lee-Chien Model for the Ethane + Hydrocarbon Systems

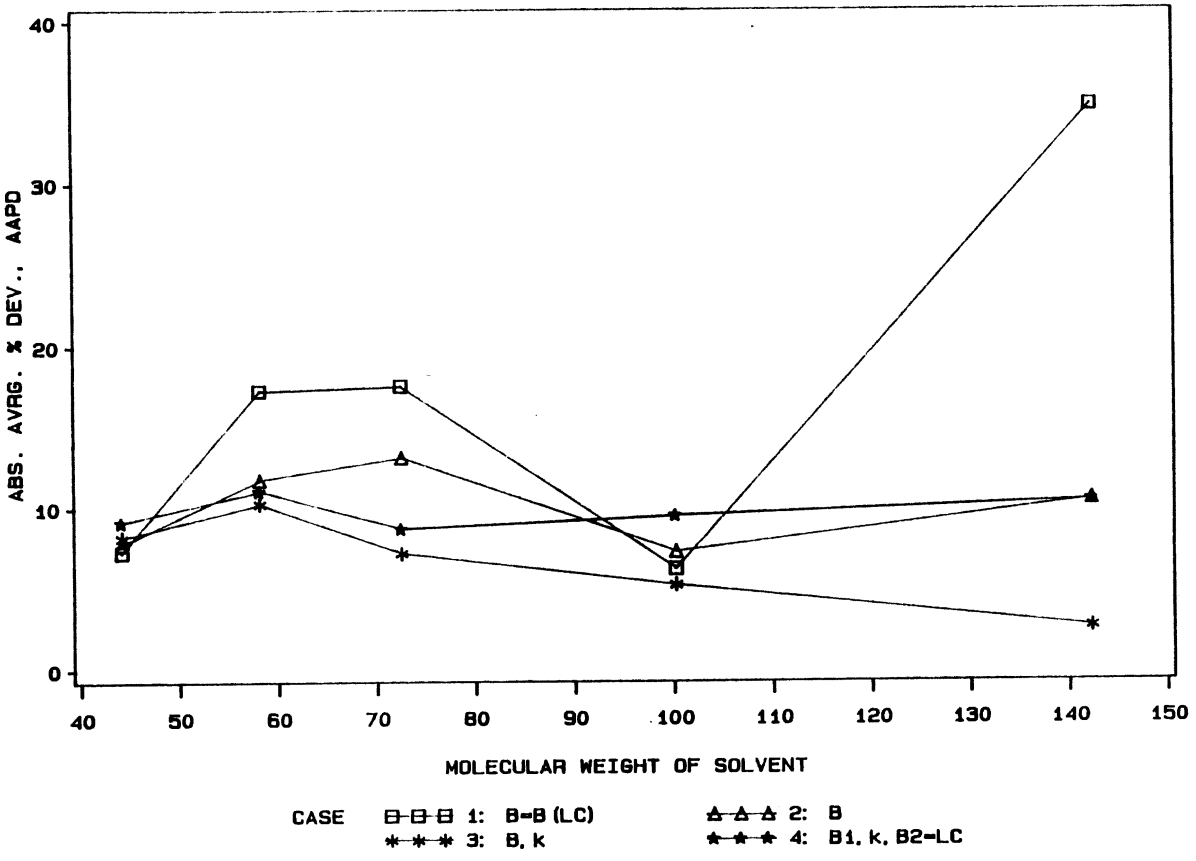

Figure 38. Case Profile of the Lee-Chien Model for the Methane + Hydrocarbon Systems

TABLE XXXIV

SUMMARY OF THE OVERALL STATISTICS FOR THE LEE-CHIEN MODEL, CASE 3,
USING DATA FOR THE CARBON DIOXIDE + HYDROCARBON SYSTEMS

ISO	T(F)	SYSTEM	PAR(1)	PAR(2)	K	C(I,J)	EMIN	EMAX	RMSE	WRMS	BIAS	AAPD	AAWPD	NO PT
1	160.	CO_2 + BENZENE	4.290	4.189	3.627	0.000	0.6297	0.9975	0.2644	1.36	-0.0676	5.55	5.04	15
2	115.	CO_2 + n-BUTANE	4.290	3.888	3.627	0.000	0.2857	0.9901	0.3232	3.29	0.1421	14.91	4.57	18
3	160.	CO_2 + n-BUTANE	4.290	3.888	3.627	0.000	0.3947	0.9805	0.0524	0.76	-0.0149	3.76	4.86	12
4	220.	CO_2 + n-BUTANE	4.290	3.888	3.627	0.000	0.3807	0.9636	0.0553	0.94	-0.0313	4.41	4.78	12
5	160.	CO_2 + CYCLOHEXANE	4.290	4.234	3.627	0.000	0.6270	0.9975	0.2959	1.62	-0.1042	6.39	5.05	14
6	160.	CO_2 + n-DECANE	4.290	5.042	3.627	0.000	0.5449	0.9930	0.4915	3.01	-0.1290	11.93	4.45	17
7	220.	CO_2 + n-DECANE	4.290	5.042	3.627	0.000	0.6274	0.9979	0.2132	1.73	-0.1056	8.20	5.44	23
8	160.	CO_2 + t-DECALIN	4.290	4.026	3.627	0.000	0.6530	0.9856	0.4147	3.20	0.1777	15.04	5.92	20
9	160.	CO_2 + TETRADECANE	4.290	5.342	3.627	0.000	0.6742	0.9952	0.1764	3.06	-0.1155	16.23	5.53	17

RMSE= 0.3003, AAPD = 10.18, BIAS = -0.0237, DMIN= -31.83, EMIN=0.2857
WRMS= 2.23, AAWPD= 5.12, WBIAS= -0.3662, DMAX= 43.29, EMAX=0.9979, NPIS = 148

TABLE XXXV

SUMMARY OF THE OVERALL STATISTICS FOR THE LEE-CHIEN MODEL, CASE 3, USING DATA FOR THE ETHANE + HYDROCARBON SYSTEMS

ISO	T(F)	SYSTEM	PAR(1)	PAR(2)	K	C(I,J)	EMIN	EMAX	RMSE	WRMS	BIAS	AAPD	AAWPD	NO PT
1	160.	C_2H_6 + n-DECANE	4.513	4.126	3.548	0.000	0.3490	0.9860	0.0421	0.30	-0.0126	1.29	4.36	20
2	160.	C_2H_6 + t-DECALIN	4.513	3.700	3.548	0.000	0.1669	0.9917	0.0805	1.06	0.0516	5.67	4.48	22
3	160	C_2H_6 + BENZENE	4.513	3.731	3.548	0.000	0.4907	0.9971	0.0596	0.77	0.0025	4.44	5.77	27

RMSE= 0.0630, AAPD = 3.92, BIAS = 0.0138, DMIN= -20.31, EMIN=0.1669
WRMS= 0.73, AAWPD= 4.95, WBIAS= -0.0393, DMAX= 17.25, EMAX=0.9971, NPIS = 69

TABLE XXXVI

SUMMARY OF THE OVERALL STATISTICS FOR THE LEE-CHIEN MODEL, CASE 3, USING DATA FOR THE METHANE + HYDROCARBON SYSTEMS

ISO	T(F)	SYSTEM	PAR(1)	PAR(2)	K	C(I,J)	EMIN	EMAX	RMSE	WRMS	BIAS	AAPD	AAWPD	NO PT
1	100.	CH_4 + n-BUTANE	4.003	3.861	3.628	0.000	0.5230	0.9937	0.1861	2.63	-0.1167	15.44	4.93	11
2	130.	CH_4 + n-BUTANE	4.003	3.861	3.628	0.000	0.5330	0.9861	0.0951	2.10	-0.0398	11.52	5.07	10
3	160.	CH_4 + n-BUTANE	4.003	3.861	3.628	0.000	0.5525	0.9945	0.0413	1.44	-0.0116	8.39	5.92	9
4	190.	CH_4 + n-BUTANE	4.003	3.861	3.628	0.000	0.5889	0.9717	0.0176	0.43	0.0067	2.70	5.62	7
5	100.	CH_4 + n-DECANE	4.003	3.838	3.628	0.000	0.3766	0.9887	0.1484	0.65	-0.0362	2.36	4.47	9
6	160.	CH_4 + n-DECANE	4.003	3.838	3.628	0.000	0.3855	0.9638	0.0807	0.68	-0.0217	2.85	4.02	8
7	100.	CH_4 + n-HEPTANE	4.003	3.798	3.628	0.000	0.0554	0.6234	0.3646	1.71	-0.0170	4.87	2.63	10
8	160.	CH_4 + n-HEPTANE	4.003	3.798	3.628	0.000	0.0564	0.7749	0.3031	1.51	0.0946	4.68	2.86	12
9	220.	CH_4 + n-HEPTANE	4.003	3.798	3.628	0.000	0.0606	0.8338	0.3197	1.86	0.1407	6.02	3.00	12
10	280.	CH_4 + n-HEPTANE	4.003	3.798	3.628	0.000	0.0683	0.7687	0.3038	1.70	0.1780	5.21	3.03	10
11	100.	CH_4 + n-PENTANE	4.003	3.746	3.628	0.000	0.4073	0.9165	0.0860	1.20	0.0375	5.17	3.60	6
12	160.	CH_4 + n-PENTANE	4.003	3.746	3.628	0.000	0.2566	0.9624	0.2382	2.03	0.1784	8.71	3.78	8
13	5.	CH_4 + n-PROPANE	4.003	3.876	3.628	0.000	0.1481	0.5160	0.3593	4.34	0.1454	15.46	3.24	5
14	50.	CH_4 + n-PROPANE	4.003	3.876	3.628	0.000	0.1145	0.6895	0.3230	1.75	-0.2272	5.54	3.39	7
15	86.	CH_4 + n-PROPANE	4.003	3.876	3.628	0.000	0.1215	0.6796	0.2746	2.96	-0.2090	11.43	3.56	12
16	113.	CH_4 + n-PROPANE	4.003	3.876	3.628	0.000	0.1972	0.5564	0.1086	1.34	-0.0942	4.71	3.64	11
17	149.	CH_4 + n-PROPANE	4.003	3.876	3.628	0.000	0.3074	0.6608	0.0357	1.08	0.0313	5.08	4.14	6

RMSE= 0.2320, AAPD = 7.12, BIAS = -0.0024, DMIN= -84.57, EMIN=0.0554
WRMS= 1.74, AAWPD= 3.90, WBIAS= -0.3194, DMAX= 50.66, EMAX=0.9945, NPIS = 153

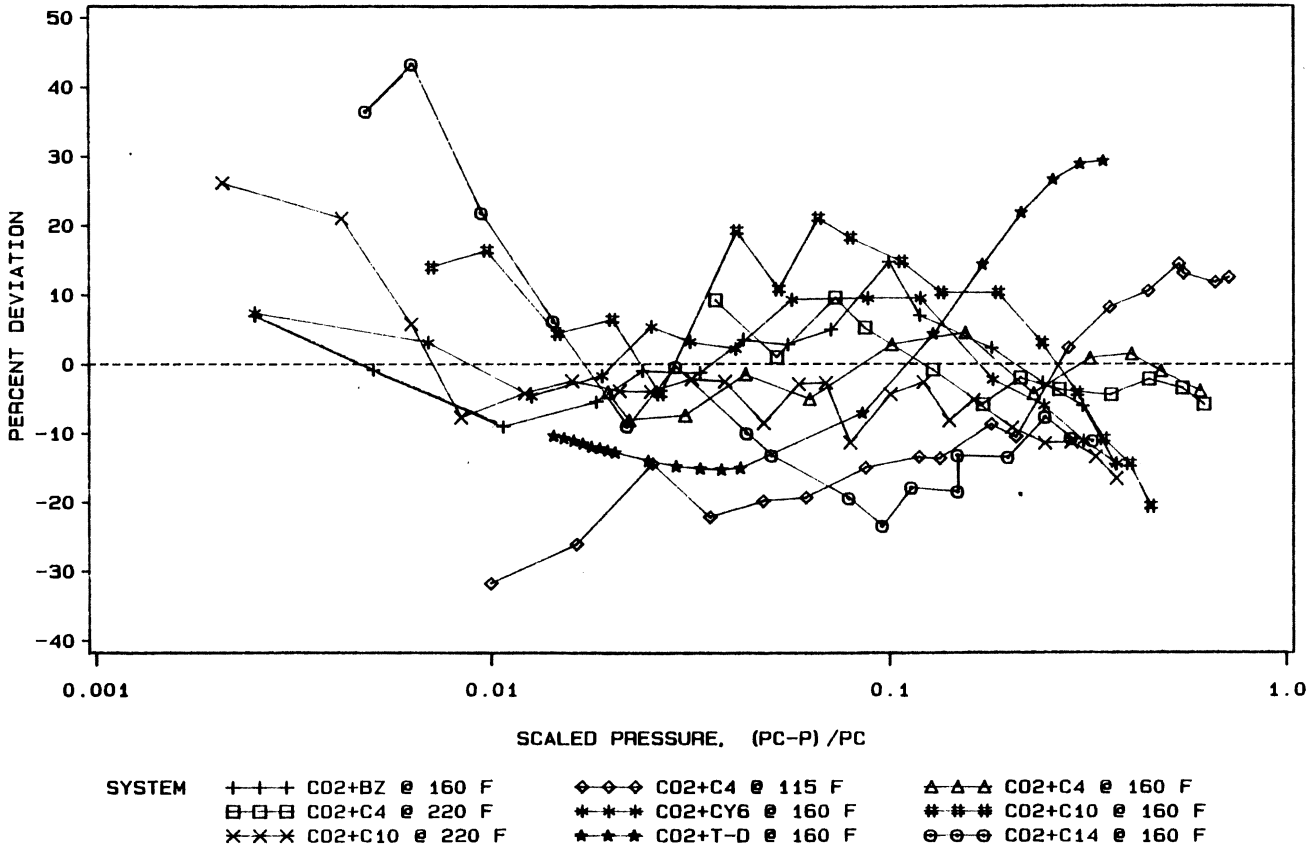

Figure 39. Evaluation of the Lee-Chien Model, Case 3, for the Carbon Dioxide + Hydrocarbon Systems. The Scaling Exponent and the Density Coexistence Curve Parameter are Regressed

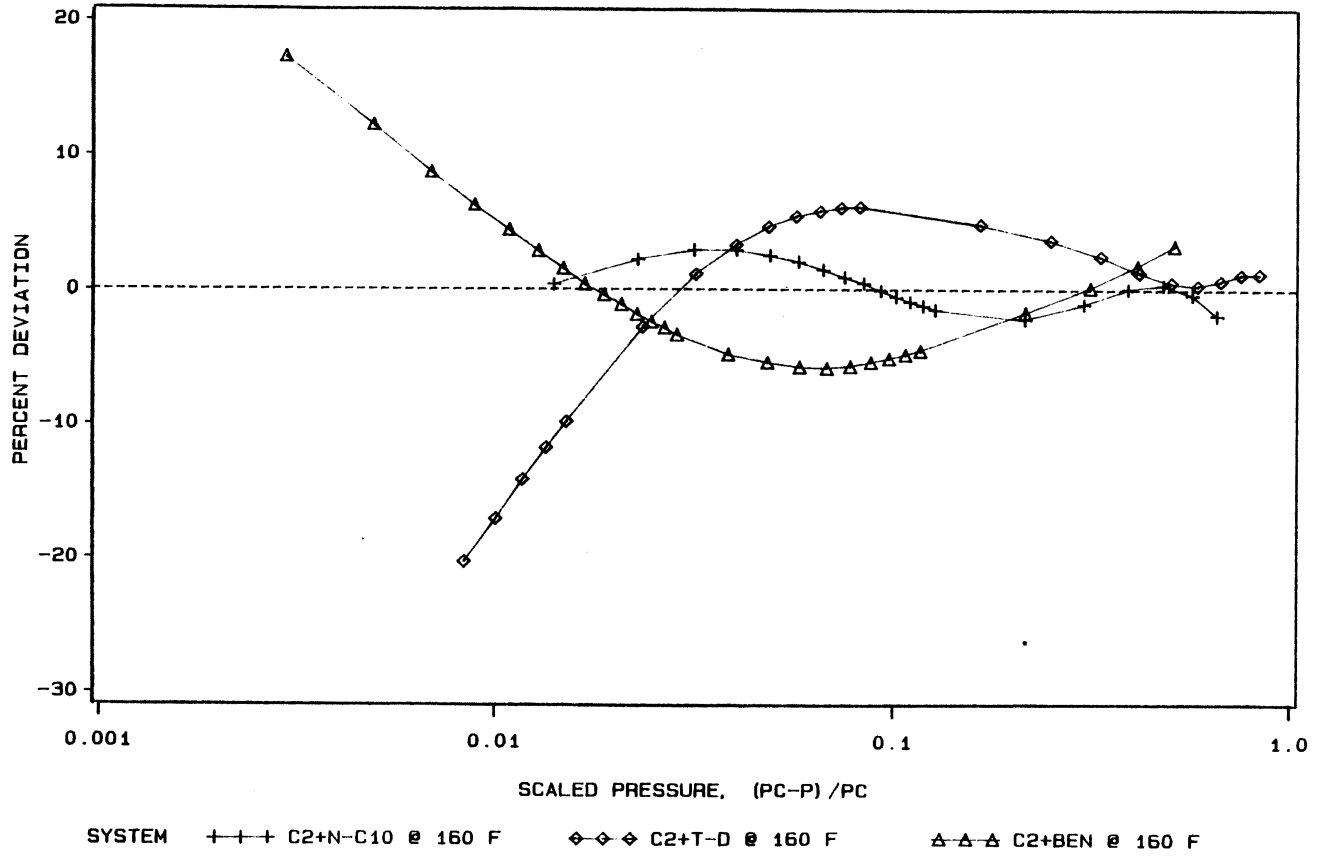

Figure 40. Evaluation of the Lee-Chien Model, Case 3, for the Ethane + Hydrocarbon Systems. The Scaling Exponent and the Density Coexistence Curve Parameter are Regressed

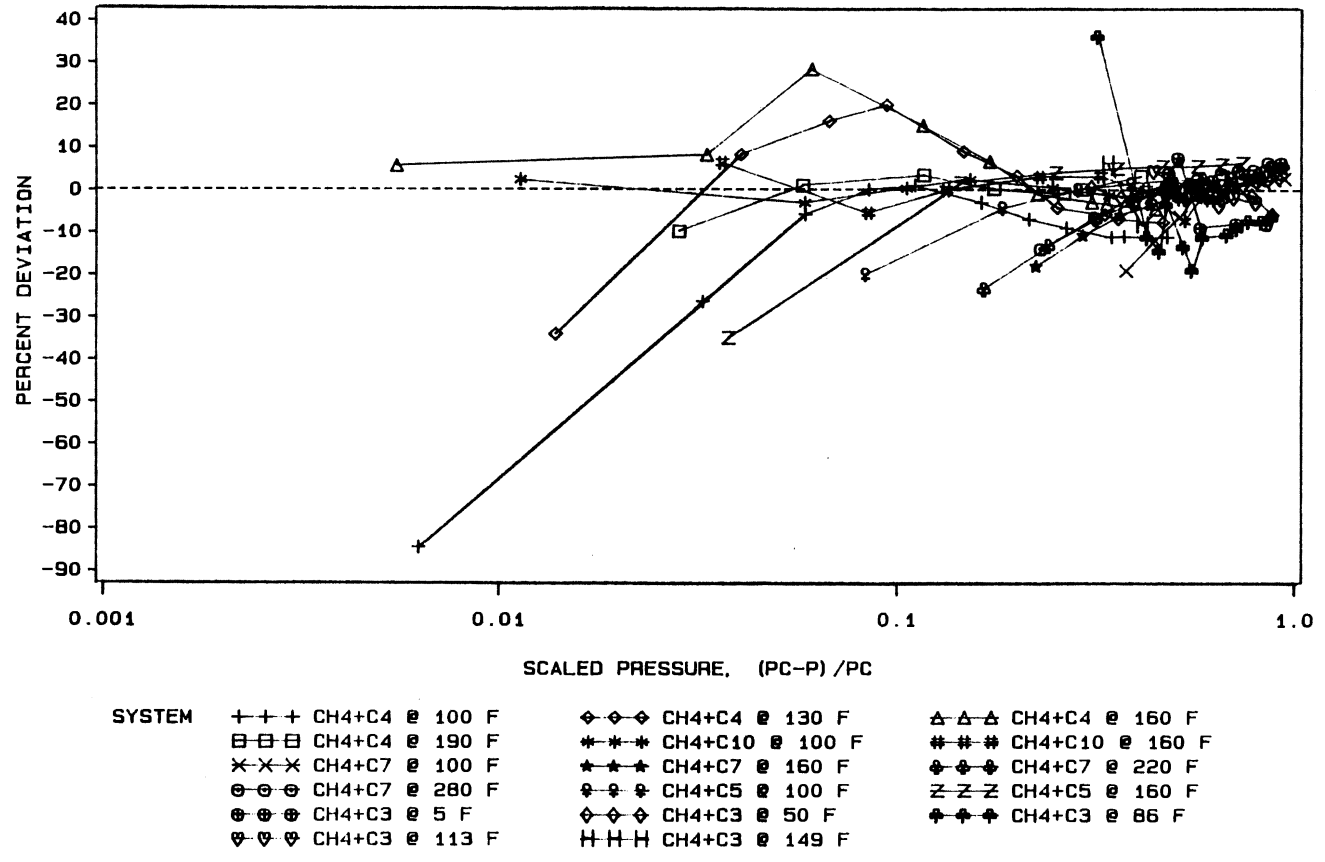

Figure 41. Evaluation of the Lee-Chien Model, Case 3, for the Methane + Hydrocarbon Systems. The Scaling Exponent and the Density Coexistence Curve Parameter are Regressed

A comparison of two of the cases studied using the Lee-Chien model is shown in Figure 42. The cases include the predictive ability of the Lee and Chien model without regressed (Case 1) and the case in which all the parameters are regressed simultaneously (Case 3).

Comparison of the Models Studied

During the evaluation of the Weinaug-Katz, Hugill-Van Welsenes, and Lee-Chien models, a case was run so that the regressed solvent parachors may be compared for the separate models. The scaling exponent in the above-mentioned cases was set to 4.0. The interaction parameter used in the HVW model was regressed. A comparison of the parachors generated for the solvent based on each solute and each model appear in Table XXXVII. Table XXXVIII complements Table XXXVII by giving values for the regressed parachors (including the solute parachors). The values listed for the Weinaug-Katz model are for Case 3, for the Hugill-Van Welsenes model are for Case 4, for the Lee-Chien model are for Case 3. The parachors listed under the subtitle "All Systems" are the values found by regressing the entire data set (i.e. all three solute systems) for each model (e.g. the regressed parachor for n-decane is common to each solute). The scaling exponents listed in Table XXXVIII are the values obtained through regressions. These values of the scaling exponent may be used to predict interfacial tensions. There is, of course, an inconsistency in using literature parachors with cases where $k \neq 4.0$ since the literature values for the solute and solvent parachors are calculated with $k = 4.0$.

The values for the parachor are consistently higher when using a scaling exponent of 3.6. This is shown in Table XXXVIII in the column

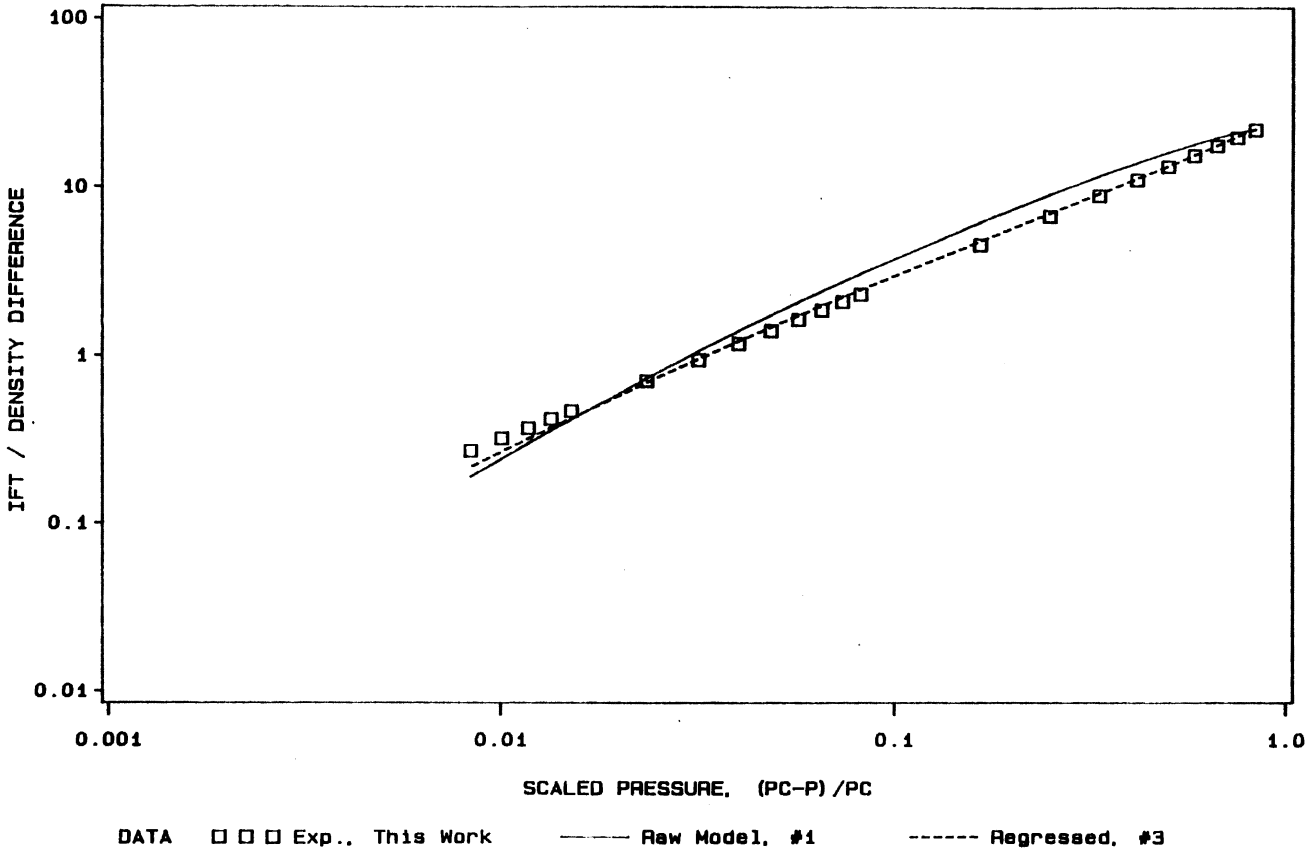

Figure 42. Comparison of the Ability of the Lee-Chien IFT Model to Predict Experimental Data for Ethane + trans-Decalin @ 344.3 K (160°F)

TABLE XXXVII

COMPARISON OF REGRESSED PARACHORS (WITH SOLUTE PARACHORS FROM QUAYLE)

Compound	Parachor	Parachor Obtained For Each Solvent											
		CO_2 SYSTEM			C_2H_6 SYSTEM			CH_4 SYSTEM			ALL SYSTEMS		
	(Quayle)	WK	HVW	LC	WK	HVW	LC	WK	HVW	LC	WK	HVW	LC
Methane	72.6							72.6	72.6	72.6	72.6	72.6	72.6
Ethane	110.5				110.5	110.5	110.5				110.5	110.5	110.5
Carbon Dioxide	77.5	77.5	77.5	77.5							77.5	77.5	77.5
n-Propane	150.8							149.1	150.9	152.6	149.1	149.7	155.9
n-Butane	190.3	199.6	171.8	199.7				201.5	182.1	206.0	200.7	201.3	199.8
n-Pentane	232.0							243.8	214.0	248.7	243.8	244.0	248.3
Benzene	206.0	205.0	157.7	205.7	196.7	178.1	206.7				200.9	203.5	192.8
Cyclohexane	242.1	239.8	195.3	234.7							239.8	242.5	212.2
n-Heptane	311.4							320.5	306.3	322.1	320.5	306.3	330.4
trans-Decalin	371.0	392.9	386.9	362.4	350.5	339.8	350.6				372.2	376.0	354.1
n-Decane	431.0	451.0	322.3	378.6	409.6	388.8	370.0	480.9	484.9	484.1	449.1	453.5	371.3
n-Tetradecane	591.3	641.3	370.2	518.0							641.3	649.1	458.4

TABLE XXXVIII

COMPARISON OF REGRESSED SOLUTE AND SOLVENT PARACHORS

Compound	Parachor	Parachor Obtained For Each Solvent											
		CO_2 SYSTEM			C_2H_6 SYSTEM			CH_4 SYSTEM			ALL SYSTEMS		
	(Quayle)	WK	HVW	LC	WK	HVW	LC	WK	HVW	LC	WK	HVW	LC
Methane	72.6							29.0	43.1	60.8	41.8	61.3	56.5
Ethane	110.5				91.0	80.7	88.3				94.3	93.8	88.9
Carbon Dioxide	77.5	79.2	105.8	69.4							76.0	76.0	60.9
n-Propane	150.8							155.9	161.4	142.2	154.9	126.9	141.6
n-Butane	190.3	199.7	198.0	181.4				194.2	210.9	182.7	197.0	180.3	181.1
n-Pentane	232.0							241.8	244.0	230.7	245.2	212.8	227.7
Benzene	206.0	200.4	247.7	182.6	223.0	193.5	205.0				210.0	176.9	209.9
Cyclohexane	242.1	234.9	275.6	207.8							238.1	223.7	237.7
n-Heptane	311.4							327.3	340.0	313.4	332.0	285.7	315.0
trans-Decalin	371.0	391.3	379.8	337.4	376.0	395.5	367.2				382.8	324.1	364.8
n-Decane	431.0	445.8	434.9	329.9	447.7	427.1	403.2	427.3	447.2	433.4	445.4	370.3	413.1
n-Tetradecane	591.3	621.1	400.7	418.7							616.3	562.9	476.6
k =		3.568	3.689	3.627	3.560	3.536	3.548	3.647	3.515	3.628	3.586	3.797	3.571

headed "All Systems" for the WK model. For instance, the parachor for n-decane has a value of 431.0 from Quayle but after regression a preferred value of 445.4 is found. This same trend has been seen in the work done by Dickson (8). The difference between Quayle's parachor and parachors obtained with a scaling exponent of 3.6 arises from the fact that the tabulated values given by Quayle were determined using data with an interfacial tension larger than one dyne/cm. The values of the parachor obtained by Quayle are expected to be lower since a scaling exponent of 4.0 rather than 3.6 was used. This arises as follows:

$$[P(k = 3.6)] = [P(k = 4.0)]_{\gamma}^{(1/3.6-1/4.0)}$$

$$= [P(k = 4.0)]_{\gamma}^{0.028}$$

so if $\gamma > 1$, $[P(k = 3.6)] > [P(k = 4.0)]$.

In evaluating each model, both the performance based on minimum deviation from experimental values and ease of application must be considered. Cross-comparisons for the cases which have common descriptions are found in Tables XXXIX, XL, and XLI. These "common" cases may be used to get a relative sense of the performance of one model compared to another. Based on the model as presented by the authors (Case 1 for each model) the model with the lowest absolute average percent deviation (AAPD) for the carbon dioxide system is the HVW model, for the ethane systems the WK model predicts the best, and for the methane systems the LC model has the lowest AAPD. However, the performance of the model cannot be judged by considering only the absolute average percent deviation, or the root-mean-square error or even the weighted values for the AAPD or RMSE, the ease in which the

TABLE XXXIX

CASE COMPARISONS FOR THE CARBON DIOXIDE + HYDROCARBON SYSTEMS

REGRESSED PARMS	FIXED PARAMETERS	ABSOLUTE AVERAGE PERCENT DEVIATION, AAPD Weinaug-Katz	Hugill-Van Welsenes	Lee-Chien
NONE	P1 and P2 = Model, k = 4.0	25.51 (1)*	23.08 (1)	30.50 (1)
k	P1 and P2 = Model	15.11 (2)	7.96 (11)	
P1, P2, k	NONE	9.07 (3)	4.94 (4)	10.18 (3)
P1, P2, k	NONE, Pr < 0.99	7.20 (4)	6.31 (6)	
P1, k	P2 = Model	14.53 (5)	7.95 (13)	13.02 (4)
k	P1 and P2 = gen. values	10.77 (6)	8.35 (7)	
NONE	P1 and P2 = gen. values, k = 3.6	10.89 (7)	10.89 (10)	
P1	P2 = Model, k = 3.6	15.47 (8)		

* Numbers in parenthesis correspond to the Case number for each model

TABLE XL

CASE COMPARISONS FOR THE ETHANE + HYDROCARBON SYSTEMS

REGRESSED PARMS	FIXED PARAMETERS	ABSOLUTE AVERAGE PERCENT DEVIATION, AAPD Weinaug-Katz	Hugill-Van Welsenes	Lee-Chien
NONE	P1 and P2 = Model, k = 4.0	15.55 (1)*	22.74 (1)	20.19 (1)
k	P1 and P2 = Model	14.91 (2)	5.57 (11)	
P1, P2, k	NONE	4.51 (3)	3.47 (4)	3.92 (3)
P1, P2, k	NONE, Pr < 0.99	4.04 (4)	5.12 (6)	
P1, k	P2 = Model	5.36 (5)	4.01 (13)	4.80 (4)
k	P1 and P2 = gen. values	8.58 (6)	4.01 (7)	
NONE	P1 and P2 = gen. values, k = 3.6	8.60 (7)	8.60 (10)	
P1	P2 = Model, k = 3.6	5.74 (8)		

* Numbers in parenthesis correspond to the Case number for each model

TABLE XLI

CASE COMPARISONS FOR THE METHANE + HYDROCARBON SYSTEMS

REGRESSED PARMS	FIXED PARAMETERS	ABSOLUTE AVERAGE PERCENT DEVIATION, AAPD Weinaug-Katz	Hugill-Van Welsenes	Lee-Chien
NONE	P1 and P2 = Model, k = 4.0	22.26 (1)*	15.97 (1)	13.39 (1)
k	P1 and P2 = Model	20.20 (2)	11.24 (11)	
P1, P2, k	NONE	6.50 (3)	5.11 (4)	7.12 (3)
P1, P2, k	NONE, Pr < 0.99	5.96 (4)	9.26 (6)	
P1, k	P2 = Model	12.66 (5)	13.02 (13)	9.81 (4)
k	P1 and P2 = gen. values	10.73 (6)	7.16 (7)	
NONE	P1 and P2 = gen. values, k = 3.6	11.59 (7)	11.59 (10)	
P1	P2 = Model, k = 3.6	14.39 (8)		

* Numbers in parenthesis correspond to the Case number for each model

model may be executed must also be taken into account. The LC model requires the values for the critical properties (including the critical volume which can vary as much as one percent in the literature and can have an effect as large as 8% on the predicted values of interfacial tension). The constants used for the evaluation of the density coexistence curve parameter in the LC model is explicitly derived for normal paraffins, which limits the use of the model and suggests that the constants used in the evaluation of B must be regeneralized for other solutes of interest.

The HVW model requires a value for the interaction parameter which must be found experimentally. However, obtaining values for this parameter is difficult. A suggested value found in this work for the interaction parameter for the ethane systems is 0.97. A single value for the other systems is elusive due to the complexity of the carbon dioxide molecule and due to the inconsistent behavior found in the methane binary isotherms.

The WK model requires only a value for the parachor, which is readily available in the literature for a fair number of organic compounds (70). This suggests that, for the models compared as originally prescribed by their authors, the easiest model to implement is the WK model, however, the other two models can give better results if the proper input variables are available.

As can be seen from Tables XXIX, XL, and XLI, the LC model is able to predict interfacial tensions for the light hydrocarbon/hydrocarbon systems better than for the carbon dioxide based systems. The HVW model has the capability to predict better than the WK model in all cases except those which have restricted data sets based on the reduced

pressure (Case 6 for the HVW model). The HVW model reduces to the WK model if the interaction parameter is equal to 1.0, as may be seen in HVW model, Case 10. The WK model is able to fit the experimental data within 4.1% of the absolute average percent deviation obtained using the HVW model for the case when all parameters are regressed (Case 3 for WK the model and Case 4 for the HVW model). Even though the LC model fits the ethane and methane data better than the WK model, the difference between the AAPD found for each model is only 0.6%.

Figure 43 compares the three "raw" models (Cases 1) the three regressed cases (Case 3 for WK model, Case 4 for HVW model, and Case 3 for LC model) and the two generalized cases (Case 7 for WK model and Case 9 for the HVW model). The data plotted in the figure are for all data points of the ethane + trans-Decalin system. In order to complement the data presented in Figure 43, Figures 44, 45, and 46 present the data in the form of $\gamma/\Delta\rho$ plotted against scaled pressure for the above mentioned cases..

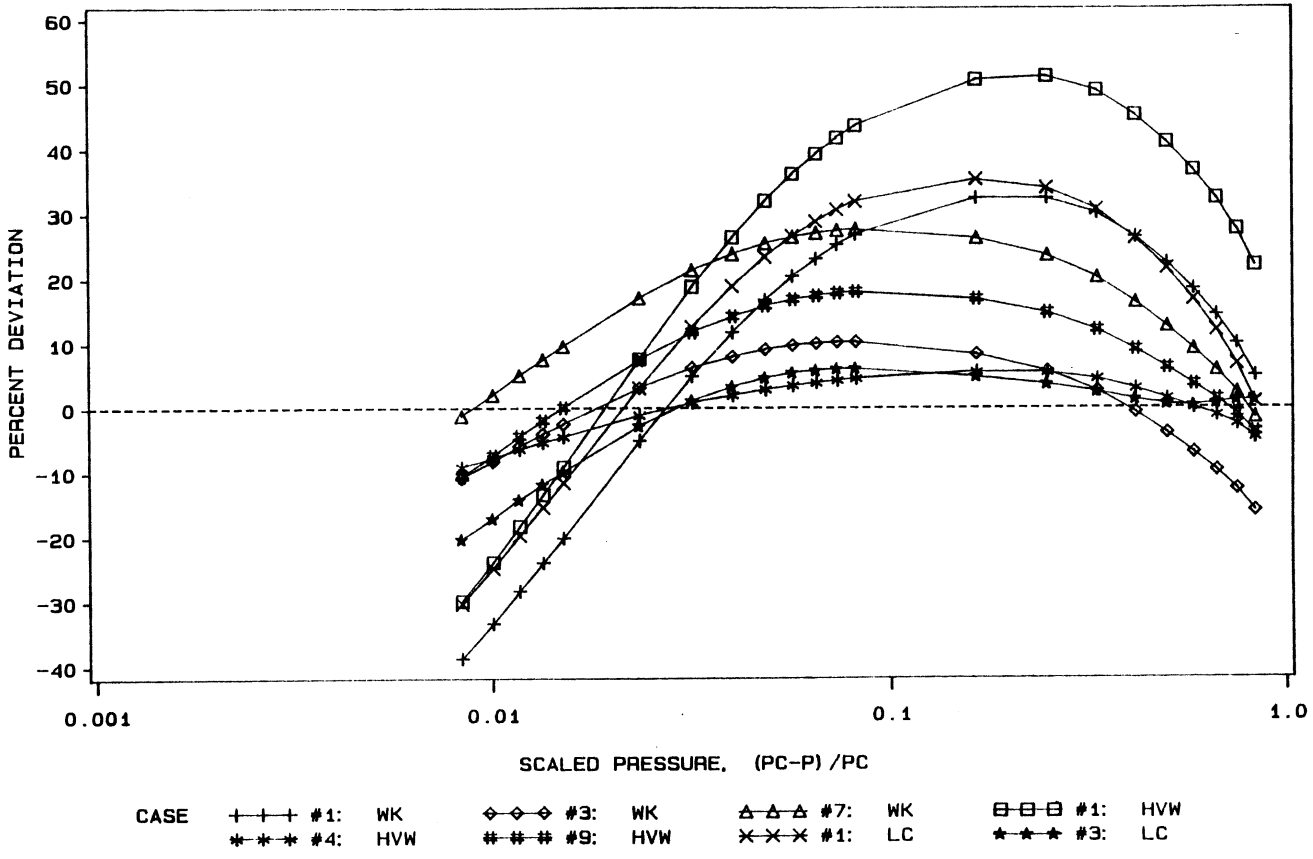

Figure 43. Comparison of the Three Models Studied Using Ethane + trans-Decalin Data @ 344.3 K (160°F)

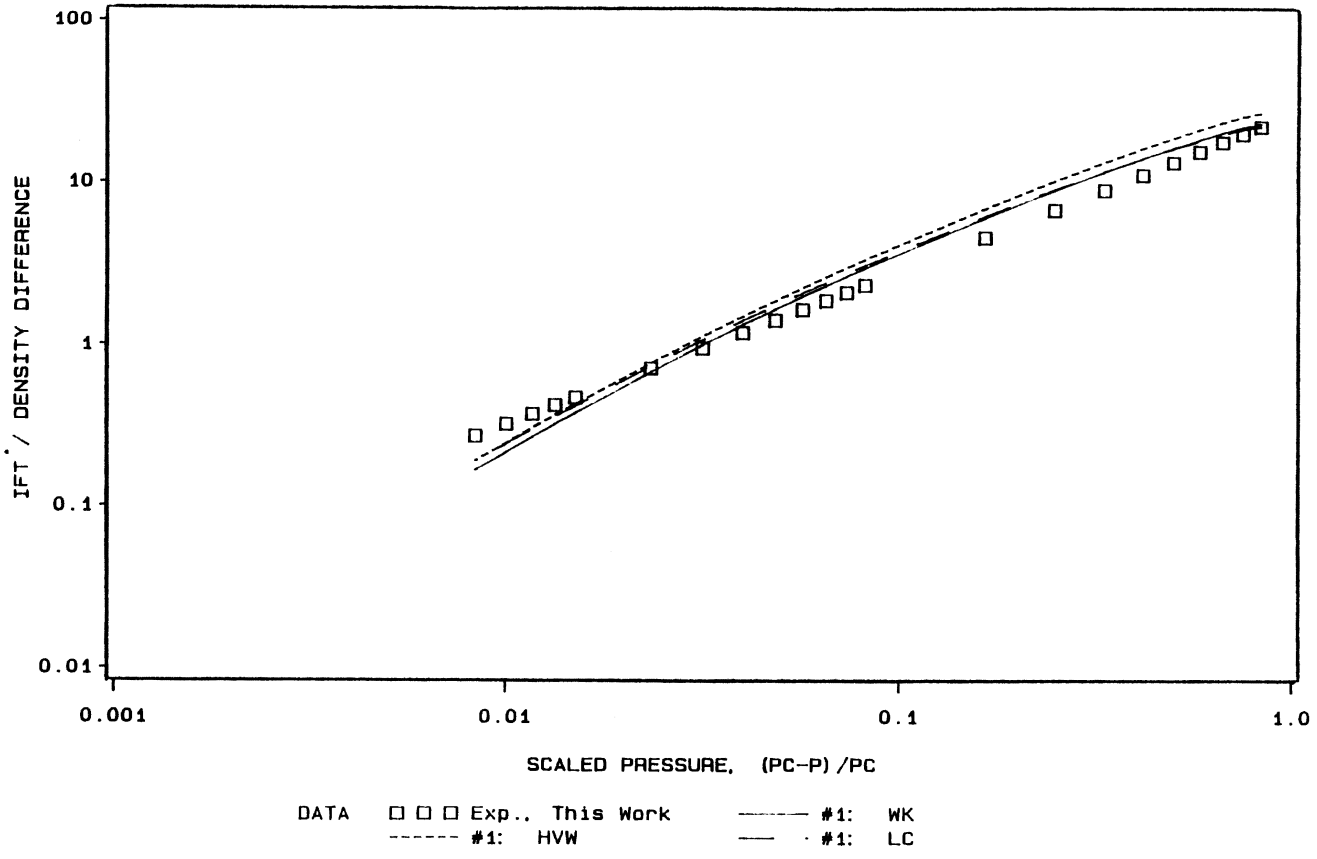

Figure 44. Comparison of the Raw Potential of the Models Studied Using Ethane + trans-Decalin Data @ 344.3 K (160°F)

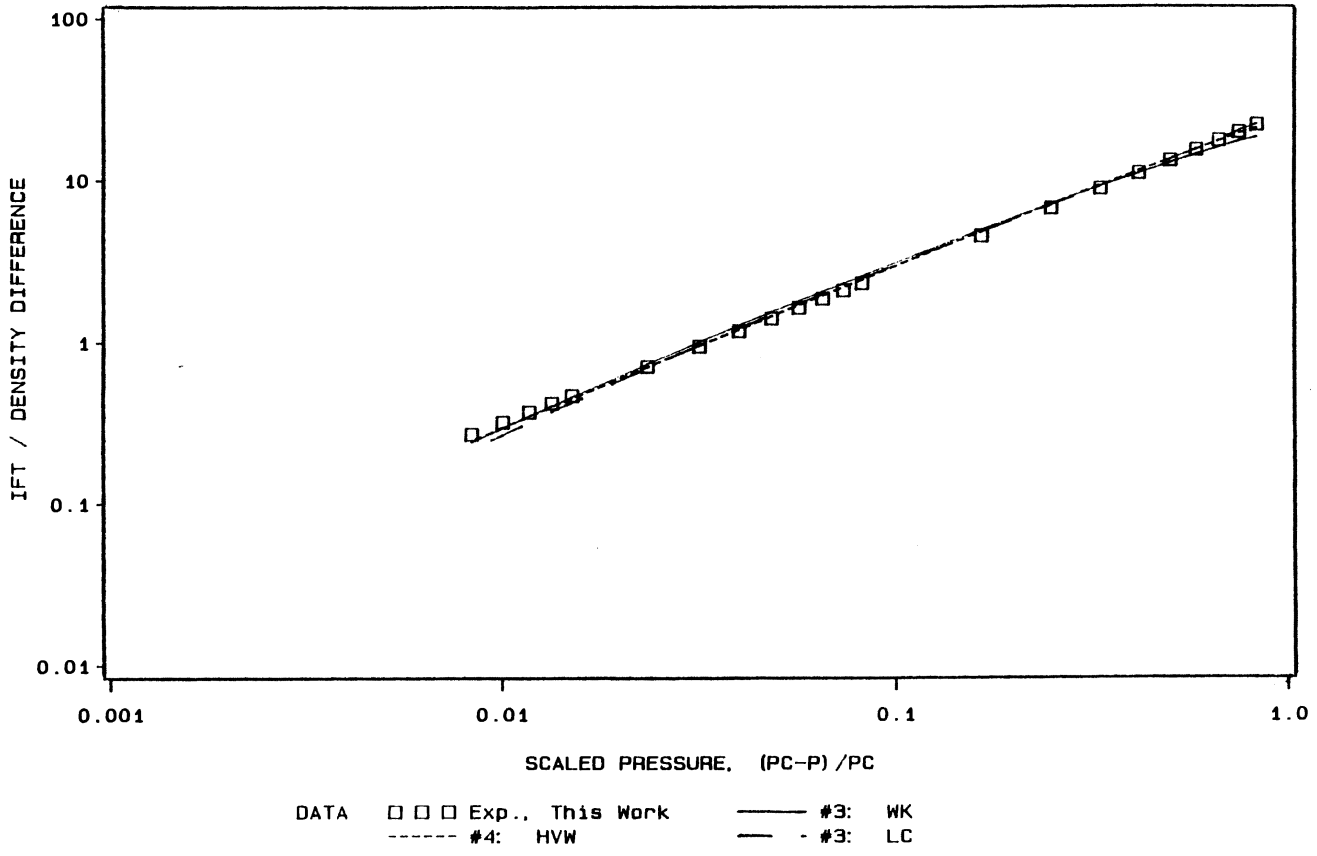

Figure 45. Comparison of the Regressed Case for the Models Studied Using Ethane + trans-Decalin Data @ 344.3 K (160°F)

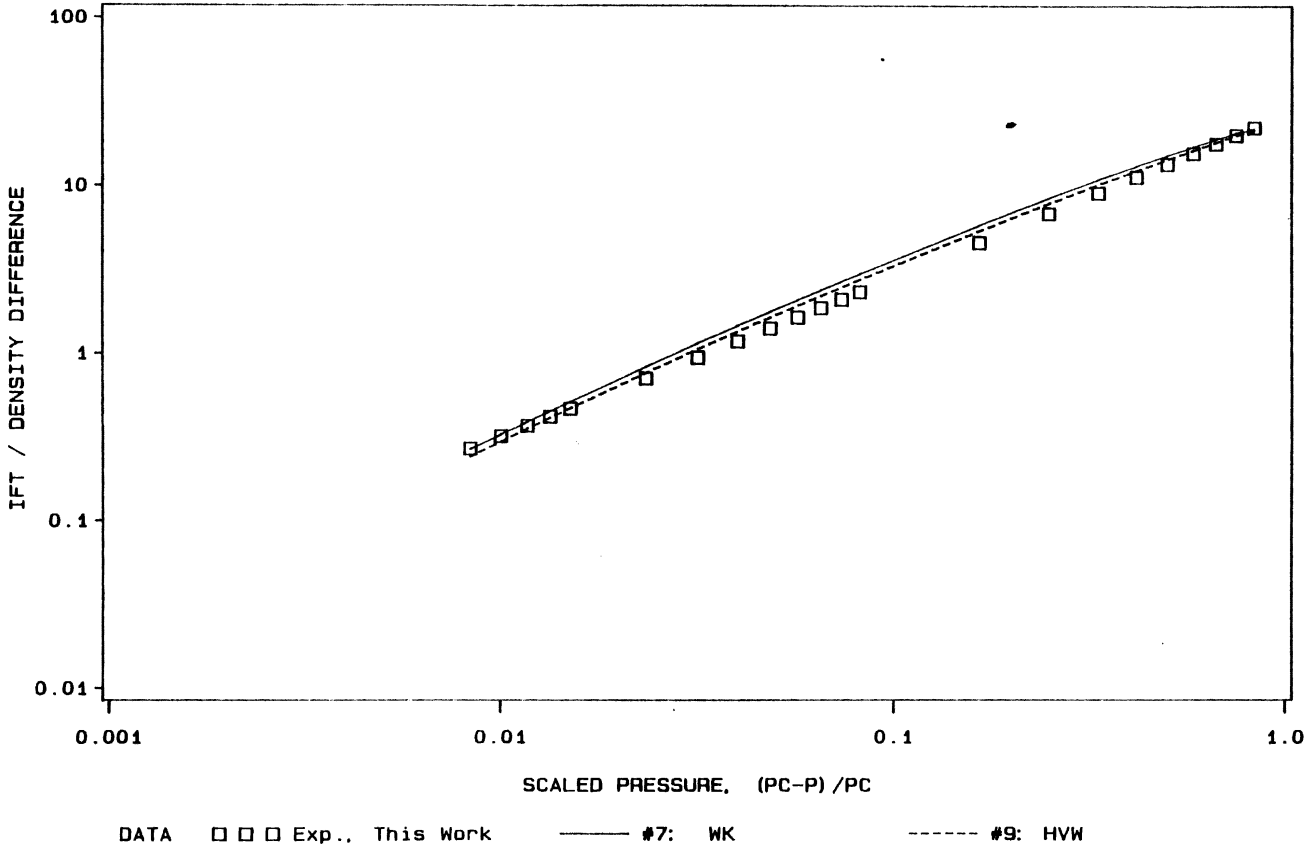

Figure 46. Comparison of the Generalized Case for the Models Studied Using Ethane + trans-Decalin Data @ 344.3 K (160°F)

CHAPTER VI

CONCLUSIONS AND RECOMMENDATIONS

Conclusions

1. The experimental data for the ethane + trans-Decalin system measured at 160°F represent a consistent set of data not previously available in the literature. The experimental accuracy is comparable to previous studies (32, 33, 34, 35, 36, 44, 45, 46, and 47) on the experimental apparatus. The consistency of these data arises from the fact that all measured properties, (x, y, ρ^L, ρ^V, $\gamma/\Delta\rho$) were obtained simultaneously in the same apparatus utilizing the same equilibrium mixture of fluids.

2. The experimental data for the ethane + trans-Decalin system measured at 160°F are represented adequately by analytic functions based on the renormalized group theory, as originally presented by Kobayashi and Charoensombut-amon (61, 62).

3. The Weinaug-Katz correlation is the preferred IFT model based on the results of the evaluations performed in this work. The WK model requires fewer input parameters than either the Hugill-Van Welsenes or Lee-Chien models. For these reasons, and because of the simplicity and ease in which this model may be applied, the recommended model is the Weinaug-Katz model. The WK model requires only the following input variables: liquid and vapor phase compositions (x, y), the liquid and vapor densities (ρ^L, ρ^L), and values for the parachor tabulated in the

work by Quayle (70).

4. The Hugill-Van Welsenes model obviously has the ability to perform better than the WK model since one additional parameter has been added to the model originated by Weinaug and Katz, a binary interaction parameter. However, the interaction parameter makes the the HVW more difficult to apply since additional experimental information is required to determine the interaction parameter.

5. The Lee-Chien correlation performs better for hydrocarbon + hydrocarbon systems than for carbon dioxide + hydrocarbon systems. This may be due to the correlation presented for the calculation of the density coexistence curve parameter, B; which is specifically for paraffins.

6. The appropriate value for the scaling exponent, k, for all three models is near 3.6 (in preference to the value of 4.0 proposed by Weinaug-Katz). The value of k = 3.6 compares favorably with the value of 3.55 suggested by Sengers, Greer, and Sengers (60).

7. All three models are relatively insensitive to the values used for the solute parachor, but the effect of the solvent parachor is substantial. In addition, all three models are very sensitive to the value of the scaling exponent, k. The Hugill-Van Welsenes model is also affected strongly by the value used for the interaction parameter.

8. The parameters in the models studied indicated that the potential for generalization may exist. However, the results in this study are not conclusive due to the limited number of solutes available for investigation.

Recommendations

1. The Weinaug-Katz correlation using generalized parameters is the recommended model for predicting interfacial tensions for hydrocarbon binary systems with carbon dioxide, ethane, or methane as the solute.

2. Further investigations should be pursued to include binary systems with one of the following as the solute constituent: carbon monoxide, nitrogen, propane, n-butane, ethylene, hydrogen or hydrogen sulfide. Through the study of these other solute systems, the viability of the generalized parameters and the fixed value of 3.6 for the scaling exponent may be further substantiated.

3. Investigations should be pursued to regeneralize the constants used in determining the density coexistence curve parameter, B, in the Lee-Chien model. Constants should be developed to properly handle solutes of interest such as carbon dioxide, carbon monoxide, nitrogen, hydrogen or hydrogen sulfide.

REFERENCES

1. Schoettle, V., Jennings, Jr., H. Y., "High-Pressure High-Temperature Visual Cell for Interfacial Tension Measurements," The Review of Scientific Instruments, Vol. 39, No. 3, 386 (1968).

2. Burkowsky, M., "The Influence of Dissolved Gas in Crude Oils on the Low-Tension Flood-Process," Papers Presented at the European Symposium on Enhanced Oil Recovery, (1979).

3. Bardon, C., Longeron, D.G., "Influence of Very Low Interfacial Tensions on Relative Permeability," Society of Petroleum Engineers Journal, October, 391-401 (1980).

4. Sevaraman, A., et al, "Correlation for Predictions of Interfacial Tensions of Pure Alkane, Naphthenic, and Aromatic Compounds Between Their Freezing and Critical Points," Fluid Phase Equilibria, 18, 225-235 (1984).

5. Weinaug, C. F., Katz, D. L., "Surface Tensions of Methane- Propane Mixtures," Industrial and Engineering Chemistry, Vol. 35, No. 2, 239-246 (1943).

6. Hugill, J. A., Van Welsenes, A. J., " Surface Tension: A Simple Correlation for Natural Gas + Condensate Systems," presented to the Fourth Int. Conf. of Fluid Properties and Phase Equilibria for Chemical Process Design, Helsingor, (May, 1986).

7. Lee, S. T., Chien, M. C. H., "A New Multicomponent Surface Tension Correlation Based on Scaling Theory," Paper 12643 Presented at the SPE/DOE Fourth Symposium on EOR, Tulsa, Oklahoma, (April, 1984).

8. Dickson, K. B., "Interfacial Tensions in Carbon Dioxide + Hydrocarbon Systems: Experimental Data and Correlations," M. S. Thesis, Oklahoma State University (1987).

9. Kittsley, S. L., "Physical Chemistry," Third Edition, Barnes and Noble Books, N. Y. (1969).

10. Modell, M. and Reid, R. C., "Thermodynamics and Its Applications," Second Edition, Prentice-Hall, Inc., Englewood Cliffs, N. J. (1974).

11. Andreas, J. M., Hauser, E. A. and Tucker, W. B., "Boundary Tension by Pendant Drops," Journal of Physical Chemistry, Vol. 42, 1001 (1938).

12. Hough, E. W., Wood, B. B. and Rzasa, M. J., "Adsorption at Water, -Helium, -Methane, -Nitrogen Interfaces at Pressures to 15,000 psia," Journal of Physical Chemistry, Vol. 56, 996 (1952).

13. Jaycock, M. J. and Parfitt, G. D., "Chemistry of Interfaces," Ellis Horwood Limited, Chichester, England (1981).

14. Gibbs, J. W., "Collected Works," Second Edition, Vol. I, Longmans, N. Y. (1928).

15. Smith, J. M. and Van Ness, H. C., "Introduction to Chemical Engineering Thermodynamics," Third Edition, McGraw-Hill Book Company, N. Y. (1975).

16. Davies, J. T. and Ridel, E. K., "Interfacial Phenomena,"Academic Press, N. Y. (1961).

17. Lewis, G. N. and Randall, M., "Thermodynamics," Second Edition, Revised by Pitzer, K. S. and Brewer, L., McGraw-Hill Book Company, N. Y. (1961).

18. Adamson, A. W., "Physical Chemistry of Surfaces," Fourth Edition, John Wiley & Sons, Inc., New York (1982).

19. Gambill, W. R., "Surface Tension for Pure Liquids," Chemical Engineering, Vol. 65, No. 7, 146 (1958).

20. Gambill, W. R., "Surface and Interfacial Tensions," Chemical Engineering, Vol. 65, No. 9, 143 (1958).

21. Eotvos, R., Annalen der Physik und Chemie N. F., Vol. 27, 448 (1886).

22. Ramsay, W. and Shields, J., Philosophical Transactions, Vol. 184, 647 (1893).

23. Katayama, M., Sci. Repts. Tohoku. Imp. Univ., Vol 4, 373 (1916); J. Chem. Soc., Vol. 110, II, 219 (1916).

24. Van der Waals, J. D., "Thermodynamische Theorie der Kapillaritat," Zeitschrift fur Physikalische Chemie, Vol. 13, 617 (1894).

25. Ferguson, A., "Studies in Capillarity," Faraday Society Transactions, Vol. 19, 407 (1923).

26. Sugden, S., "The Variation of Surface Tension with Temperature and Some Related Functions," J. Chem. Soc., 32-41 (1924).

27. Macleod, D. B., "On a Relation between Surface Tension and Density," Faraday Society Transactions, Vol. 19, 38 (1923).

28. Fowler, R. H., Proceedings of Royal Society (London), Vol. 159, 229 (1937).

29. Reilly, J. and Rae, W. N., "Physico-Chemical Methods," Third Edition, Princeton, N. J. (1939).

30. Hough, E. W. and Warren, H. G., "Correlation of Interfacial Tension of Hydrocarbons," Soc. Pet. Eng. J., 345-348 (December 1966).

31. Hsu, J. C., Nagarajan, N. and Robinson, Jr., R. L., "Equilibrium Phase Compositions, Phase Densities, and Interfacial Tensions for CO2 + Hydrocarbon Systems. 1. CO2 + n-Butane," Journal of Chemical & Engineering Data, Vol. 30, 485 (1985).

32. Nagarajan, N. and Robinson, Jr., R. L., "Equilibrium Phase Compositions, Phase Densities, and Interfacial Tensions for CO2 + Hydrocarbon Systems. 2. CO2 + n-Decane," Journal of Chemical & Engineering Data, Vol. 31, 168 (1986).

33. Gasem, K. A., Dickson, K. B., Dulcamara, P. B., and Robinson, Jr., R. L., "Interfacial Tensions in Carbon Dioxide-Hydrocarbon Systems: Development of Experimental Facilities and Acquisition of Experimental Data. Experimental Data for CO2 + n-Tetradecane", Technical Progress Report (September 20, 1985).

34. Nagarajan, N., Chen, Y.-K., and Robinson, Jr., R. L., "Interfacial Tensions in Carbon Dioxide-Hydrocarbon Systems: Development of Experimental Facilities and Acquisition of Experimental Data. Experimental Data for CO2 + Cyclohexane", Technical Progress Report (May, 1984).

35. Nagarajan, N., Chen, Y.-K., and Robinson, Jr., R. L., "Interfacial Tensions in Carbon Dioxide-Hydrocarbon Systems: Development of Experimental Facilities and Acquisition of Experimental Data. Experimental Data for CO2 + Benzene", Technical Progress Report (June 15, 1984).

36. Gasem, K. A., and Robinson, Jr., R. L., "Interfacial Tensions in Carbon Dioxide-Hydrocarbon Systems: Development of Experimental Facilities and Acquisition of Experimental Data. Experimental Data for CO2 + Trans Decalin", Technical Progress Report (October 10, 1986).

37. Pennington, B. F. and Hough, E. W., "Interfacial Tension of the Methane-normal Butane System," Producers Monthly, vol. 29, 4 (1965).

38. Sage, B. H., Hicks, B. L., and Lacey, W. N., "Phase Equilibria in Hydrocarbon Sytems," Industrial and Engineering Chemistry, Vol. 32, no. 8, 1085-1092 (1940).

39. Stegemeier, G. L. and Hough, E. W., "Interfacial Tension of the Methane-normal Pentane System," Producers Monthly, Vol. 25, 6 (1961).

40. Sage, B. H., Reamer, H. H., Olds, R. H., and Lacey, W. N., "Phase Equilibria in Hydrocarbon Sytems," Industrial and Engineering Chemistry, Vol. 34, No. 9, 1108-1117 (1942).

41. Warren, H. G., Ph. D. Dissertation, Mississippi State University (1965).

42. Sage, B. H., Reamer, H. H., and Lacey, W. N., "Phase Equilibria in Hydrocarbon Sytems," Industrial and Engineering Chemistry, Vol. 1, No. 1, 29-42 (1956).

43. Sage, B. H., Reamer, H. H., Olds, R. H., and Lacey, W. N., "Phase Equilibria in Hydrocarbon Sytems," Industrial and Engineering Chemistry, Vol. 34, No. 12, 1526-1531 (1942).

44. Gasem, K. A., and Robinson, Jr., R. L., "Interfacial Tensions in Ethane-Hydrocarbon Systems: Development of Experimental Facilities and Acquisition of Experimental Data. Experimental Data for Ethane + n-Decane", Technical Progress Report (September 25, 1985).

45. Gasem, K. A. M., Dulcamara, P. B., and Robinson, Jr., R. L., "Interfacial Tensions in Ethane-Hydrocarbon Systems: Acquisition of Experimental Data. Experimental Data for Ethane + Benzene," Technical Progress Report (July 24, 1987).

46. Nagarajan, N., and Robinson, Jr., R. L., "Interfacial Tensions in Carbon Dioxide-Hydrocarbon Systems: Development of Experimental Facilities and Acquisition of Experimental Data. Experimental Data for CO2/n-Butane/n-Decane Ternary System", Technical Progress Report to Amoco Production Co. (January, 1984).

47. Gasem, K. A., Dickson, K. B., and Robinson, Jr., R. L., "Interfacial Tensions in Carbon Dioxide-Hydrocarbon Systems: Development of Experimental Facilities and Acquisition of Experimental Data. Experimental Data for Carbon Dioxide + a Recombined Reservoir Oil", Technical Progress Report (March 28, 1986).

48. Bashforth, S. and Adams, J. C., "An Attempt To Test the Theories of Capillary Action, Part I," University Press Cambridge, England (1883).

49. Jennings, Jr., H. Y., "Apparatus for Measuring Very Low Interfacial Tensions," The Review of Scientific Instruments, Vol. 39, No. 3, 386 (1968).

50. Andreas, J. M., Hauser, E. A., Tucker, W. B., J. Phys. Chem., 42, 1001 (1938); see also Niederhauser, D. O., Bartell, F. E., "Report of progress. Fundamental Research on Occurance and Recovery of Petroleum," 1948-49, American Petroleum Institute, Baltimore, Md., p. 144, (1950).

51. Deam, J. R., "Interfacial Tension in Hydrocarbon Systems,"Ph. D. Dissertation, Oklahoma State University (1966).

52. Goodin, R. D., Roder, H. M., and Straty, G. C., "Thermophysical Properties of Ethane, from 90 to 600 K at Pressures to 700 Bar", NBS Technical Note 684, Boulder, Colorado, 53-54 (1976).

53. Douslin, D. R. and Harrison, R. H., J. Chem. Thermodynamics, Vol. 5, 491 (1973).

54. Sage, B. H., Reamer, H. H., Olds, R. H., and Lacey, W. N., Industrial and Engineering Chemistry, Vol. 36, 956 (1944).

55. Laplace, P. S., "Mecanique Celeste," Supplement to the 10th Book, Duprat, Paris (1806).

56. Mills, O. S., "Tables for Use in Measurement of Interfacial Between Liquids with Small Density Differences," British Journal of Applied Physics, Vol. 4, (1953).

57. Stegemeier, G. L., "Interfacial Tension of Synthetic Condensate Systems," Ph. D. Dissertation, University of Texas, Austin, Texas (1959).

58. Robinson, Jr., R. L., "Interfacial Tensions in Carbon Dioxide-Hydrocarbon Systems: Development of Data Correlation, Final Technical Report", Submitted to AMOCO Production Company, (1983).

59. Le Guillou, J. C., and J. Zinn-Hustin, Phys. Rev., B 21, 3976 (1980).

60. Levelt-Sengers, J. M. H., Greer, W. L., and J. V. Sengers, J. Phys. Chem. Ref. Data, Vol. 5, 1 (1976).

61. Wichterle, I., Chappelear, P. S., and R. Kobayashi, Journal of Computational Phys., Vol. 7, 606 (1971).

62. Charoensombut-amon, T., Ph.D. Dissertation, Rice University, 1985. See also: Charoensombut-amon, T. and Kobayashi, R., Fluid Phase Equilibria, Vol. 31, 23 (1986).

63. Wegner, F. J., Phys. Rev., B 5, 4529 (1972).

64. Nagarajan, N., Kumar, A., Gopal, E. S. R., and S. C. Greer, J. Phys. Chem., Vol. 84, 2883 (1980).

65. Bufkin, B. A., M. S. Thesis, Oklahoma State University (1986).

66. Mapes, J. L., Personal Communication, Oklahoma State University, (February, 1987).

67. Anderson, J. M., Barrick, M. W. and Robinson, Jr., R. L., Journal of Chemical & Engineering Data, Vol. 31, 172 (1986).

68. Soave, G., Chem. Eng. Sci., Vol. 27, 1197 (1972).

69. Faraday, J. E. and Freeborn, A. S., "Faraday's Encyclopedia of Hydrocarbon Compounds," Chemical Publishing Company, Vol. 7, 9 (1961).

70. Quayle, O. R., "The Parachors of Organic Compounds," Chem. Review, Vol. 53, pp. 439-586 (1953).

71. Jackson, L. W., "A Comparison of Selected Gradient Methods for Solving Nonlinear Least Squares Problem," M. S. Thesis, Oklahoma State University, Stillwater, Oklahoma (1978).

72. Robinson, Jr., R. L., Regents Professor and Head, School of Chemical Engineering, Oklahoma State University, Stillwater, Oklahoma 74078.

73. Ely, J. F. and Hanley, H. J. M., NBS Technical Note No. 1039 (1981).

74. Sugden, S., J. Chem. Soc., p. 1177 (1924).

75. Rossini, F. D., et al., "Selected Values of Physical and Thermodynamic Properties of Hydrocarbons and Related Compounds," p. 318, Carnegie Press, Pittsburgh (1953).

76. Sage, B. H. and Lacey, W. N., "Thermodynamic Properties of the Lighter Paraffin Hydrocarbons and Nitrogen," American Petroleum Institute, New York (1950).

77. Katz, D. L., "Phase Relationships in Oil and Gas Reservoirs," Bulletin of the Agricultural and Mechanical College of Texas, No. 114, pp. 38-41, College Station, Texas (1949).

78. Tschiekuna, J., Personal Communication, Oklahoma State University, September, 1987.

APPENDIXES

APPENDIX A

DATA ACQUISITION FORMS

The typical format of the forms used in preparation to collecting data and for actual data acquisition are contained in this appendix. Before the injection of any components, to be studied, a thorough cleaning of the apparatus is performed. Figure 47 contains the form used to collect pertinent information during cleaning, including, the pressure at which circulation was established for each circulation pattern (liquid or vapor), the pump speed required to meet circulation needs, the effect of closing the GC by-pass valve on the circulation rate (a purely subjective rating by the operator from 0-4, where 4 is the best), and the status of cleanliness of the window through which the pendant drop photo graphs are taken.

Figure 48 is an example of the form used during calibrations of the pressure gauges. The data collected are the pressure of the three gauges used in determining the system pressure and the pressure of the fluids being injected.

The calibration of the densitometers is recorded on the form presented in Figure 49. Space is provided to record all system thermocouple readings and system pressure along with the density meter count (DMC) for either the liquid or vapor cell.

Before actually heating up the oven for either calibration or collection of data, a check is made on some prerequisites for startup of

Date: System: + Temp: OP:

TIME HR:MN	TYPE OF CIRCUL.	CLEANING PRESSURE (psi_)	CIRCULATION GC VALVE OPEN CLOSED (0,1,2,3,4)		PUMP SPEED	STATUS OF IFT WINDOW
	L V					
.	L V					
	L V					
	L V					
	L V					
	L V					
	L V					
	L V					
	L V					
	L V					
	L V					
	L V					

COMMENTS:

Figure 47. Form Used During the Cleaning of the System

Date: System: Temp: ° F OP:

ID#	MASS (grams)	TEMP. ° C	DEAD WT.P (psig)	RUSKA P (psig)	SYS P (psia)	SENSO. P. (psig)
1	855.686		144.73			
1,5	1711.486		289.47			
1,5,6	2567.252		434.21			
1,2	4278.661		723.67			
1,2,5,6	5990.227		1013.17			
1,2,3	7701.640		1302.62			
1,2,3,5,6	9413.206		1592.11			
1,2,3,4	11124.695		1881.59			
1,2,3,4,5	11980.495		2026.33			
1,2,3,4,5,6	12836.261		2171.07			
1,2,3,4,5,6,7	13692.036		2315.82			

D.W. P (psig)	SENSO P (psig)	SYS P (psia)	DEL P1 DW-SENSO	DEL P2 DW-SYS	COMMENTS
144.73					
289.47					
434.21					
723.67					
1013.17					
1302.62					
1592.11					
1881.59					
2026.33					
2171.07					
2315.82					

P(senc) = P(sen) + { - P(sen)}

P(sysc) = P(sys) + { - P(sys)}

P(rusc) = P(rus) + { - P(rus)}

Figure 48. Form Used During Calibration of the Pressure Gauges

Date: System: Temp: OP:

PVT 1	IFT 2	DMV 3	DML 4	RM. 5/0	P psi_	TIME	DP1 5/2	DP1 5/3	DP1 5/4	DP1 5/5	DP1 5/6
DMC :											
PRES: psig; psia											
COMM:											
DMC :											
PRES: psig; psia											
COMM:											
DMC :											
PRES: psig; psia											
COMM:											
DMC :											
PRES: psig; psia											
COMM:											
DMC :											
PRES: psig; psia											
COMM:											
DMC :											
PRES: psig; psia											
COMM:											
DMC :											
PRES: psig; psia											
COMM:											
DMC :											
PRES: psig; psia											
COMM:											

Figure 49. Form Used During Calibration of the Densitometers

the apparatus. These checks are shown on the check list in Figure 50.

Figure 51 is an example of the form typically used to record information during the injection of components for a response factor calibration, a total system volume determination, or a material balance during the determination of a bubble point.

The form used to record the bulk of the data for an individual system is displayed in Figure 52. Space is provided to record the temperatures of the thermocouples, the system pressure, the circulation pattern chosen, the pump rate, the rating given by the operator for the relative acceptability of the circulation, the density meter counts (period of ocsillation within densitometer), and area (or % area) given by the gas chromatograph for each component in the mixture of interest.

Once the photographs of the pendant drop have been taken at each pressure of interest, the negatives are measured; specifically, the distances of the major perimeter of the drop, X_{de}, and the minor perimeter at a distance X_{de} from the lowest point on the drop, X_{ds} are determined. The information is recorded onto a form similar to the one shown in Figure 53.

Figure 54 presents the form used to record the information required to determine the bubble point of particular composition.

(The following items should be checked before heating the oven)

---

1) System was leak (and pressure) tested at a pressure of psi_.

2) Does the IFT turret ring rotate while operated by the exterior handles? yes no

3) Were the Valco sampling valves (#1, 3, and 5) actuated with air? yes no

4) Is the magnetic pump running smoothly? yes no

5) Circulation was observed for liquid at a pressure of psi_.
Pump rate = strokes/min.

6) Circulation was observed for vapor at a pressure of psi_.
Pump rate = strokes/min.

7) Are both liquid and vapor DMAs working properly? comment:

8) Are all valve handles fitting tightly to shafts? Check the valves:
Valve #2 __ #3 __ #4 __ #7 __ #8 __ #9 __

9) All thermocouples working properly? Check the thermocouples.
TC #1 __ #2 __ #3 __ #4 __ #5/0 __ #5/2 __#5/3 __ #5/4 __ #5/5__ #5/6 __

10) Is the light source for the IFT centered? yes no

COMMENTS:

Figure 50. Startup Check-list Sheet

Date: System: Temp: OP:

	1 initial final	2 initial final	3 initial final	4 initial final
Component				
V (cc)				
T (F)				
P (psig)				
dV (cc)				
	TIME=	DATE=	OP=	
Component				
V (cc)				
T (F)				
P (psig)				
dV (cc)				
	TIME=	DATE=	OP=	
Component				
V (cc)				
T (F)				
P (psig)				
dV (cc)				
	TIME=	DATE=	OP=	
Component				
V (cc)				
T (F)				
P (psig)				
dV (cc)				

NOTE: During the injection of the hydrocarbon be sure that valve # 3 and valve # 9 are closed. After injecting the hydrocarbon pulse some of the solute into the system, then open valve # 3.

Figure 51. Form Used During Injections

Date: System: Temp: OP:

PVT 1	IFT 2	DMV 3	DML 4	RM. 5/0	P psi_	TIME	DP1 5/2	DP1 5/3	DP1 5/4	DP1 5/5	DP1 5/6
P (psi_)											
		DMC L V :									

TYPE: vap liq	COMP.	AREA	% AREA
CIRC: 0 1 2 3 4	N2		
PUMP:	C2 CO2		
DMC :	HC		
PRES: psig; psia	TOTAL		
COMM:	C/HC		
TYPE: vap liq	COMP.	AREA	% AREA
CIRC: 0 1 2 3 4	N2		
PUMP:	C2 CO2		
DMC :	HC		
PRES: psig; psia	TOTAL		
COMM:	C/HC		
TYPE: vap liq	COMP.	AREA	% AREA
CIRC: 0 1 2 3 4	N2		
PUMP:	C2 CO2		
DMC :	HC		
PRES: psig; psia	TOTAL		
COMM:	C/HC		
TYPE: vap liq	COMP.	AREA	% AREA
CIRC: 0 1 2 3 4	N2		
PUMP:	C2 CO2		
DMC :	HC		
PRES: psig; psia	TOTAL		
COMM:	C/HC		

Figure 52. Form Used During Data Acquisition

Date: System: Temp: F OP:

Picture No.: Pressure : psig; psia Needle O.D.: inches Ref. N.O.D.: inches Date : Xde = - = Y = + = Xds = - = OD = - = ROD = - = S = (Xds/Xde) = 1/H = (FROM TABLES) M.R.= Ref. Act. O.D. / Ref. Mag. O.D. = De = M.R. x 2.54 x Xde = IFTR =980 x (1/H) x De² =	Picture No.: Pressure : psig; psia Needle O.D.: inches Ref. N.O.D.: inches Date : Xde = - = Y = + = Xds = - = OD = - = ROD = - = S = (Xds/Xde) = 1/H = (FROM TABLES) M.R.= Ref. Act. O.D. / Ref. Mag. O.D. = De = M.R. x 2.54 x Xde = IFTR =980 x (1/H) x De² =
Picture No.: Pressure : psig; psia Needle O.D.: inches Ref. N.O.D.: inches Date : Xde = - = Y = + = Xds = - = OD = - = ROD = - = S = (Xds/Xde) = 1/H = (FROM TABLES) M.R.= Ref. Act. O.D. / Ref. Mag. O.D. = De = M.R. x 2.54 x Xde = IFTR =980 x (1/H) x De² =	Picture No.: Pressure : psig; psia Needle O.D.: inches Ref. N.O.D.: inches Date : Xde = - = Y = + = Xds = - = OD = - = ROD = - = S = (Xds/Xde) = 1/H = (FROM TABLES) M.R.= Ref. Act. O.D. / Ref. Mag. O.D. = De = M.R. x 2.54 x Xde = IFTR =980 x (1/H) x De² =

LEGEND:
OD - outside diameter of the needle that the pendant drop hangs from.
ROD - outside diameter of the reference needle.
M.R. - magnification ratio.
IFTR - gamma over delta rho

Figure 53. Form Used During Measurement of the Pendant Drop Photographs

Date:		System:		Temp: F		OP:	
TIME OF INJECTION	RUSKA T (F)	VOL INJ (CC)	DENSITY (GM/CC)	PRESSURE (PSI_)	MOLES INJECTED	TOTAL MOLES	MOLE FRC.

COMMENTS:

Figure 54. Form Used During Determination of the Bubble Point

APPENDIX B

SMOOTHED LITERATURE DATA

In conjunction with the smoothed data produced during the course of this work the smoothing procedure described in Chapter IV was used to smooth other data measured at Oklahoma State University by Robinson, et al. (31, 32, 34, 35). A summary of the root-mean-square error, the weighted root-mean-square error, and the weighting factors from the smoothed data sets appear in Table XLII. A summary of the number of points rejected from the original data set appear in Table XLIII. Table XLIV contains the pressures at which points were rejected. The smoothed data, the regressed parameters for the smoothing function, and the statis tics representing the smoothed data for the carbon dioxide + (benzene at 160°F, n-butane at 115°F, n-butane at 160°F, n-butane at 220°F, cyclohexane at 160°F, n-decane at 160°F, and n-decane at 220°F) appear in Tables XLV through LXV.

The range of applicability for the above mentioned smoothing function does not include extrapolation to pressures lower than the stated pressures in the tables containing the smoothed data. In fact, the smoothing function fails in low pressure regions, this evident in the carbon dioxide + n-butane systems. This is due to the inadequacy of using a polynomial equation as a background term for the scaling law at pressures far removed from the critical point.

TABLE XLII

SUMMARY OF STATISTICAL ERRORS FOR THE CARBON DIOXIDE SYSTEMS STUDIED AT OSU

System	Temp. (°F)	Crit. P. (psia)	No. of data Points	RMSE	WRMS	Prime Error
---------- PHASE COMPOSITION ----------						
CO_2 + C_6H_6	160	1588	30	0.00075	0.998	0.000580
CO_2 + n-C_4	115	1106	29	0.00060	0.934	0.000400
CO_2 + n-C_4	160	1178	27	0.00024	1.015	0.000040
CO_2 + n-C_4	220	1098	24	0.00080	0.987	0.000700
CO_2 + C_6H_{12}	160	1590	30	0.00118	1.000	0.000631
CO_2 + n-C_{10}	160	1848	35	0.00181	0.999	0.001670
CO_2 + n-C_{10}	220	2391	48	0.00111	0.994	0.000998
---------- PHASE DENSITY ----------						
CO_2 + C_6H_6	160	1588	28	0.00073	0.997	0.000335
CO_2 + n-C_4	115	1106	35	0.00143	0.997	0.000850
CO_2 + n-C_4	160	1178	30	0.00060	1.016	0.000220
CO_2 + n-C_4	220	1098	29	0.00083	1.002	0.000648
CO_2 + C_6H_{12}	160	1590	26	0.00107	0.983	0.000189
CO_2 + n-C_{10}	160	1848	30	0.00141	0.997	0.000610
CO_2 + n-C_{10}	220	2391	45	0.00104	1.022	0.000500
---------- INTERFACIAL TENSION/DENSITY DIFFERENCE ----------						
				% AAPD		
CO_2 + C_6H_6	160	1588	14	1.4180	0.995	0.0080
CO_2 + N-C_4	115	1106	18	2.9035	1.000	0.0333
CO_2 + N-C_4	160	1178	12	2.5178	1.000	0.0342
CO_2 + N-C_4	220	1098	12	3.3823	1.000	0.0473
CO_2 + C_6H_{12}	160	1590	14	3.4695	0.990	0.0347
CO_2 + N-C_{10}	160	1848	16	2.6857	0.998	0.0267
CO_2 + N-C_{10}	220	2391	23	4.1226	0.991	0.0365

TABLE XLIII

SUMMARY OF REJECTED DATA POINTS FOR THE CARBON DIOXIDE SYSTEMS STUDIED AT OSU

System	Temp. (°F)	Crit. P. (psia)	No. of data Points	Points Rejected Liq.	Vap.
---------- PHASE COMPOSITION ----------					
CO_2 + C_6H_6	160	1588	30	0	0
CO_2 + n-C_4	115	1106	40	5	6
CO_2 + n-C_4	160	1178	30	1	2
CO_2 + n-C_4	220	1098	30	3	3
CO_2 + C_6H_{12}	160	1590	30	0	0
CO_2 + n-C_{10}	160	1848	36	1	0
CO_2 + n-C_{10}	220	2391	48	0	0
---------- PHASE DENSITY ----------					
CO_2 + C_6H_6	160	1588	30	1	1
CO_2 + n-C_4	115	1106	40	1	4
CO_2 + n-C_4	160	1178	30	0	0
CO_2 + n-C_4	220	1098	30	1	0
CO_2 + C_6H_{12}	160	1590	30	2	2
CO_2 + n-C_{10}	160	1848	36	3	3
CO_2 + n-C_{10}	220	2391	48	2	1
----------INTERFACIAL TENSION/DENSITY DIFFERENCE----------					
CO_2 + C_6H_6	160	1588	15	1	
CO_2 + n-C_4	115	1106	18	0	
CO_2 + n-C_4	160	1178	12	0	
CO_2 + n-C_4	220	1098	12	0	
CO_2 + C_6H_{12}	160	1590	14	0	
CO_2 + n-C_{10}	160	1848	17	1	
CO_2 + n-C_{10}	220	2391	23	0	

TABLE XLIV

SUMMARY OF REJECTED PRESSURES FOR THE CARBON DIOXIDE SYSTEMS STUDIED AT OSU

CO_2+C_6H_6 at 160°F Pc=1588	CO_2+n-C_4 at 115°F Pc=1106	CO_2+n-C_4 at 160°F Pc=1178	CO_2+n-C_4 at 220°F Pc=1098	CO_2+C_6H_{12} at 160°F Pc=1590	CO_2+n-C_{10} at 160°F Pc=1848	CO_2+n-C_{10} at 220°F Pc=2391
PHASE COMPOSITION						
	316(L)	465(L)	418(L)		1811(L)	
	375(L)	465(V)	498(L)			
	497(L)	610(V)	604(L)			
	514(L)		418(V)			
	610(L)		498(V)			
	316(V)		604(V)			
	375(V)					
	497(V)					
	514(V)					
	610(V)					
	710(V)					
PHASE DENSITY						
1430(L)	1010(L)		1003(L)	1300(L)	1007(L)	1801(L)
1430(V)	375(V)			1400(L)	1104(L)	2100(L)
	514(V)			1300(V)	1210(L)	2386(V)
	875(V)			1400(V)	1007(V)	
	906(V)				1104(V)	
					1210(V)	
INTERFACIAL TENSION/DENSITY DIFFERENCE						
1430					1799	

TABLE XLV

SMOOTHED PHASE EQUILIBRIA AND INTERFACIAL TENSIONS FOR CARBON DIOXIDE + BENZENE AT 344.3 K (160°F)

Pressure (psia)	Phase Compositions, (Mole Fraction CO_2) Liquid	Vapor	Phase Densities, (kg/m^3) x 10^{-3} Liquid	Vapor	IFT Ratio, $(mN/m)/(kg/m^3)$ IFTR
1000	0.4528	0.9316	0.8150	0.1560	9.9778
1100	0.5067	0.9371	0.8093	0.1772	8.0010
1200	0.5627	0.9413	0.8018	0.2048	6.1652
1300	0.6251	0.9400	0.7869	0.2367	4.4622
1400	0.6924	0.9355	0.7639	0.2800	2.8771
1500	0.7630	0.9262	0.7141	0.3404	1.3769
1510	0.7708	0.9246	0.7066	0.3488	1.2287
1520	0.7789	0.9227	0.6985	0.3580	1.0802
1530	0.7874	0.9205	0.6897	0.3682	0.9310
1540	0.7964	0.9180	0.6799	0.3796	0.7809
1550	0.8059	0.9151	0.6690	0.3925	0.6291
1560	0.8161	0.9116	0.6562	0.4075	0.4748
1570	0.8273	0.9075	0.6402	0.4255	0.3164
1580	0.8401	0.9018	0.6162	0.4496	0.1504
1582	0.8431	0.9002	0.6090	0.4562	0.1155
1584	0.8466	0.8981	0.5997	0.4644	0.0796
1586	(0.8513)*	(0.8947)	(0.5861)	(0.4761)	(0.0421)
1588**	(0.8736)	(0.8736)	(0.5286)	(0.5286)	(0.0000)

*Numbers in parentheses are extrapolated beyond highest measured pressures.

** Estimated critical point

TABLE XLVI

PARAMETERS USED TO GENERATE SMOOTHED PROPERTIES FOR CARBON DIOXIDE + BENZENE AT 160°F

PHASE COMPOSITIONS
Units: Mole Fraction Carbon Dioxide

PC	1588.
ZC	0.8735925
AZ0	0.2393224
AZ1	-1.0090831
AZ2	4.0853050
AZ3	-34.7325388
AZ4	153.6018742
AZ5	-330.8548116
AZ6	275.7054590
BZ0	0.5152262
BZ1	-4.5974699
BZ2	46.6217096
BZ3	-210.7428597
BZ4	504.7042860
BZ5	-605.7471574
BZ6	285.7994841

PHASE DENSITIES
Units: $(kg/m^3) \times 10^{-3}$ or (gm/cc)

RHOC	0.528630
AR0	3.263565
AR1	-5.591445
AR2	23.837960
AR3	-180.957742
AR4	771.610969
AR5	-1651.995363
AR6	1385.710694
BR0	1.117555
BR1	-3.722776
BR2	30.602698
BR3	-113.762179
BR4	216.140308
BR5	-207.915684
BR6	80.340935

IFT-DENSITY DIFFERENCE RATIO
Units: $[(mN/m)/(kg/m^3)] \times 10^{-3}$ or [(mN/m)/(gm/cc)]

BG0	20.75488997
BG1	-9.01034781
BG2	26.41632766

TABLE XLVII

SUMMARY OF STATISTICS FOR CARBON DIOXIDE + BENZENE AT 160°F

VARIABLE	MEAN
SUMMARY OF RESULTS FOR PHASE COMPOSITION	
CO2 MOLE FRACTION	0.8206233
ROOT-MEAN-SQUARED ERROR	0.0007543
WEIGHTED ROOT-MEAN-SQUARED ERROR	0.9978836
ABSLOUTE AVERAGE % DEVIATION	0.0000000
DEVIATION,YEXP-YCALC	0.0000003
% DEVIATION	-0.0000128
SCALED PRESSURE,(PC-P)/PC	0.1055835
CRITICAL PRESSURE	1588.0000000
WEIGHTED DEVIATION, DEV/SIGMA	-0.0014097
MOLE FRACTION PRIME ERROR	0.0005800
PRESSURE PRIME ERROR	1.0000000
SUMMARY OF RESULTS FOR PHASE DENSITY	
PHASE DENSITY	0.5205393
ROOT-MEAN-SQUARED ERROR	0.0007346
WEIGHTED ROOT-MEAN-SQUARED ERROR	0.9968315
ABSLOUTE AVERAGE % DEVIATION	0.1720924
DEVIATION,YEXP-YCALC	0.0000010
% DEVIATION	0.0000218
SCALED PRESSURE,(PC-P)/PC	0.1060184
CRITICAL PRESSURE	1588.0000000
WEIGHTED DEVIATION, DEV/SIGMA	0.0005882
DENSITY PRIME ERROR	0.0003350
PRESSURE PRIME ERROR	1.0000000
SUMMARY OF RESULTS FOR IFTR	
GAMMA/DRHO	2.7243571
ROOT-MEAN-SQUARED ERROR	0.0439186
WEIGHTED ROOT-MEAN-SQUARED ERROR	0.9948464
ABSLOUTE AVERAGE % DEVIATION	1.4180488
DEVIATION,YEXP-YCALC	-0.0022248
% DEVIATION	0.2924876
SCALED PRESSURE,(PC-P)/PC	0.1060184
CRITICAL PRESSURE	1588.0000000
WEIGHTED DEVIATION, DEV/SIGMA	-0.1100255
GAMMA/DRHO PRIME ERROR C1	0.0080000
GAMMA/DRHO PRIME ERROR C2	0.8100000
PRESSURE PRIME ERROR	1.0000000

TABLE XLVIII

SMOOTHED PHASE EQUILIBRIA AND INTERFACIAL TENSIONS
FOR CARBON DIOXIDE + N-BUTANE AT 319.3 K (115°F)

Pressure (psia)	Phase Compositions, (Mole Fraction CO_2) Liquid	Vapor	Phase Densities, (kg/m^3) x 10^{-3} Liquid	Vapor	IFT Ratio, $(mN/m)/(kg/m^3)$ IFTR
300			0.5637	0.0497	11.4563
400			0.5689	0.0591	10.1424
500			0.5776	0.0767	8.7754
600			0.5836	0.0971	7.3618
700	0.5055		0.5861	0.1209	5.9096
800	0.5976	0.8864	0.5841	0.1501	4.4303
900	0.6866	0.8928	0.5741	0.1861	2.9405
1000	0.7694	0.8982	0.5482	0.2336	1.4687
1010	0.7773	0.8986	0.5443	0.2396	1.3243
1020	0.7853	0.8989	0.5399	0.2462	1.1808
1030	0.7933	0.8990	0.5351	0.2532	1.0382
1040	0.8014	0.8989	0.5298	0.2610	0.8967
1050	0.8096	0.8985	0.5239	0.2697	0.7563
1060	0.8179	0.8979	0.5172	0.2796	0.6174
1070	0.8265	0.8969	0.5095	0.2911	0.4800
1080	0.8354	0.8955	0.5001	0.3052	0.3444
1090	0.8447	0.8933	0.4878	0.3238	0.2110
1100	0.8553	0.8888	0.4683	0.3528	(0.0799)*
1102	0.8580	0.8870	0.4618	0.3619	(0.0538)
1104	0.8615	0.8843	0.4526	0.3745	(0.0275)
1106**	(0.8727)	(0.8727)	(0.4162)	(0.4162)	(0.0000)

*Numbers in parentheses are extrapolated beyond highest measured pressures.
**Estimated critical point

TABLE XLIX

PARAMETERS USED TO GENERATE SMOOTHED PROPERTIES FOR CARBON DIOXIDE + N-BUTANE AT 115°F

PHASE COMPOSITIONS
Units: Mole Fraction Carbon Dioxide

PC	1106.
ZC	0.8727433
AZ0	0.7270614
AZ1	-1.5350701
AZ2	3.1781622
AZ3	-24.4017740
AZ4	100.3489062
AZ5	-185.9407908
AZ6	99.6759545
BZ0	0.1816164
BZ1	0.2359510
BZ2	-3.9299613
BZ3	42.9627129
BZ4	-167.6001569
BZ5	293.9700697
BZ6	-190.4921168

PHASE DENSITIES
Units: $(kg/m^3) \times 10^{-3}$ or (gm/cc)

RHOC	0.41620446
AR0	-1.53639548
AR1	1.90554938
AR2	-1.11700198
AR3	-0.91235064
AR4	7.54625215
AR5	-11.96169756
AR6	6.29698762
BR0	0.60873649
BR1	0.93133357
BR2	-4.42101474
BR3	11.35318774
BR4	-16.98006240
BR5	12.97117377
BR6	-3.97039261

IFT-DENSITY DIFFERENCE RATIO
Units: $[(mN/m)/(kg/m^3)] \times 10^{-3}$ or [(mN/m)/(gm/cc)]

BG0	8.92484260
BG1	15.87321069
BG2	-9.76385501

TABLE L

SUMMARY OF STATISTICS FOR CARBON DIOXIDE + N-BUTANE AT 115° F

VARIABLE	MEAN
SUMMARY OF RESULTS FOR PHASE COMPOSITION	
CO2 MOLE FRACTION	0.8246552
ROOT-MEAN-SQUARED ERROR	0.0005962
WEIGHTED ROOT-MEAN-SQUARED ERROR	0.9336893
ABSLOUTE AVERAGE % DEVIATION	0.0000000
DEVIATION,YEXP-YCALC	0.0000003
% DEVIATION	-0.0000133
SCALED PRESSURE,(PC-P)/PC	0.0960279
CRITICAL PRESSURE	1106.0000000
WEIGHTED DEVIATION, DEV/SIGMA	0.0104180
MOLE FRACTION PRIME ERROR	0.0004000
PRESSURE PRIME ERROR	1.0000000
SUMMARY OF RESULTS FOR PHASE DENSITY	
PHASE DENSITY	0.3983714
ROOT-MEAN-SQUARED ERROR	0.0014278
WEIGHTED ROOT-MEAN-SQUARED ERROR	0.9967575
ABSLOUTE AVERAGE % DEVIATION	0.4128742
DEVIATION,YERP-YCALC	-0.0000009
% DEVIATION	-0.0009846
SCALED PRESSURE,(PC-P)/PC	0.2082666
CRITICAL PRESSURE	1106.0000000
WEIGHTED DEVIATION, DEV/SIGMA	-0.0067767
DENSITY PRIME ERROR	0.0008500
PRESSURE PRIME ERROR	1.0000000
SUMMARY OF RESULTS FOR IFTR	
GAMMA/DRHO	3.9438333
ROOT-MEAN-SQUARED ERROR	0.0615102
WEIGHTED ROOT-MEAN-SQUARED ERROR	0.9996257
ABSLOUTE AVERAGE % DEVIATION	2.9034638
DEVIATION,YEXP-YCALC	0.0026734
% DEVIATION	1.4915570
SCALED PRESSURE,(PC-P)/PC	0.2485935
CRITICAL PRESSURE	1106.0000000
WEIGHTED DEVIATION, DEV/SIGMA	0.2034912
GAMMA/DRHO PRIME ERROR C1	0.0333000
GAMMA/DRHO PRIME ERROR C2	0.8100000
PRESSURE PRIME ERROR	1.0000000

TABLE LI

SMOOTHED PHASE EQUILIBRIA AND INTERFACIAL TENSIONS
FOR CARBON DIOXIDE + N-BUTANE AT 344.3 K (160°F)

Pressure (psia)	Phase Compositions, (Mole Fraction CO_2) Liquid	Vapor	Phase Densities, (kg/m^3) x 10^{-3} Liquid	Vapor	IFT Ratio, $(mN/m)/(kg/m^3)$ IFTR
400			0.5135	0.0589	10.2772
500	0.2243		0.5219	0.0749	8.8595
600	0.2909		0.5234	0.0928	7.4790
700	0.3531	0.7608	0.5227	0.1129	6.1343
800	0.4170	0.7767	0.5210	0.1355	4.8234
900	0.4819	0.7879	0.5165	0.1616	3.5429
1000	0.5486	0.7907	0.5051	0.1949	2.2861
1100	0.6196	0.7834	0.4799	0.2465	1.0361
1110	0.6272	0.7817	0.4758	0.2536	0.9098
1120	0.6350	0.7796	0.4713	0.2613	0.7828
1130	0.6430	0.7770	0.4660	0.2698	0.6549
1140	0.6515	0.7738	0.4597	0.2792	0.5258
1150	0.6606	0.7697	0.4519	0.2899	0.3949
1160	0.6711	0.7639	0.4414	0.3027	0.2614
1170	0.6849	0.7544	0.4249	0.3202	(0.1228)*
1172	0.6887	0.7515	0.4199	0.3250	(0.0940)
1174	(0.6932)	(0.7478)	(0.4136)	(0.3310)	(0.0645)
1176	(0.6994)	(0.7424)	(0.4045)	(0.3393)	(0.0339)
1178**	(0.7213)	(0.7213)	(0.3708)	(0.3708)	(0.0000)

*Numbers in parentheses are extrapolated beyond highest measured pressures.
**Estimated critical point

TABLE LII

PARAMETERS USED TO GENERATE SMOOTHED PROPERTIES FOR CARBON DIOXIDE + N-BUTANE AT 160°F

PHASE COMPOSITIONS
Units: Mole Fraction Carbon Dioxide

PC	1178.
ZC	0.72135000
AZ0	-0.04427455
AZ1	-0.15178708
AZ2	-1.83907408
AZ3	10.19026668
AZ4	-32.90938122
AZ5	51.46981839
AZ6	-30.18745259
BZ0	0.35127892
BZ1	0.24975315
BZ2	-1.07663241
BZ3	4.74050919
BZ4	-3.65762684
BZ5	-5.37369067
BZ6	6.25119736

PHASE DENSITIES
Units: $(kg/m^3) \times 10^{-3}$ or (gm/cc)

RHOC	0.37078708
AR0	1.11608850
AR1	-1.84295218
AR2	2.94183633
AR3	-8.70170176
AR4	15.26181604
AR5	-13.58290619
AR6	4.61362816
BR0	0.53860778
BR1	0.23176301
BR2	-1.14324988
BR3	7.15610018
BR4	-21.59621845
BR5	27.16170645
BR6	-12.14627516

IFT-DENSITY DIFFERENCE RATIO
Units: $[(mN/m)/(kg/m^3)] \times 10^{-3}$ or [(mN/m)/(gm/cc)]

BG0	12.47889281
BG1	0.46369960
BG2	3.39023062

TABLE LIII

SUMMARY OF STATISTICS FOR CARBON DIOXIDE + N-BUTANE AT 160°F

VARIABLE	MEAN
SUMMARY OF RESULTS FOR PHASE COMPOSITION	
CO2 MOLE FRACTION	0.6676222
ROOT-MEAN-SQUARED ERROR	0.0002380
WEIGHTED ROOT-MEAN-SQUARED ERROR	1.0147708
ABSLOUTE AVERAGE % DEVIATION	0.0000000
DEVIATION,YEXP-YCALC	-0.0000021
% DEVIATION	-0.0002780
SCALED PRESSURE,(PC-P)/PC	0.1223668
CRITICAL PRESSURE	1178.0000000
WEIGHTED DEVIATION, DEV/SIGMA	-0.0942246
MOLE FRACTION PRIME ERROR	0.0000400
PRESSURE PRIME ERROR	1.0000000
SUMMARY OF RESULTS FOR PHASE DENSITY	
PHASE DENSITY	0.3504833
ROOT-MEAN-SQUARED ERROR	0.0005980
WEIGHTED ROOT-MEAN-SQUARED ERROR	1.0158783
ABSLOUTE AVERAGE % DEVIATION	0.2172108
DEVIATION,YERP-YCALC	-0.0000001
% DEVIATION	-0.0002108
SCALED PRESSURE,(PC-P)/PC	0.1665535
CRITICAL PRESSURE	1178.0000000
WEIGHTED DEVIATION, DEV/SIGMA	0.0005412
DENSITY PRIME ERROR	0.0002200
PRESSURE PRIME ERROR	1.0000000
SUMMARY OF RESULTS FOR IFTR	
GAMMA/DRHO	3.1459167
ROOT-MEAN-SQUARED ERROR	0.0700318
WEIGHTED ROOT-MEAN-SQUARED ERROR	0.9998811
ABSLOUTE AVERAGE % DEVIATION	2.5178176
DEVIATION,YEXP-YCALC	0.0108033
% DEVIATION	-1.6423414
SCALED PRESSURE,(PC-P)/PC	0.2065648
CRITICAL PRESSURE	1178.0000000
WEIGHTED DEVIATION, DEV/SIGMA	-0.3746359
GAMMA/DRHO PRIME ERROR C1	0.0342000
GAMMA/DRHO PRIME ERROR C2	0.8100000
PRESSURE PRIME ERROR	1.0000000

TABLE LIV

SMOOTHED PHASE EQUILIBRIA AND INTERFACIAL TENSIONS
FOR CARBON DIOXIDE + N-BUTANE AT 377.6 K (220°F)

Pressure (psia)	Phase Compositions, (Mole Fraction CO_2) Liquid	Vapor	Phase Densities, (kg/m^3) x 10^{-3} Liquid	Vapor	IFT Ratio, $(mN/m)/(kg/m^3)$ IFTR
400			0.4579	0.0679	7.0618
500			0.4545	0.0846	6.0579
600			0.4527	0.1012	5.0490
700	0.2288	0.5240	0.4480	0.1211	4.0367
800	0.2820	0.5551	0.4398	0.1452	3.0228
850	0.3073	0.5636	0.4347	0.1587	2.5161
900	0.3354	0.5697	0.4286	0.1734	2.0100
950	0.3650	0.5733	0.4211	0.1898	1.5048
1000	0.3950	0.5738	0.4102	0.2099	1.0008
1050	0.4286	0.5666	0.3915	0.2381	0.4971
1060	0.4367	0.5630	0.3860	0.2456	(0.3961)*
1070	0.4457	0.5581	0.3793	0.2541	(0.2947)
1080	0.4561	0.5515	0.3711	0.2643	(0.1926)
1090	0.4688	0.5419	0.3595	0.2777	(0.0888)
1092	0.4720	0.5392	0.3562	0.2813	(0.0676)
1094	0.4758	0.5360	0.3521	0.2857	(0.0461)
1096	0.4810	0.5313	0.3462	0.2919	(0.0240)
1098**	(0.5063)	(0.5063)	(0.3191)	(0.3191)	(0.0000)

*Numbers in parentheses are extrapolated beyond highest measured pressures.
**Estimated critical point

TABLE LV

PARAMETERS USED TO GENERATE SMOOTHED PROPERTIES FOR CARBON DIOXIDE + N-BUTANE AT 220°F

PHASE COMPOSITIONS
Units: Mole Fraction Carbon Dioxide

PC	1098.
ZC	0.5063495
AZ0	0.0206900
AZ1	-0.1602876
AZ2	-2.1492001
AZ3	15.0078981
AZ4	-75.0071799
AZ5	206.8617098
AZ6	-225.8505326
BZ0	0.5240264
BZ1	-4.0056423
BZ2	39.3542222
BZ3	-181.1553161
BZ4	432.0063928
BZ5	-512.8482781
BZ6	238.9085611

PHASE DENSITIES
Units: $(kg/m^3) \times 10^{-3}$ or (gm/cc)

RHOC	0.3191186
AR0	0.1016651
AR1	-0.2623076
AR2	0.3500999
AR3	-1.3002957
AR4	3.2791645
AR5	-4.3401773
AR6	2.2693642
BR0	0.5048617
BR1	-2.0601985
BR2	17.5244125
BR3	-65.4132669
BR4	123.3246842
BR5	-114.7747014
BR6	41.8426495

IFT-DENSITY DIFFERENCE RATIO
Units: $[(mN/m)/(kg/m^3)] \times 10^{-3}$ or [(mN/m)/(gm/cc)]

BG0	8.089530095
BG1	4.975472352
BG2	-2.062009189

TABLE LVI

SUMMARY OF STATISTICS FOR CARBON DIOXIDE + N-BUTANE AT 220°F

VARIABLE	MEAN
SUMMARY OF RESULTS FOR PHASE COMPOSITION	
CO2 MOLE FRACTION	0.4707875
ROOT-MEAN-SQUARED ERROR	0.0007975
WEIGHTED ROOT-MEAN-SQUARED ERROR	0.9869794
ABSLOUTE AVERAGE % DEVIATION	0.0000000
DEVIATION,YEXP-YCALC	0.0000305
% DEVIATION	0.0051838
SCALED PRESSURE,(PC-P)/PC	0.1180176
CRITICAL PRESSURE	1098.0000000
WEIGHTED DEVIATION, DEV/SIGMA	0.0421451
MOLE FRACTION PRIME ERROR	0.0007000
PRESSURE PRIME ERROR	1.0000000
SUMMARY OF RESULTS FOR PHASE DENSITY	
PHASE DENSITY	0.2962724
ROOT-MEAN-SQUARED ERROR	0.0008312
WEIGHTED ROOT-MEAN-SQUARED ERROR	1.0019332
ABSLOUTE AVERAGE % DEVIATION	0.4076574
DEVIATION,YERP-YCALC	0.0000000
% DEVIATION	-0.0003707
SCALED PRESSURE,(PC-P)/PC	0.2061114
CRITICAL PRESSURE	1098.0000000
WEIGHTED DEVIATION, DEV/SIGMA	0.0012063
DENSITY PRIME ERROR	0.0006480
PRESSURE PRIME ERROR	1.0000000
SUMMARY OF RESULTS FOR IFTR	
GAMMA/DRHO	2.7773333
ROOT-MEAN-SQUARED ERROR	0.0528357
WEIGHTED ROOT-MEAN-SQUARED ERROR	0.9995417
ABSLOUTE AVERAGE % DEVIATION	3.3822802
DEVIATION,YEXP-YCALC	-0.0142332
% DEVIATION	-2.5969396
SCALED PRESSURE,(PC-P)/PC	0.2505313
CRITICAL PRESSURE	1098.0000000
WEIGHTED DEVIATION, DEV/SIGMA	-0.4737508
GAMMA/DRHO PRIME ERROR C1	0.0472500
GAMMA/DRHO PRIME ERROR C2	0.8100000
PRESSURE PRIME ERROR	1.0000000

TABLE LVII

SMOOTHED PHASE EQUILIBRIA AND INTERFACIAL TENSIONS FOR CARBON DIOXIDE + CYCLOHEXANE AT 344.3 K (160°F)

Pressure (psia)	Phase Compositions, (Mole Fraction CO_2) Liquid	Vapor	Phase Densities, (kg/m^3) x 10^{-3} Liquid	Vapor	IFT Ratio, $(mN/m)/(kg/m^3)$ IFTR
1000	0.4271	0.9508	0.7397	0.1548	10.7823
1100	0.4801	0.9470	0.7341	0.1759	8.9746
1200	0.5351	0.9485	0.7307	0.2055	7.1001
1300	0.5952	0.9458	0.7564	0.2678	5.2037
1400	0.6659	0.9402	0.7270	0.2908	3.3350
1500	0.7448	0.9270	0.6783	0.3365	1.5468
1510	0.7535	0.9252	0.6736	0.3454	1.3741
1520	0.7624	0.9232	0.6684	0.3550	1.2027
1530	0.7717	0.9211	0.6624	0.3652	1.0323
1540	0.7815	0.9189	0.6553	0.3761	0.8629
1550	0.7918	0.9163	0.6464	0.3878	0.6943
1560	0.8028	0.9132	0.6352	0.4009	0.5260
1570	0.8147	0.9090	0.6207	0.4170	0.3572
1580	0.8283	0.9021	0.6010	0.4414	0.1858
1582	0.8314	0.8999	0.5961	0.4487	0.1508
1584	0.8348	0.8973	0.5905	0.4575	0.1152
1586	0.8387	0.8937	0.5838	0.4690	0.0790
1588	0.8439	0.8882	0.5749	0.4856	(0.0415)*
1590**	(0.8647)	(0.8647)	(0.5392)	(0.5392)	(0.0000)

*Numbers in parentheses are extrapolated beyond highest measured pressures.
**Estimated critical point

TABLE LVIII

PARAMETERS USED TO GENERATE SMOOTHED PROPERTIES FOR CARBON DIOXIDE + CYCLOHEXANE AT 160°F

PHASE COMPOSITIONS

Units: Mole Fraction Carbon Dioxide

PC	1590.
ZC	0.864695
AZ0	2.563725
AZ1	-4.859309
AZ2	17.750072
AZ3	-128.848042
AZ4	548.174813
AZ5	-1181.285647
AZ6	998.795069
BZ0	0.446088
BZ1	-1.453035
BZ2	14.929698
BZ3	-61.077967
BZ4	151.848406
BZ5	-202.841191
BZ6	108.408061

PHASE DENSITIES

Units: $(kg/m^3) \times 10^{-3}$ or (gm/cc)

RHOC	0.53919
AR0	-11.29760
AR1	19.03330
AR2	-101.06075
AR3	956.70118
AR4	-4836.04948
AR5	11628.61767
AR6	-10533.06282
BR0	0.75691
BR1	2.75265
BR2	-25.80013
BR3	127.50313
BR4	-331.35679
BR5	420.56594
BR6	-205.83365

IFT-DENSITY DIFFERENCE RATIO

Units: $[(mN/m)/(kg/m^3)] \times 10^{-3}$ or [(mN/m)/(gm/cc)]

BG0	20.21939689
BG1	-2.26396998
BG2	57.08735031
BG3	-57.52919286

TABLE LIX

SUMMARY OF STATISTICS FOR CARBON DIOXIDE + CYCLOHEXANE AT 160°F

VARIABLE	MEAN
SUMMARY OF RESULTS FOR PHASE COMPOSITION	
CO2 MOLE FRACTION	0.8159200
ROOT-MEAN-SQUARED ERROR	0.0011831
WEIGHTED ROOT-MEAN-SQUARED ERROR	0.9995143
ABSLOUTE AVERAGE % DEVIATION	0.0000000
DEVIATION,YEXP-YCALC	0.0000052
% DEVIATION	0.0005361
SCALED PRESSURE,(PC-P)/PC	0.1007547
CRITICAL PRESSURE	1590.0000000
WEIGHTED DEVIATION, DEV/SIGMA	-0.0246850
MOLE FRACTION PRIME ERROR	0.0006310
PRESSURE PRIME ERROR	1.0000000
SUMMARY OF RESULTS FOR PHASE DENSITY	
PHASE DENSITY	0.5029385
ROOT-MEAN-SQUARED ERROR	0.0010656
WEIGHTED ROOT-MEAN-SQUARED ERROR	0.9824350
ABSLOUTE AVERAGE % DEVIATION	0.1847732
DEVIATION,YERP-YCALC	0.0000157
% DEVIATION	0.0041345
SCALED PRESSURE,(PC-P)/PC	0.0930334
CRITICAL PRESSURE	1590.0000000
WEIGHTED DEVIATION, DEV/SIGMA	0.0738133
DENSITY PRIME ERROR	0.0001890
PRESSURE PRIME ERROR	1.0000000
SUMMARY OF RESULTS FOR IFTR	
GAMMA/DRHO	3.098071
ROOT-MEAN-SQUARED ERROR	0.057960
WEIGHTED ROOT-MEAN-SQUARED ERROR	0.990404
ABSLOUTE AVERAGE % DEVIATION	3.469472
DEVIATION,YEXP-YCALC	-0.009188
% DEVIATION	-2.554058
SCALED PRESSURE,(PC-P)/PC	0.107907
CRITICAL PRESSURE	1590.000000
WEIGHTED DEVIATION, DEV/SIGMA	-0.412857
GAMMA/DRHO PRIME ERROR C1	0.034700
GAMMA/DRHO PRIME ERROR C2	0.810000
PRESSURE PRIME ERROR	1.000000

TABLE LX

SMOOTHED PHASE EQUILIBRIA AND INTERFACIAL TENSIONS
FOR CARBON DIOXIDE + N-DECANE AT 344.3 K (160°F)

Pressure (psia)	Phase Compositions, (Mole Fraction CO_2) Liquid	Vapor	Phase Densities, (kg/m^3) x 10^{-3} Liquid	Vapor	IFT Ratio, $(mN/m)/(kg/m^3)$ IFTR
1000	0.4858	0.9941			13.9307
1100	0.5320	0.9961			12.3480
1200	0.5726	0.9943	0.6146	0.1183	10.7545
1300	0.6139	0.9935	0.7154	0.2119	9.1497
1400	0.6569	0.9930	0.7166	0.2416	7.5332
1500	0.7019	0.9909	0.7160	0.2775	5.9040
1600	0.7503	0.9870	0.7152	0.3191	4.2595
1700	0.8036	0.9822	0.7072	0.3741	2.5939
1800	0.8642	0.9715	0.6840	0.4602	0.8865
1810	0.8715	0.9686	0.6783	0.4727	0.7104
1820	0.8795	0.9647	0.6708	0.4877	0.5323
1830	0.8889	0.9590	0.6603	0.5076	0.3509
1840	0.9014	0.9497	0.6435	0.5389	(0.1639)*
1842	0.9047	0.9469	0.6385	0.5482	(0.1252)
1844	0.9087	0.9434	0.6325	0.5597	(0.0857)
1846	0.9137	0.9387	0.6245	0.5749	(0.0449)
1848**	(0.9263)	(0.9263)	(0.6064)	(0.6064)	(0.0000)

*Numbers in parentheses are extrapolated beyond highest measured pressures.
**Estimated critical point

TABLE LXI

PARAMETERS USED TO GENERATE SMOOTHED PROPERTIES FOR CARBON DIOXIDE + N-DECANE AT 160°F

PHASE COMPOSITIONS
Units: Mole Fraction Carbon Dioxide

PC	1848.
ZC	0.9262887
AZ0	0.2983464
AZ1	-0.7506805
AZ2	-2.3078493
AZ3	24.0004876
AZ4	-99.9582652
AZ5	193.8914225
AZ6	-143.3938195
BZ0	0.1585863
BZ1	3.2157354
BZ2	-21.7982704
BZ3	81.2882838
BZ4	-153.1792714
BZ5	142.1277766
BZ6	-51.3506468

PHASE DENSITIES
Units: $(kg/m^3) \times 10^{-3}$ or (gm/cc)

RHOC	0.606353
AR0	-7.452247
AR1	11.402195
AR2	-45.545982
AR3	377.043633
AR4	-1858.754290
AR5	4731.139861
AR6	-4785.113005
BR0	0.180960
BR1	12.238741
BR2	-106.731438
BR3	483.662647
BR4	-1182.386185
BR5	1473.832660
BR6	-734.189588

IFT-DENSITY DIFFERENCE RATIO
Units: $[(mN/m)/(kg/m^3)] \times 10^{-3}$ or [(mN/m)/(gm/cc)]

BG0	24.86451534
BG1	8.40992966
BG2	-4.11563517

TABLE LXII

SUMMARY OF STATISTICS FOR CARBON DIOXIDE + N-DECANE AT 160°F

VARIABLE	MEAN
SUMMARY OF RESULTS FOR PHASE COMPOSITION	
CO2 MOLE FRACTION	0.8700114
ROOT-MEAN-SQUARED ERROR	0.0018142
WEIGHTED ROOT-MEAN-SQUARED ERROR	0.9985521
ABSLOUTE AVERAGE % DEVIATION	0.0000000
DEVIATION,YEXP-YCALC	-0.0000061
% DEVIATION	-0.0009606
SCALED PRESSURE,(PC-P)/PC	0.1416976
CRITICAL PRESSURE	1848.0000000
WEIGHTED DEVIATION, DEV/SIGMA	-0.0026408
MOLE FRACTION PRIME ERROR	0.0016700
PRESSURE PRIME ERROR	1.0000000
SUMMARY OF RESULTS FOR PHASE DENSITY	
PHASE DENSITY	0.5462100
ROOT-MEAN-SQUARED ERROR	0.0014127
WEIGHTED ROOT-MEAN-SQUARED ERROR	0.9970447
ABSLOUTE AVERAGE % DEVIATION	0.2353375
DEVIATION,YERP-YCALC	0.0000015
% DEVIATION	0.0001749
SCALED PRESSURE,(PC-P)/PC	0.0857864
CRITICAL PRESSURE	1848.0000000
WEIGHTED DEVIATION, DEV/SIGMA	0.0021343
DENSITY PRIME ERROR	0.0006100
PRESSURE PRIME ERROR	1.0000000
SUMMARY OF RESULTS FOR IFTR	
GAMMA/DRHO	4.7968125
ROOT-MEAN-SQUARED ERROR	0.0786414
WEIGHTED ROOT-MEAN-SQUARED ERROR	0.9982699
ABSLOUTE AVERAGE % DEVIATION	2.6857312
DEVIATION,YEXP-YCALC	0.0065048
% DEVIATION	0.4143038
SCALED PRESSURE,(PC-P)/PC	0.1539164
CRITICAL PRESSURE	1848.0000000
WEIGHTED DEVIATION, DEV/SIGMA	0.2088592
GAMMA/DRHO PRIME ERROR C1	0.0267000
GAMMA/DRHO PRIME ERROR C2	0.8100000
PRESSURE PRIME ERROR	1.0000000

TABLE LXIII

SMOOTHED PHASE EQUILIBRIA AND INTERFACIAL TENSIONS
FOR CARBON DIOXIDE + N-DECANE AT 377.6 K (220°F)

Pressure (psia)	Phase Compositions, (Mole Fraction CO_2) Liquid	Vapor	Phase Densities, (kg/m^3) x 10^{-3} Liquid	Vapor	IFT Ratio, (mN/m)/(kg/m^3) IFTR
1500	0.5654	0.9868	0.6764	0.2049	9.3135
1600	0.5943	0.9864	0.6752	0.2243	8.2831
1700	0.6242	0.9831	0.6750	0.2455	7.2643
1800	0.6564	0.9808	0.6737	0.2683	6.2544
1900	0.6882	0.9786	0.6710	0.2933	5.2497
2000	0.7176	0.9753	0.6674	0.3212	4.2453
2100	0.7453	0.9704	0.6625	0.3523	3.2337
2200	0.7755	0.9640	0.6543	0.3884	2.2024
2300	0.8148	0.9529	0.6375	0.4366	1.1246
2310	0.8195	0.9511	0.6349	0.4427	1.0121
2320	0.8244	0.9491	0.6319	0.4493	0.8982
2330	0.8294	0.9468	0.6286	0.4562	0.7827
2340	0.8347	0.9442	0.6249	0.4637	0.6653
2350	0.8401	0.9412	0.6206	0.4718	0.5457
2360	0.8459	0.9377	0.6154	0.4808	0.4232
2370	0.8521	0.9332	0.6090	0.4911	0.2968
2380	0.8595	0.9269	0.6000	0.5038	0.1644
2382	0.8613	0.9252	0.5975	0.5070	0.1368
2384	0.8634	0.9232	0.5946	0.5105	0.1086
2386	0.8659	0.9206	0.5910	0.5148	0.0798
2388	0.8692	0.9171	0.5860	0.5203	(0.0499)*
2390	(0.8752)	(0.9106)	(0.5771)	(0.5295)	(0.0181)
2391**	(0.8926)	(0.8926)	(0.5533)	(0.5533)	(0.0000)

*Numbers in parentheses are extrapolated beyond highest measured pressures.
**Estimated critical point

TABLE LXIV

PARAMETERS USED TO GENERATE SMOOTHED PROPERTIES FOR CARBON DIOXIDE + N-DECANE AT 220°F

PHASE COMPOSITIONS
Units: Mole Fraction Carbon Dioxide

PC	2391.
ZC	0.8926220
AZ0	0.8056595
AZ1	-1.4441537
AZ2	-1.0256210
AZ3	35.6863003
AZ4	-224.8969866
AZ5	572.3106685
AZ6	-522.0894160
BZ0	0.5299663
BZ1	-3.2837509
BZ2	27.3426941
BZ3	-100.2481565
BZ4	184.2823320
BZ5	-158.4812414
BZ6	48.6917162

PHASE DENSITIES
Units: $(kg/m^3) \times 10^{-3}$ or (gm/cc)

RHOC	0.5533101
AR0	0.5543431
AR1	-1.4157818
AR2	5.1575923
AR3	-33.5824260
AR4	133.9667554
AR5	-276.8770949
AR6	227.4601947
BR0	0.6906370
BR1	-3.2651955
BR2	31.7946671
BR3	-137.9798517
BR4	308.8787565
BR5	-346.2488464
BR6	153.7531526

IFT-DENSITY DIFFERENCE RATIO
Units: $[(mN/m)/(kg/m^3)] \times 10^{-3}$ or [(mN/m)/(gm/cc)]

BG0	24.6798000
BG1	-9.6624379
BG2	11.9845949

TABLE LXV

SUMMARY OF STATISTICS FOR CARBON DIOXIDE + N-DECANE AT 220°F

VARIABLE	MEAN
SUMMARY OF RESULTS FOR PHASE COMPOSITION	
CO2 MOLE FRACTION	0.8641708
ROOT-MEAN-SQUARED ERROR	0.0011143
WEIGHTED ROOT-MEAN-SQUARED ERROR	0.9939047
ABSLOUTE AVERAGE % DEVIATION	0.0000000
DEVIATION,YEXP-YCALC	0.0000014
% DEVIATION	0.0000464
SCALED PRESSURE,(PC-P)/PC	0.0995574
CRITICAL PRESSURE	2391.0000000
WEIGHTED DEVIATION, DEV/SIGMA	0.0009838
MOLE FRACTION PRIME ERROR	0.0009980
PRESSURE PRIME ERROR	1.0000000
SUMMARY OF RESULTS FOR PHASE DENSITY	
PHASE DENSITY	0.5121729
ROOT-MEAN-SQUARED ERROR	0.0010350
WEIGHTED ROOT-MEAN-SQUARED ERROR	1.0215922
ABSLOUTE AVERAGE % DEVIATION	0.2002314
DEVIATION,YERP-YCALC	0.0000020
% DEVIATION	0.0002424
SCALED PRESSURE,(PC-P)/PC	0.0979599
CRITICAL PRESSURE	2391.0000000
WEIGHTED DEVIATION, DEV/SIGMA	-0.0052005
DENSITY PRIME ERROR	0.0005000
PRESSURE PRIME ERROR	1.0000000
SUMMARY OF RESULTS FOR IFTR	
GAMMA/DRHO	2.7112174
ROOT-MEAN-SQUARED ERROR	0.0633012
WEIGHTED ROOT-MEAN-SQUARED ERROR	0.9907447
ABSLOUTE AVERAGE % DEVIATION	4.1226228
DEVIATION,YEXP-YCALC	-0.0058867
% DEVIATION	-1.5255035
SCALED PRESSURE,(PC-P)/PC	0.1038314
CRITICAL PRESSURE	2391.0000000
WEIGHTED DEVIATION, DEV/SIGMA	-0.2780087
GAMMA/DRHO PRIME ERROR C1	0.0365000
GAMMA/DRHO PRIME ERROR C2	0.8100000
PRESSURE PRIME ERROR	1.0000000

APPENDIX C

PHYSICAL PROPERTY DATA

Table LXVI presents the pure property data, including molecular weight (MW), normal boiling point (T_b), critical temperature (T_c), critical pressure (P_c), critical specific volume (V_c), critical compressability factor (Z_c), and the Pitzer acentric factor, for the substances studied during the course of this investigation. These pure property data were acquired from the National Bureau of Standards (73).

TABLE LXVI

PHYSICAL PROPERTY DATA SET FROM THE NATIONAL BUREAU OF STANDARDS

Compound	MW	T_b, K	T_c, K	P_c, atm	V_c, cc/mol	ω
Methane	16.043	111.63	190.555	45.387	97.752	0.011314
Ethane	30.070	184.55	305.33	48.077	147.060	0.10038
Carbon Dioxide	44.010	194.6	304.21	72.86	94.43	0.2251
n-Propane	44.097	231.05	369.82	41.914	201.61	0.15418
n-Butane	58.124	272.65	425.16	37.465	256.41	0.20038
n-Pentane	72.151	309.21	469.75	33.319	313.60	0.25109
Benzene	78.114	353.24	562.16	48.34	259.0	0.212
Cyclohexane	84.16	353.88	553.5	40.168	308.0	0.212
n-Heptane	100.206	371.58	540.14	26.997	431.97	0.34991
trans-Decalin	138.254	460.4	690.0	31.0	480.0	0.250
n-Decane	142.287	447.3	617.55	20.693	607.53	0.48847
n-Tetradecane	198.395	526.73	692.95	15.525	827.13	0.64416

APPENDIX D

PARACHORS USED DURING THIS WORK

The Macleod-Sugden correlation (26, 27, 74), introduced in 1923, suggested a relationship between γ and the liquid and vapor densities:

$$\gamma^{1/4} = [P](\rho^L - \rho^V) \qquad (D\text{-}1)$$

Where [P] is a temperature independent parameter called the parachor.

The values of the interfacial tension predicted by the above relation are sensitively dependent on the value used for the parachor. Quayle (70) used experimental values for surface tension and density to evaluate parachors for many compounds. Table LXVII lists pertinent values for parachors. The values listed include those are from Quayles' work, Stegemeiers' work and values obtained from the Hugill-Van Welsenes and Lee-Chien models.

The Quayle parachors are from his tables (70). Stegemeier obtained parachors in his work from the Guggenheim parachor equation:

$$[P] = \frac{M\,\gamma^{3/11}}{\Delta\rho} \qquad (D\text{-}2)$$

The experimental data used to obtain the parachors came from the work of Rossini (75) for methane, ethane and n-decane; the n-pentane data was from the work of Sage and Lacey (76) and Katz (77); the propane and n-

TABLE LXVII

SUMMARY OF COMPONENT PARACHORS

Compound	Parachor (Quayle)	Parachor (Stegemeier)	Parachor (HVW)	Parachor (LC)
Methane	72.6	77.9	72.5	67.8
Ethane	110.5	118.0	112.6	110.7
Carbon Dioxide	77.5		76.8	81.7
n-Propane	150.8	158.0	153.3	152.1
n-Butane	190.3	200.0	193.4	193.5
n-Pentane	232.0	246.0	234.5	235.1
Benzene	206.0		211.1	208.3
Cyclohexane	242.1		242.2	240.0
n-Heptane	311.4		316.7	318.6
n-Nonane	391.0		397.4	396.5
trans-Decalin	371.0		377.9	363.7
n-Decane	431.0	463.0	439.8	432.1
n-Tetradecane	591.3		605.4	553.0

butane data were from the work of Sage and Lacey (76) and his own work (57). The Hugill-Van Welsenes (HVW) parachors were obtained using the reduced parachor correlation, where this reduced parachor is found from the linear relation between the reduced parachor and the acentric factor:

$$[P_r] = 0.151 - 0.0464\omega \qquad \text{(D-3)}$$

The parachor is then found from:

$$[P] = \frac{40.1684\ [P_r]\ T_c^{13/12}}{P_c^{5/6}} \qquad \text{(D-4)}$$

where P_c - critical pressure expressed in atmospheres

T_c - critical temperature expressed in Kelvin

The Lee-Chien parachors were obtained from their suggested method:

$$[P] = \frac{A_c^{\beta/\theta}\ V_c}{B} \qquad \text{(D-5)}$$

where $\beta/\theta = 45/176 = 1/3.911...$

$A_c - P_c^{2/3}\ T_c^{1/3}\ (0.133\ \alpha_c) - 0.281)$

$\alpha - 0.9078(1+(T_{br} \ln P_c)/(1-T_{br})$

$B - 1.854426\ Z_c^{-0.52402}$

P_c - Critical Pressure

T_c - Critical Temperature

V_c - Critical Volume

The density coexistence curve parameter, B, defined in the work by Lee and Chien was defined for normal paraffins as:

$$B = 1.854426\ Z_c^{-0.52402} \qquad (D\text{-}6)$$

The critical properties used to evaluate the parachor were obtained from the NBS data set found in Appendix C.

A graphical comparison of the various sources for the parachor is shown in Figure 55.

The value of the exponent, k, was found to be dependent on the value of P_c, where P_r is the ratio of the pressure to the critical pressure, P/P_c. For pressures far from the critical $P_r < 0.7$ the value of the exponent, k, was predominantly 4.0. As the critical pressure was approached and scaling law behavior became the major factor the value for which k gave the best predictions was $k = 2\nu/\beta = 3.78$. This poses a difficulty in understanding the validity of using the parachor of the pure substances for binary systems, since the pure components in the the binary may be below 0.7 P_c or well above 0.7 P_c, in some instances supercritical, for one of the pure substances. This could mean that the parachor for a pure substance should be found using a k of 4.0, but in the calculation of the binary interfacial tension a value of 3.78 should be used.

A generalized prediction for the parachors of the solvent or solute in a binary was arrived at during this work. Using the parachors presented by Quayle and multipling them by a fluctuation factor predictions had a lower absolute average percent deviation as compared to using the value of the parachors as just presented by Quayles. Tabulated values of the generalized arrived at values of the parachors used are presented in Table LXVIII. The solute parachor is obtained by

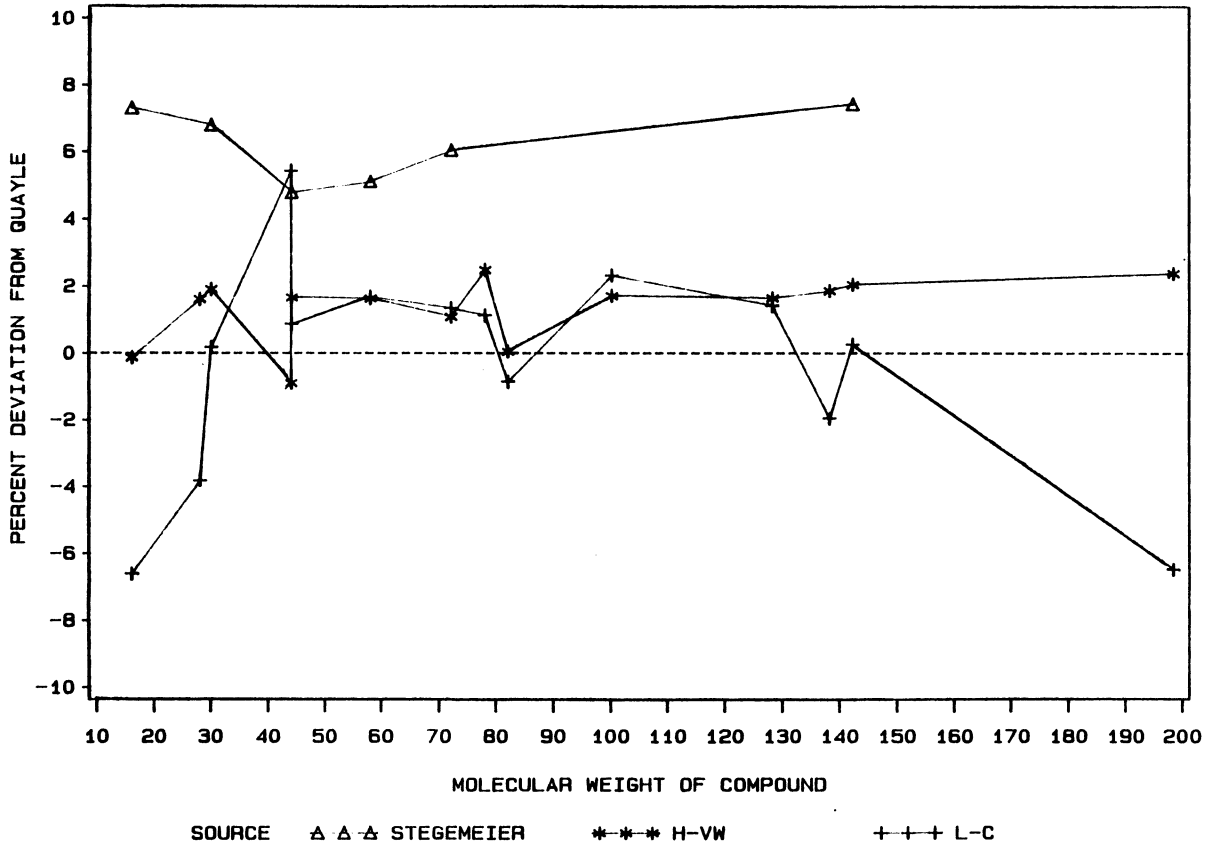

Figure 55. Deviation of Calculated Parachors From Literature Values Pure Compounds

TABLE LXVIII

SUMMARY OF GENERALIZED PARACHORS

Compound	Parachor (Quayle)	Parachor (Solute)	Parachor (Solvent)
Methane	72.6	63.1	
Ethane	110.5	96.1	
Carbon Dioxide	77.5	67.4	
n-Propane	150.8		158.3
n-Butane	190.3		199.8
n-Pentane	232.0		243.6
Benzene	206.0		216.3
Cyclohexane	242.1		254.2
n-Heptane	311.4		327.0
n-Nonane	391.0		410.6
trans-Decalin	371.0		389.6
n-Decane	431.0		452.6
n-Tetradecane	591.3		620.9

reducing the value given for the parachor by Quayle by 15%. The solvent parachor is obtained by increasing the Quayle parachor by 5%.

VITA

PETER BRIAN DULCAMARA JR.

Candidate for the Degree of

Master of Science

Thesis: INTERFACIAL TENSIONS FOR CARBON DIOXIDE OR LIGHT HYDROCARBONS IN HYDROCARBON SOLVENTS: EXPERIMENTAL DATA AND CORRELATIONS

Major Field: Chemical Engineering

Biographical:

Personal Data: Born at Fort Meade, Maryland, June 10, 1961, to Peter and Carol Dulcamara.

Education: Graduated from Stuttgart American High School, Stuttgart, Germany, December, 1978; received Bachelor of Science in Chemistry from Cameron University in December, 1983; received Bachelor of Science in Chemical Engineering from the Oklahoma State University in July, 1986; completed the requirements for the Master of Science degree at Oklahoma State University in December, 1987.

Professional Experience: Research Associate, Department of Chemical Engineering, Oklahoma State University, May, 1984 to September, 1987.